UCID-20112

KOVEC STUDIES OF RADIOISOTOPE THERMOELECTRIC GENERATOR RESPONSE (In connection with possible NASA Space Shuttle Accident Explosion Scenarios)

J. Walton
A. Weston
E. Lee

June 26, 1984

Lawrence Livermore National Laboratory

DISCLAIMER

Printed in the United States of America
Available from
National Technical Information Service
U.S. Department of Commerce
5285 Port Royal Road
Springfield, VA 22161
Price: Printed Copy $; Microfiche $4.50

Page Range	Domestic Price	Page Range	Domestic Price
001-025	$ 7.00	326-350	$ 26.50
026-050	8.50	351-375	28.00
051-075	10.00	376-400	29.50
076-100	11.50	401-426	31.00
101-125	13.00	427-450	32.50
126-150	14.50	451-475	34.00
151-175	16.00	476-500	35.50
176-200	17.50	501-525	37.00
201-225	19.00	526-550	38.50
226-250	20.50	551-575	40.00
251-275	22.00	576-600	41.50
276-300	23.50	601-up[1]	
301-325	25.00		

[1]Add 1.50 for each additional 25 page increment, or portion thereof from 601 pages up.

KOVEC STUDIES OF RADIOISOTOPE THERMOELECTRIC GENERATOR RESPONSE (In connection with possible NASA Space Shuttle Accident Explosion Scenarios)

J. Walton, A. Weston, and E. Lee
Lawrence Livermore National Laboratory
University of California
Livermore, California 94550

ABSTRACT

The Department of Energy (DOE) commissioned a study leading to a final report (NUS-4543, "Report of the Shuttle Transportation System (STS) Explosion Working Group (EWG)," June 8, 1984), concerned with PuO_2 dispersal should the NASA space shuttle explode during the proposed Galileo and ISPN launches planned for 1986. At DOE's request, LLNL furnished appendices that describe hydrocode KOVEC calculations of potential damage to the Radioisotope Thermoelectric Generators, fueled by PuO_2, should certain explosion scenarios occur. These appendices are contained in this report.

INTRODUCTION

The Department of Energy (DOE) commissioned a study directed by the NUS Corporation (Gaithersburg, MD) to estimate the probabilities and magnitudes of various postulated Shuttle Transportation System (STS) accident explosions involving mixtures of on board hydrogen and oxygen, as well as possible explosions of the solid rocket booster (SRB) propellant. The focus of concern was damage to and dispersal of Plutonium dioxide fuel elements in the Radioisotope Thermoelectric Generator (RTG) power sources to be included in the planned 1986 launches of the Galileo and ISPM spacecraft. LLNL was requested to participate by performing a series of explosion calculations using the KOVEC computer program to estimate STS and RTG responses to various explosion scenarios. The three (3) appendices furnished by LLNL to NUS that describe the LLNL studies are presented here.

The master NUS report is NUS-4543, "Report of the Shuttle Transportation System (STS) Explosion Working Group (EWG)," June 8, 1984.

*Work performed under the auspices of the U.S. Department of Energy by the Lawrence Livermore National Laboratory under contract No. W-7405-ENG-48.

SUMMARY

In 1983, there was a large ANFO explosion (609 tons) named, Direct Course, in which an RTG was exposed in a region where free field overpressure is estimated to have been somewhere between 1300 psi and 2000 psi. KOVEC was used to calculate this explosion and estimate the RTG response. This work is described in Appendix B2.2 which is a self contained section.

A shock tube test was conducted at Sandia National Laboratory, Albuquerque, in which an RTG working element, the General Purpose Heat Source (GPHS) was subjected to a shock corresponding to a free field overpressure of 1070 psi. KOVEC was used to calculate the GPHS response to this test. This work is described in Appendix B2.3, a section that relies on Appendix B2.2 as a source of essential information.

The major elements of the STS, the Centaur rocket, and the Galileo space craft were examined and analyzed. Various mixtures of liquid hydrogen and frozen oxygen, at various locations were assumed to detonate, pursuant to scenarios postulated by the EWG. Intervening structures and materials between the detonations and the RTG were modeled as material layers for one dimensional KOVEC calculations. Four explosion scenarios were studied. These are,

(1) External fuel tank to RTG
(2) Onboard Centaur fuel tank to RTG
(3) Assumed initial velocity flyer plate impacts to the RTG
(4) External fuel tank to solid rocket booster propellant.

These KOVEC calculations are summarized and described in Appendix I, mostly a stand alone section, although descriptive material on KOVEC from Appendix B2.2 is referenced.

APPENDIX B2.2, DIRECT COURSE

Introduction

The mechanical response of the RTG to the Direct Course explosion has been calculated at the Lawrence Livermore National Laboratory, LLNL, using the hydrocode, KOVEC*, that operates on the Cray computer. KOVEC solves the Lagrangian finite difference equations for one dimensional, elastic-plastic flow**. One dimensional problems can be formulated for solution in planar, cylindrical, or spherical plane strain geometries. These Direct Course problems were all formulated in spherical geometry.***

The RTG is a small, heavy (119 lbs) body located in a large explosive field, 56.5 ft. from the center of the 609 ton ANFO explosive. The radius of the spherical ANFO case was on the order of 17.5 ft. The actual RTG blast response is multidimensional. Therefore, interpretation of response calculations based upon spherical one dimensional, plane strain, layered material (flyer plate), impacts involve judgemental assumptions, based on physical reasoning.

The ANFO explosion not only produced an air shock front and free field overpressure but it also produced a large flow of explosive products traveling at a high particle velocity, (4.6 mm/μs, 15000 ft/sec) behind the shock front. The momentum of this flow created a dynamic pressure much larger than the free field overpressure, when it was caused to slow and move around the RTG in the vicinity of its geometric "stagnation region." It seems reasonable to suppose that RTG response, calculated using a one dimensional explosion model, should be of the same order of magnitude as that calculated using a two dimensional model when the target body has a drag coefficient on the order of 1.0.

It proved necessary to perform several one dimensional model calculations to measure the sensitivity of calculated results to various reasonable assumptions. These "explosion models" are next described.

Explosion Models

The target RTG model material layers are illustrated on Fig. B2.2-1. Associated dimensional and zoning data is tabulated in Table B2.2-1. The ANFO detonated in the center and ANFO case model is illustrated on Fig. B2.2-2. Associated zoning and dimensional data is tabulated in Table B2.2-2. Tables B2.2-1 and B2.2-2 also list a number designating the KOVEC equations of state (EOS) for each material layer. The EOS are described in detail in the next section.

---

* J. P. Woodruff, "KOVEC User's Manual," Nov. 23, 1976, UCID-17306.

** M. L. Wilkins, "Calculation of Elastic-Plastic Flow," UCRL-7322, Rev. 1 (1969)

*** Explosions described in Appendix I were formulated in all three geometries.

The RTG model, Figure B2.2-1, did not completely represent the configuration in the Direct Course event. The gas space between the molybdenum and the graphite also was filled with "Cerafelt." Cerafelt is a light weight expanded material, that is "snowplow" compressed to a nearly solid condition by the explosion. Since the total mass of the omitted Cerafelt is small, its absence will not significantly affect the calculated pressures in the graphite and uranium dioxide layers.

Table B2.2-3 lists the five (5) explosion models for which comparative results are presented. In run 14, all void spaces including the space between the ANFO case and the first aluminum layer of the RTG, was assumed to be empty, i.e., at a perfect vacuum. In this run, the ANFO case material first strikes the RTG. In run 15, all void spaces are assumed to be full of atmospheric air. Here the air between the ANFO case and the first RTG layer is trapped and becomes a "cushion" that limits RTG response. RTG response will be overestimated in run 14 and underestimated in run 15.

Actually, most of the air between the ANFO case and the RTG will flow around it and will not be trapped. In runs 16 and 21, a 12 inch layer of air adjacent to the RTG was included to represent the small amount of air cushion effect that was present in the real explosion. The material yield strength in the graphite and UO_2 layers of the RTG were varied between runs 16 and 21. Yield strength proved to be of secondary importance to these calculations and therefore the results of these two runs appear to be substantially the same. Also, the calculated RTG responses for runs 16 and 21 appear to be of the same magnitude as those calculated for the vacuum case, run 14.

In run 23, the ANFO and its case are exploded in air. No RTG model is present. This calculation results in free field overpressure versus time at the location of the RTG. In run 24, an uncased gas explosion with no case was created that would produce nearly the same free field air shock overpressure at the RTG as that produced by cased ANFO in run 23.

In run 24, the RTG was present and the free field overpressure to be expected at the RTG radius was estimated by applying a radius ratio to the pressure peak at a middle air zone initially located 37 ft. from the explosion center.

Equations of State

In KOVEC, any given material state is represented as the sum of isotropic volumetric behavior and deviatoric shearing behavior. The model for volumetric behavior is termed the "equation of state," i.e., EOS. In this study deviatoric shearing behavior is represented by a yield stress and a shear modulus. Fracturing behavior, was not considered. A condition of no material separation was imposed on all solid material layers. This caused both high positive and negative oscillatory peak pressures to be calculated in response to the explosion. Here, the absolute magnitudes of various calculated pressures were so high that it must be assumed that all target materials failed.

Under the intense impact conditions imposed by the explosion, volumetric pressures are very high and swamp deviatoric shearing behavior. It is a good approximation to assume that the magnitude of the principal stress equals that of the pressure.

A volumetric EOS is an equation that relates pressure, P, to dimensionless relative volume, V, and internal energy per unit volume, E. Both P and E are expressed in the same units of pressure. The initial material density, ρ_0, or specific volume, $V_0 = 1/\rho_0$, also is a part of the EOS. In some EOS formats, a variable named compression, μ, is used, which is related to relative volume, as

$$\mu = 1/V - 1$$

In KOVEC, a particular consistent unit system is used for both input and output. Density is expressed as gm/cc; pressure and energy are expressed as Mb; position is in cm; time is in μs; velocity is expressed as cm/μs. The EOS data is tabulated in these units.

In this study four (4) EOS formats are of interest. The ANFO explosive is described by the JWL EOS, KOVEC form 1.

$$P = A\left(1 - \frac{\omega}{R_1 V}\right)e^{-R_1 V} + B\left(1 - \frac{\omega}{R_2 V}\right)^{-R_2 V} + \frac{\omega E}{V}$$

The gas explosion was described by the Gamma Law EOS, KOVEC form 1, A = B = 0

$$P = \omega E/V$$

Both explosive EOS require an initial energy designated as E_0.
Non-reactive solid materials frequently are described by a linear polynomial, KOVEC form 2.

$$P = A_0 + A_1\mu + A_2\mu^2 + A_3\mu^3 + (B_0 + B_1\mu + B_2\mu^2)E$$

Light weight foam materials and also non reactive solids are sometimes described by a Gruneisen EOS, KOVEC form 4.

$$P = \frac{\rho_0 C^2 \mu\left[1 + (1 - \frac{\gamma_0}{2})\mu - \frac{a}{2}\mu^2\right]}{\left[1 - (S_1 - 1)\mu - S_2\frac{\mu}{\mu+1} - S_3\frac{\mu^3}{(\mu+1)^2}\right]^2} + (\gamma_0 + a\mu)E$$

Almost any non-reactive material, porous or solid, can be represented by a very general ratio of polynomial's, the 32 bit EOS, KOVEC forms 3, 6, and 7.

$$\frac{F_1 + F_2E + F_3E^2 + F_4E^3}{F_5 + F_6E + F_7E^2}$$

where $F_i = \sum_j^3 A_{ij}\mu^j$

The constants built into the 32 bit EOS automatically are available when a number designating the material is called, unless overridden by an outside input. Here two such materials are used, UO_2, and dynasil (a particular type of silicon expanded material).

Input data for all materials used in this study is tabulated in Table B2.2-4.

Results

Calculated results are tabulated on Table B2.2-5. First note that two sets of numbers are given for the "vacuum" explosion designated as (1) coarse resolution output (run 14), and (2) fine resolution output (run 14A). To calculate the RTG response, it is first necessary to compute the entire explosion process to the RTG, a matter of 4 ms and 56.5 ft. The succeeding essential response at the radius when the shock reaches the RTG is very short, a matter of 12 inches and about 200 μs. The RTG is made up of thin material layers which in turn are transited by the shock front in a fraction of a microsecond. KOVEC chooses its own time step according to the "Courant criteria", based on the smallest cell transit time, a number that varies with cell compression. This "calculation" time increment was typically on the order of 0.02 microseconds.

The output time step is requested by the code user. Since the storage available for output plot files is limited, the code user must first request coarse output that will span the entire process. Then, the user can see when the essential action occurs and can then rerun the problem and request a small "window" of fine resolution output. Here, coarse resolution output was requested every 40 μs. Subsequent fine resolution output was requested every 1 μs. Refer to Figs. B2.2-3 and B2.2-4 that plot UO_2 pellet velocity versus time. Note that coarse resolution Fig. B2.2-3 is very "spikey" and that the absolute maximum spike amplitude is always less than the maximum peak or maximum valley illustrated on the fine resolution shown on Fig. B2.2-4.

Figures B2.2-3 to B2.2-14 show a set of comparative coarse and fine resolution outputs for the vacuum explosion, for selected pressures and velocities throughout the model. Since the calculation is Lagrangian, each output shows pressure or velocity in a particular piece of matter (calculation cell) as it moves in time. Each output is identified at the bottom of each figure. Run 14 is for coarse time resolution and run 14A is for fine time resolution. Figures B2.2-15 to B2.2-18 illustrate coarse resolution position versus time for run 16, with vacuum plus 12 inches of air in front of the RTG. Calculated results for run 16 are substantially similar to those for run 14. Therefore, these position versus time outputs should also be representative of run 14.

Refer again to the summary results on Table B2.2-5. Run 23 calculated an ANFO explosion into the air. No RTG was present so that the calculated air pressure versus time represents free field pressure. The cell pressure versus time on Figs. B2.2-19 and B2.2-20 bracket the free field response to be expected at the location of the RTG. Interpolating between these two figures yields the estimated free field overpressure at the RTG location to be .1245 Kb (1806 psi).

Figure B2.2-21 shows the free field air cell particle velocity corresponding to the air pressure of Fig. B2.2-20. Its peak value is 2.84 mm/μs. The free field air shock velocity near the RTG is calculated from the peak values on Figs. B2.2-20 and B2.2-21.

$$U_s = \frac{P}{\rho_o U_p} = 3.54 \text{ mm/}\mu\text{s}$$

Figure B2.2-22 presents pressure versus time for the last air cell between the ANFO casing and the RTG, directly in front of the RTG, for the explosion in air, run 15. Figure B2.2-23 presents particle velocity versus time for the same cell. Figures B2.2-24 and B2.2-25 present information for the same cell in the uncased gas explosion, run 24. Comparing these figures will give a measure of the relative intensity of the Direct Course explosion with cased ANFO, to a gas explosion without the casing that produces about the same free field overpressure at the RTG radius. From these figures it is apparent that run 15 was more severe than run 24.

Discussion of Results

With regard to the RTG model, Figs. B2.2-1 and Table B2.2-1, note that no single material layer is divided into more than three (3) zones. This means that the wave travel through any given layer is not represented with precision. Sharp shock and release fronts relative to the thickness of a layer, is not computed. On the other hand, all of the mass and compressibility in the array of layers is represented, so that the calculated pressures and particle velocities for the elements of array should be quite accurate.

From the summary of results on Table B2.2-5, the following is concluded.

1. Calculated response for runs 16 and 21 are similar to those for the vacuum case run 14. The data scatter reflects coarse time resolution output. Run 14A fine time resolution output applies to all three runs 14, 16, and 21.
   Therefore: the graphite responded to pressures as high as 186 Kb and then failed; the UO_2 reacted to pressures as high as 137 Kb and then failed; the aluminum reacted to pressures as high as 58 Kb and then failed. In total, the RTG failed early as the shock front passed over it.

2. In comparing run 15 for the cased ANFO explosion in air, to run 24 for the gas explosion without the casing, it appears that the impact of the ANFO case on the RTG greatly increased the RTG response and, therefore, the damage.

3. In comparing runs 14 and 23, it appears that shock front radial momentum greatly increases RTG stresses over those that would be induced by only the free field overpressure.

APPENDIX B2.3, KOVEC SIMULATION OF SHOCK TUBE TEST

Introduction

A shock tube test* of a heated (1095°C) General Purpose Heat Sourse (GPHS) was performed at Sandia, Albuquerque, on March 9, 1983. As for the Direct Course Explosion, Appendix B2.2, the mechanical response of the GPHS was calculated at Lawrence Livermore National Laboratory using the KOVEC hydrocode.

Two experimental pressure versus time gauge records are included in the test report, one measured in the shock tube sidewall 10.3 ft. upstream from the GPHS location, and another measured in the sidewall 4.28 ft. upstream from the GPHS location. The 1070 psi peak overpressure at the test station was estimated using a curve fit to the pressure pulse "times of arrival" at these two upstream gauge positions, assuming ambient temperature nitrogen gas and using the perfect gas laws. The 10.3 ft. upstream record indicated a peak pressure of about 1180 psig and the 4.28 ft. upstream record indicated a peak pressure of about 965 psig.

For the simulation calculation, it was decided to approximate the pressure versus time profile of the 10.3 ft. upstream pressure gauge (1180 psi), using the spherical gas explosion comparison model discussed in the Direct Course Appendix B2.2, run 24.

A free field calculation using the gas explosion model into air resulted in a reasonable approximation to the selected nitrogen gas shock tube record. See Fig. B2.3-1.

The GPHS model was abstracted from the RTG model, Direct Course Fig. B2.2-1 and Table B2.2-1. Zoning and dimensional data are included in Table B2.3-1.

Results

The GPHS was placed at the air cell where the experimental pressure profile was simulated. Figure B2.3-2 shows pressure versus time in the first graphite cell. Figure B2.3-3 shows pressure versus time in the first UO_2 cell. The calculated peak graphite pressure of 8267 psi and peak UO_2 pressure of 6600 psi for a pulse with a free field overpressure peak in air of 1180 psi, is in reasonable agreement with the test report estimate of a peak nitrogen gas reflected pressure acting on the carbon block of 7500 psi for a place with a free field overpressure peak of 1070 psi. Figure B2.3-4 shows velocity versus time for the first graphite cell and Fig. B2.3-5 shows position versus time for the first graphite cell. GPHS acceleration estimated from Fig. B2.3-4 is 21000 gees, a value that is in reasonable agreement with the test report estimate of 19000 gees.

---

* F. H. Mathews, "Test of a General Purpose Heat Source Heated to 1095°C and Subjected to a Blast at 1070 psi Static Overpressure," Sandia National Laboratory, Albuquerque, NM, March 17, 1983, directed to Stan Bronisz, CMB-5, LANL.

APPENDIX I
STS FLYER PLATE STUDY

I1. Introduction

The mechanical response of the RTG to various flyer plate (fragment) scenarios that could result from accident induced explosions of the STS has been calculated at the Lawrence Livermore National Laboratory, LLNL, using the one dimensional, plane strain, Lagrangian, finite difference, hydrocode KOVEC. Such problems can be formulated in planar, cylindrical, and spherical coordinate systems. Many different layers of several different materials, described by different equations of state (EOS) can be represented in a KOVEC problem statement. Details about KOVEC and a general discussion of EOS are included in the Direct Course Appendix B2.2.

The one dimensional RTG model illustrated in Fig. B2.2-1 and described in Table B2.2-1 has been simplified. The molybdenum layers were eliminated and the corresponding mass has been added to the dynasil layers. The irridium layers were eliminated and replaced by graphite. Dimensional and zoning data plus the KOVEC EOS identification number are tabulated in Table I-1. Elimination of the thin cells of molybdenum and irridium reduced computation time by 30 percent with no significant effect on the pressures calculated in the layers of graphite and UO_2. In addition, the "32 bit" EOS format for the dynasil was changed to the Gruneisen EOS format for cellular silicone of the same density. This was done because in one of the STS explosion models, computation was stopped by the calculation instability in a dynasil layer.

Input material data for these STS explosion models are listed in Table I-2. The format of Table I-2 is the same as that for Direct Course, Table B2.2-4. The EOS section of Appendix B2.2 is a general explanatory reference for this data. In the Direct Course study, a condition of no material failure was imposed on the calculation models. Here, that condition has been removed and, for the most part, no material is allowed to carry negative pressure (tension). This change was made so that STS elements formulated in cylindrical and spherical coordinate systems would not be slowed by unrealistic levels of tension in responding to explosion environments that are much less intense than that caused by the Direct Course ANFO detonation.

I2. The LOX-LH_2 Explosion EOS

The STS explosion scenarios discussed here involve the reaction of various weights of mixed LOX and LH_2. There is a program named TIGER* that takes into account the equilibrium thermochemical data of reactive materials and then calculates all the important parameters of the processes, ending with the final states on the fully reacted Hugoniot. This program was applied to a stoichiometric mixture of LOX and LH_2. The results were then fitted by a JWL format explosion EOS for code KOVEC computations. The correspondence between the JWL EOS and the TIGER data is illustrated on Figs. I-1 to I-3. Note in Fig. I-1, the Chapman-Jouguet (CJ) detonation pressure is about 40 kb and the "volume burn" pressure (at V = 1.0) is 18.6 kb. The CJ detonation velocity is 5.42 mm/μs.

---

* M. Cowperthwaite and W. H. Zeisler, "TIGER Computer Program Documentation," SRI publication No. Z106, January 1973.

In the STS explosion scenarios, a small dense (0.4025 g/cc) region of stoichiometric LOX and LH_2 is volume burned. The initial high pressure region then produces a pressure wave through a thick blanket of LH_2 (density = 0.07 g/cc), to impact and accelerate a confining shell array composed of layers of metal and insulation. Figure I-4 shows the non-reactive shock velocity versus particle velocity Hugoniot for LH_2. The data of Fig. I-4 were translated into the polynomial EOS coefficients listed in Table I-2.

There is no experimental evidence that such an intense explosion has yet been produced in mixtures of LOX and LH_2. The Pyro test data, Appendix A, are associated with free field pressures of 2000 psi, measured close to the center of the explosion. The Pyro test data suggest that the chemical energy release there has occurred in a rapid deflagration process over a significant time period.

Gaseous detonations of well mixed, cold (-260°F), fairly dense oxy-hydrogen mixtures at low initial pressures (100 mm Hg) have been produced in large containers with a single spark plug discharge.* The temperature difference between LOX and LH_2 means that the mixtures of interest here will be pieces of frozen oxygen in a matrix of liquid and gaseous hydrogen. The Direct Course ANFO detonation was produced in a mixture of ammonium nitrate "rocks" and oil with an explosive booster charge that weighed 115 lbs. A very strong LOX and LH_2 explosion, and even true detonation, is theoretically possible. Whether or not such an event occurs, and of what intensity, will depend on the size and distribution of the solid oxygen "rocks" and on the strength of the initiation.

For the calculations in this appendix, an adequate initiator is assumed. Several computer runs are made for each scenario, in which the weight of combustible mixture is varied. The resulting calculated pre-impact velocities of the flyer plates (fragments) that strike the RTG range between 0.5 mm/μs to 3 mm/μs.

I3. Flyer Plate Definition in General

A trip was made to Rockwell in Los Angeles and to General Dynamics in San Diego, where drawings, schematics, and verbal information was obtained relating to the STS, the Centaur, and the Galileo space craft. Additional drawings and data were obtained as a result of conversations with personnel at Rockwell, General Dynamics, JPL, and Thiokol. The space shuttle mockup at Rockwell was observed as were Centaur parts at General Dynamics.

This information was used to generate a scaled schematic drawing (SH-RTG-AMW-1) in which STS, Centaur, and Galileo parts were located in relation to the RTG, with all parts in their nominal position. Representative, nominal explosion paths were identified and flyer plates (fragments) were defined from the details of the intervening material.

---

* A. J. Laderman, A. K. Oppenheim, "Study of Detonation of Mixtures of Gaseous Hydrogen and Gaseous Oxygen," Final Report on Contract NAS8-2634, April 1965, Space Science Laboratory, UC, Berkeley, CA.

Accidents generate large forces and accelerations. The Galileo support to the Centaur fails at about 7 gees; the RTG support to the Galileo fails at about 20 gees. It is unlikely that the chosen flyer plates will impact a nominally located RTG. However, it is assumed that fragments somewhat like the chosen flyer plates are likely to strike the RTG wherever it might be.

Various layers of different densities of insulation and ablation materials are included in the flyer plate (fragment) definitions. These materials range from light to very light. The dynasil in the RTG model is an expanded material with a density of 8 pcf (0.128 g/cc). To reduce the number of different EOS, the masses of all these layers of different densities were maintained but the thicknesses were all normalized to a density of 8 pcf. Thus, all insulation and ablation materials fall within the same Gruneisen format EOS for cellular silicone foam.

I4. Annular Explosion in ET to RTG

In this scenario there is a shaft of LOX along the center line of the ET, bounded by an annular ring of stoichiometric LOX plus LH_2 mixture, bounded by a thick blanket of LH_2, which in turn is bounded by the ET tank shell. Such cylindrical explosions can be described by an equivalent planar explosion with the same ratio of explosive weight to shell weight. Here, both cylindrical and planar explosion models were created. The explosion accelerates the ET tank shell into the orbiter floor and then into the RTG.

Figure I-5 shows both the cylindrical and planar explosion models. Figure I-6 illustrates the details of the flyer plate that represents the ET tank wall. Figure I-7 illustrates the details of the flyer plate that represents the orbiter floor.

Calculated ET and orbiter floor pre-impact velocities (cylindrical and planar values are averaged) are plotted versus stoichiometric mixture weight per ft. of ET tank length, in Fig. I-8A. Associated averaged graphite and UO_2 pressures are plotted in Fig. I-9A.

I5. Centaur Tank Explosion to RTG

In this scenario there is spherical ball of stoichiometric mixture of LOX and LH_2, bounded by the Centaur tank dome. The explosion accelerates the Centaur tank into its purge diaphragm, then into the magnesium lower Galileo adapter shell, and then into the RTG model. Figure I-8 illustrates the explosive model. Figure I-9B illustrates the Centaur tank model. Figure I-10 illustrates a flyer plate model that combines the purge diaphragm and the Galileo lower adapter.

Calculated Centaur steel dome and adapter magnesium pre-impact velocities are plotted versus the weight of the stoichiometric mixture in Fig. I-11. Associated averaged graphite and UO_2 pressures are plotted in Fig. I-12.

I6. Flyer Plate Initial Velocity Impacts

The ET shell model, Fig. I-6, was placed against the orbiter floor model, Fig. I-7. The array was located 12 inches from the RTG model in a planar coordinate system. All elements of the ET shell model were given

an initial velocity. This accelerated the ET shell-orbiter floor array into the RTG. Three ET shell initial velocity cases were calculated; 1000 fps (.3048 mm/μs), 3000 fps (.9144 mm/μs), and 5249 fps (1.6 mm/μs.). Orbiter floor pre-impact velocity is plotted against assumed ET shell initial velocity in Fig. I-13. Associated averaged graphite and UO_2 pressures are plotted in Fig. I-14.

Note that the greater than linear falloff in pressures for the pre-impact velocities below 3000 fps. At high velocities, the low density non-metallic materials are compressed to an almost solid state. As the pre-impact velocity is reduced, these materials become a more effective cushion and act to attenuate the RTG response.

I7. Annular Explosion in ET to SRB

This explosion scenario is similar to the largest that is described in Section I4, but the target is an SRB, not the RTG. The explosion model and SRB "flyer plate" are illustrated on Figs. I15 and I16. The objective of this calculation is to compute the pressure pulse into the SRB propellant, calculate the energy fluence, and compare the result with flyer plate impacts into the more sensitive "Project Sophy" propellants.* The Project Sophy data (samples containing 5 percent to 10 percent RDX) was recently reanalyzed** in connection with several shock initiation tests commonly applied to explosives and more sensitive propellants that contain HMX.

The project Sophy propellants were similar to the SRB propellant, but for the purpose of determining critical diameter, they were salted with differing amounts of RDX to make them sensitive enough to achieve measurable reactions in the test program. There were three formulations with measured failure diameters of 2.7 ins. 5.2 ins. and 11.5 ins. The unsalted Sophy propellant (which is almost identical in composition to the STS SRM) failed to detonate at a diameter of 5 feet and detonated in a test at 6 feet diameter. SRB propellant has an unmeasured failure diameter estimated from the Sophy tests to be about 6 feet.

The reanalysis indicated that the RDX salted Sophy materials required a pressure pulse of more than 19 Kb to initiate. The least sensitive (D_F = 11.5 ins salted with 5 percent RDX) also required a critical energy fluence greater than 10 MJ/M^2.

Figure I-17 shows the pressure pulse that transits the first cell of the propellant after an external tank explosion with 1662 lbs/ft of stoichiometric mixture of LOX and LH_2. While there are some pressure spikes that reach 10.5 Kb on the front of this pulse, it is basically flat topped at 7 Kb with an effective duration on the order of 700 μs. Figure I-18 illustrates the particle velocity for the same cell, a value

---

* R. B. Elwell, O. R. Irwin, R. W. Vail, "Project Sophy-Solid Propellant Hazards Program," AFRPL-TR-67-211-Vol I, August 1961.

** A. M. Weston, J. F. Kincaid, et al., "Correlation of the Results of Shock Initiation Test," 7the Symposium on Detonation, NSWC MP 82-334, pp. 887-897.

of 0.2 mm/μs when pressure is high. From this information, the shock velocity is estimated at about 3 mm/μs and the energy fluence is estimated at about 60 MJ/M^2. This value for energy fluence is between 5 and 6 times the critical value estimated for the least sensitive 5 percent RDX salted Sophy propellant, a value of only 10 MJ/M^2.

Energy fluence is a concept that relates the response of an explosive to initiation, to the pressure and duration of a load applied to the explosive. The higher the energy fluence, the more difficult it is to initiate a reaction in the propellant. Although this concept has not been widely accepted (B. Brown, L. Green, et al., "Scaling Relationship for Impact Initiated Detonations," in Proceedings called 16 JANNAF Combustion Meeting, Sept. 1979), if properly used, it can result in a reasonable correlation between tests performed under differing conditions.

No estimates were made of the energy fluence required for initiation of unadulterated Project Sophy propellant. However, it is expected to be substantially higher than the RDX salted propellant. This is because the unadulterated or unsalted propellant is relatively insensitive. As pointed out in Appendix A-4, the RDX salted propellants are classed as high explosives (Class 1.1), and the composite propellants, as in the SRB, are classed as a non-mass detonating material (Class 1.3).

The low pressure means that the SRB propellant will not detonate. These calculations cannot reveal what lower level reactions may occur. They may range from no reaction to a deflagration or a yield of less than 6 percent, as shown in Table A-1, Appendix A. The 6 percent yield was for an already burning propellant which is more sensitive than an unburnt propellant.

As for other items of interest, the pre-impact velocity for the ET aluminum is 2.3 mm/μs. The last cell of the SRB steel case has a spiky peak velocity of 0.37 mm/μs but an average flat velocity of only 0.2 mm/μs. The low steel case velocity relative to the high ET shell aluminum velocity is because the thick steel case of the SRB is much heavier than the thin aluminum shell of the ET.

I8. Summarized Results

Table I-3 is a tabulation of all essential flyer plate scenario results, including those from the Direct Course explosion, Appendix B2.2. The Direct Course explosion was substantially more severe than the most severe ET to RTG explosion case. The ET to RTG explosions are somewhat more severe than the Centaur to RTG explosions. The assumed 1000 fps (.3048 mm/μs) initial velocity flyer plate case was much less severe than any of the explosion scenarios. The assumed 3000 fps (.9144 mm/μs) initial velocity flyer plate case appears equivalent to the smaller ET to RTG and Centaur to RTG explosions, so far as pressures produced in the graphite and UO_2 are concerned.

It is of interest to crossplot the averages of ET flyer plate velocity versus average values for graphite plus UO_2 stresses. This results in a
fairly clean looking line that covers three decades in stress and two decades in flyer plate velocity, Figure I-19. The data for the figure

are from the cases discussed in Section I-4 (Annular Explosion in ET to RTG) and Section I-6 (Flyer Plate Initial Velocity Impact). Recognize that the plotted data are for course time resolution response. Therefore, peak analyzed values are likely to be higher.

DESCRIPTION	KOVEC EOS EOS NO.	THICKNESS CM	NO OF ZONES	CUMULATED DIMENSIONS CM
				0.0
ALUMINUM CASE	25	0.3175	3	0.3175
CERAFELT (DYNASIL)	67	1.905	1	2.2225
MOLYBDENUM	114	0.0254	1	2.2479
ARGON AIR	51	8.1331	3	10.3810
GRAPHITE	73	1.1881	3	11.5691
IRIDIUM	79	0.070	1	11.6341
URANIUM DIOXIDE	95	2.833	3	14.4721
IRIDIUM	79	0.070	1	14.5421
GRAPHITE	73	1.2958	3	15.9379
IRIDIUM	79	0.070	1	16.0079
URANIUM DIOXIDE	95	2.833	3	18.8409
IRIDIUM	79	0.070	1	18.9109
GRAPHITE	73	1.1881	3	20.0990
ARGON (AIR)	51	8.1331	3	28.2321
MOLYBDENUM	114	0.0254	1	28.2575
CERAFELT (DYNASIL)	67	1.905	1	30.1625
ALUMINUM	25	0.3175	3	30.48

TABLE B2.2-1 RTG MODEL DIMENSIONS, ZONES, AND MATERIAL IDENTITY FOR DIRECT COURSE CALCULATIONS.

DESCRIPTION	KOVEC EOS NO.	THICKNESS CM	NO. OF ZONES	CUMULATED DIMENSION CM
				0
ANFO	6	553.21	55	553.21
KEVLAR SHELL	53	1.27	3	534.48
POLYURETHANE	34	7.62	3	542.10
KEVLAR SHELL	53	1.27	3	543.37
AIR OR VACUUM	51	1160.97	55	1704.34
RTG MODEL		30.48	35	1734.82

TABLE. 2.2-2 ANFO PLUS CASE DIMENSIONS, ZONES, MATERIAL IDENTITY FOR DIRECT COURSE CALCULATIONS.

RUNS 14,14A ANFO PLUS CASE EXPLOSION INTO VACUUM TO RTG.
RUN 15 ANFO PLUS CASE EXPLOSION INTO AIR TO RTG.
RUNS 16, 21 ANFO PLUS CASE EXPLOSION INTO VACUUM, 12 INCHES OF AIR IN FRONT OF RTG. RUN 16 UO_2 YS = 0.1 kb Graphite YS = 1.3 kb RUN 21 UO_2 YS = 10. kb Graphite YS = 10. kb
RUN 23 ANFO PLUS CASE EXPLOSION INTO AIR, NO RTG.
RUN 24 GAS EXPLOSION, NO CASE INTO AIR TO RTG.

TABLE 2.2-3 EXPLOSION MODELS FOR DIRECT COURSE CALCULATIONS.

ACTUAL MATERIAL	DENSITY	KOVEC MATERIAL	DENSITY	EOS TYPE	CONSTANTS FOR EQUATION OF STATE	SHEAR MODULUS	YIELD STRESS
ANFO		ANFO	0.85	JWL	A = 0.476 R1 = 3.5 W = 0.31 B = 0.005235 R2 = 0.9 E_0 = 0.0325	0	0
		No case Explosion gas	0.0012	JWL (gamma law)	A = 0. W = 0.4 B = 0. E_0 = 0.003	0	0
Aluminum		Aluminum 6061-T6	2.703	Gruneisen	C = 0.524 S2 = 0 γ_0 = 1.97 S1 = 1.4 S3 = 0 a = 0.48	0.276	0.0029
Cerofelt	8 pcf	Dynasil	0.128	32 bit	A11 = 0.7745 A13 = 30.15 A50 = 1. A12 = -4.404 A20 = 0.0752 A72 = 70.37	0.001	0.0001
Molybdenum		Molybdenum	10.2	Cruneisen	C = 0.5143 S2 = 0 γ_0 = 1.59 S1 = 1.255 S3 = 0 a = 0.30	1.25	0.0093
Iridium		Iridium	22.484	Gruneisen	C = 0.3916 S2 = 0 γ_0 = 0 S1 = 1.457 S3 = 0 a = 0	0.81	0.0055
Graphite		Graphite	1.98	Gruneisen	C = 0.39 S2 = 1.54 γ_0 = 0.24 S1 = 2.16 S1 = -9.43 a = 0	0.02	0.0001
Air and Argon		Air	0.001195	JWL (Gamma law)	A = 0 W = 0.4 B = 0 E_0 = 2.533E-06	0	0
Uranium Dioxide		Uranium Dioxide	10.5	32 bit	A11 = 1.638 A21 = 1.545 A31 = 0.1662 A12 = 0.00371 A22 = 3.243 A32 = 0.02028 A13 = 0.03645 A23 = 0.0002098 A50 = 0.77255 A20 = 0.3445 A30 = 1.261 A60 = 1. A70 = -70.37	0.365	0.0013
Fiberglass		Kevlar	1.538	Polynomial	A0 = 0 A2 = 0.369 B0 = 0.783 A1 = 0.197 A3 = 0.197 B1 = 0.783 B2 = 0	0.18	0.0103
Balsa		Polyurethane	0.192	Polynomial	A0 = 6.205E-5 A2 = 0 B0 = 0.4 A1 = 0 A3 = 0 B1 = 0.4 B2 = 0.	0.01	0.0001

No material was allowed to fracture

TABLE B2.2-4 Materials Data for Direct Course Calculations

RUN NO.	DESCRIPTION	ANFO PEAK PRESS Kb	ANFO CASE VEL mm/μs	AIR PRESS AT RTG Kb	ANFO CASE ΔV mm/μs	RTG RESPONSE PEAKS				REMARKS
						AL ΔV mm/μs	AL PRESS Kb	GRAPHITE PRESS Kb	UO_2 PRESS Kb	
14A	Vacuum	47	4.6		5	3.3/-2	58/-42	186/-72	137/-114	3850 s 4200 s.
14						2.35	11.7	53	64	Coarse resolution output* 0-8000 s
15	Air	47	3.		3.95	.77	4.6	11	37.5	All remaining data is coarse resolution output.
16	V.+Air Blkt	47	4.6		6.4	1.8	18.8	104	36	UO_2 YS=0.1 Kb; Graphite YS = 1.3Kb;
21	12" fwd of RTG					1.95	18.8	46	31	UO_2 + Graphite YS = 10 Kb
23	ANFO + Case NO RTG			0.1245						Pressure at zone 135 extrapolated between profiles for zones 120 & 140
24	Gas, no case	12		0.1100		.5	2.6	2.8	5.6	RTG present. Pressure radius ratioed from early time profile.

* Coarse Resolution outputs are absolute (+ or -) peak values.

TABLE B2.2-5 Summary of Hydrocode Calculation Results for Direct Course Calculations.

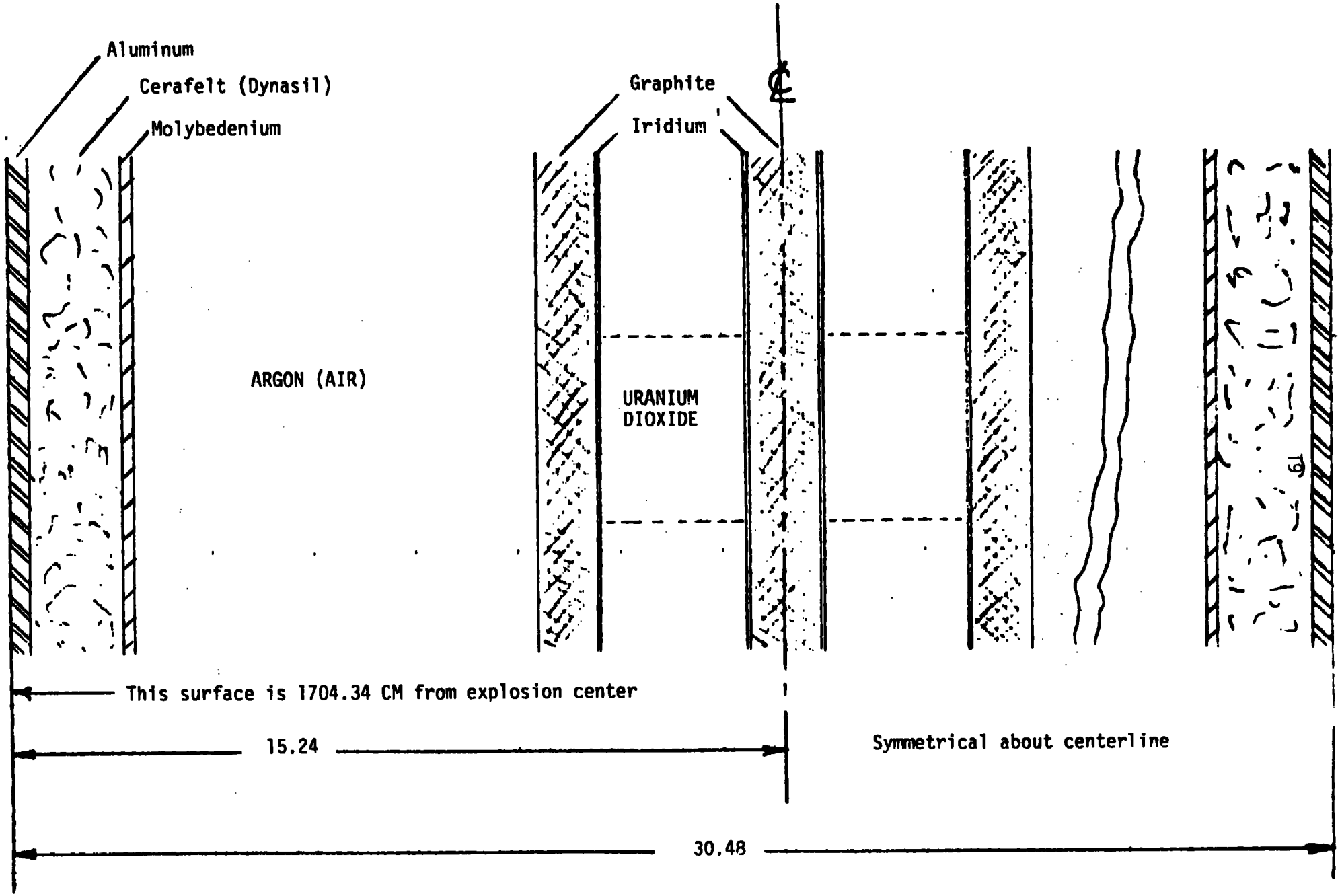

Figure B2.2-1 1D Layered (flyer plate) Model of RTG for Direct Course Calculations.

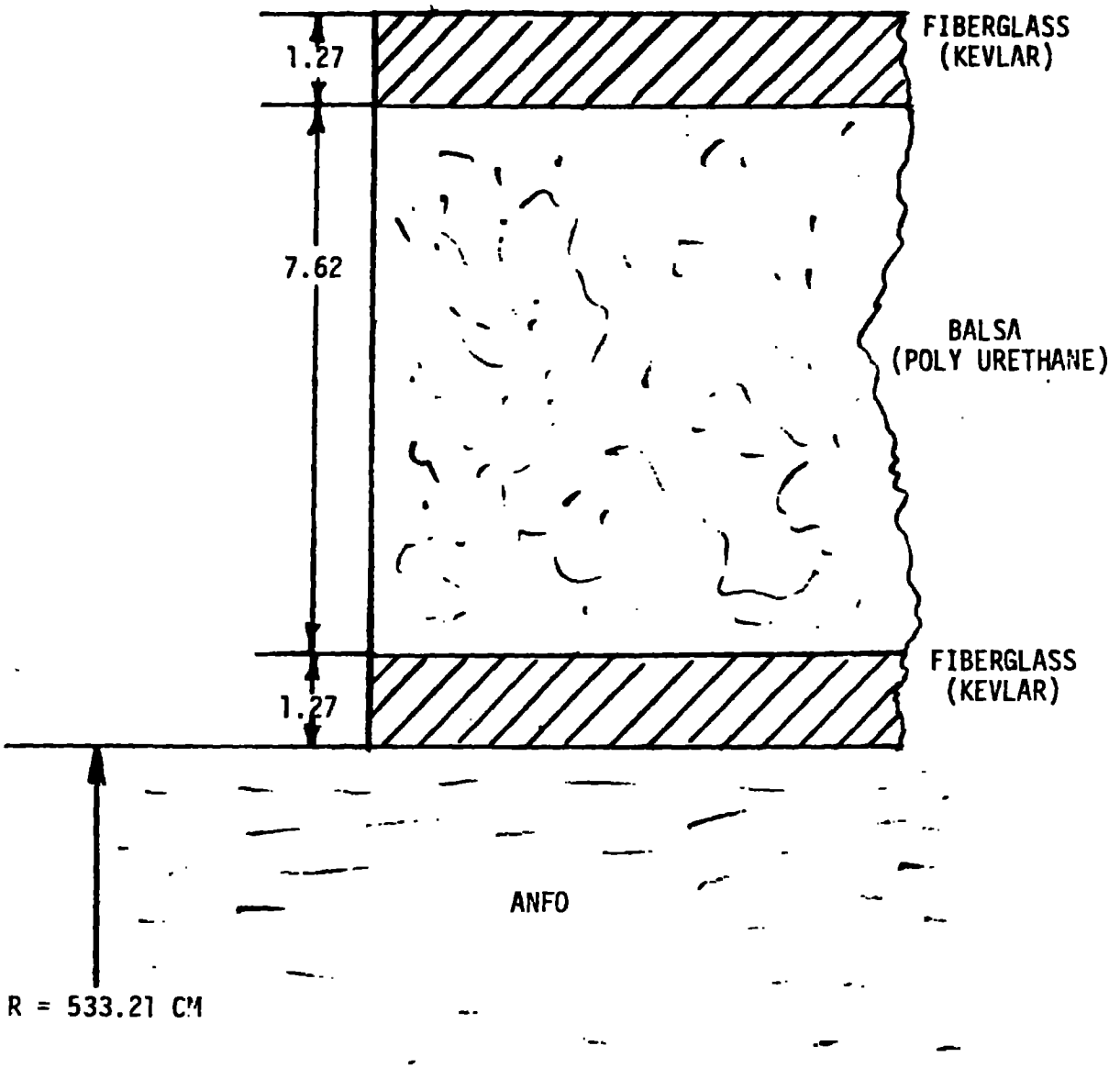

Figure B2.2-2 Spherical Model of ANFO and ANDO case for Direct Course Calculations

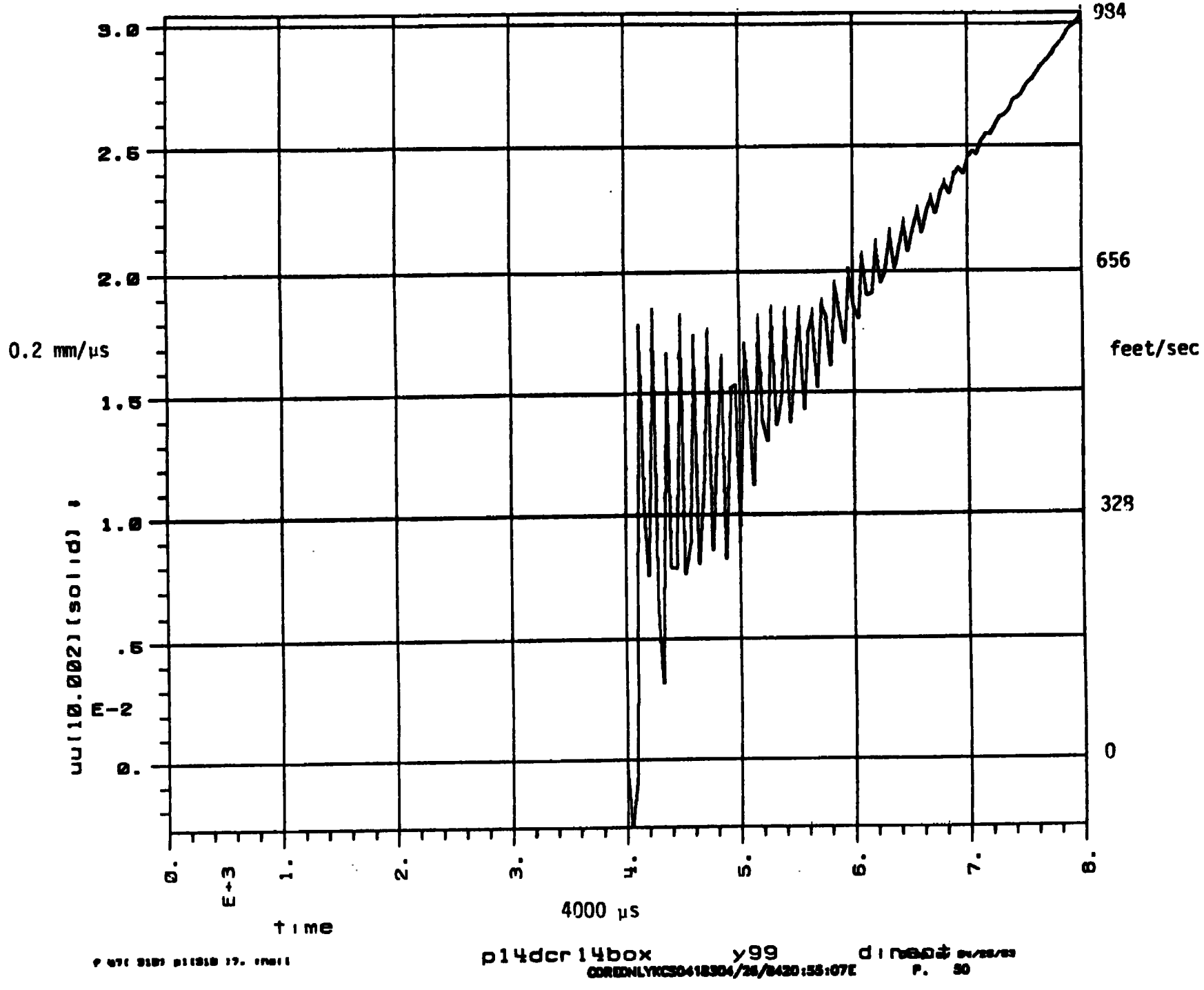

Figure B2.2-3 Uranium Dioxide velocity versus time coarse resolution.

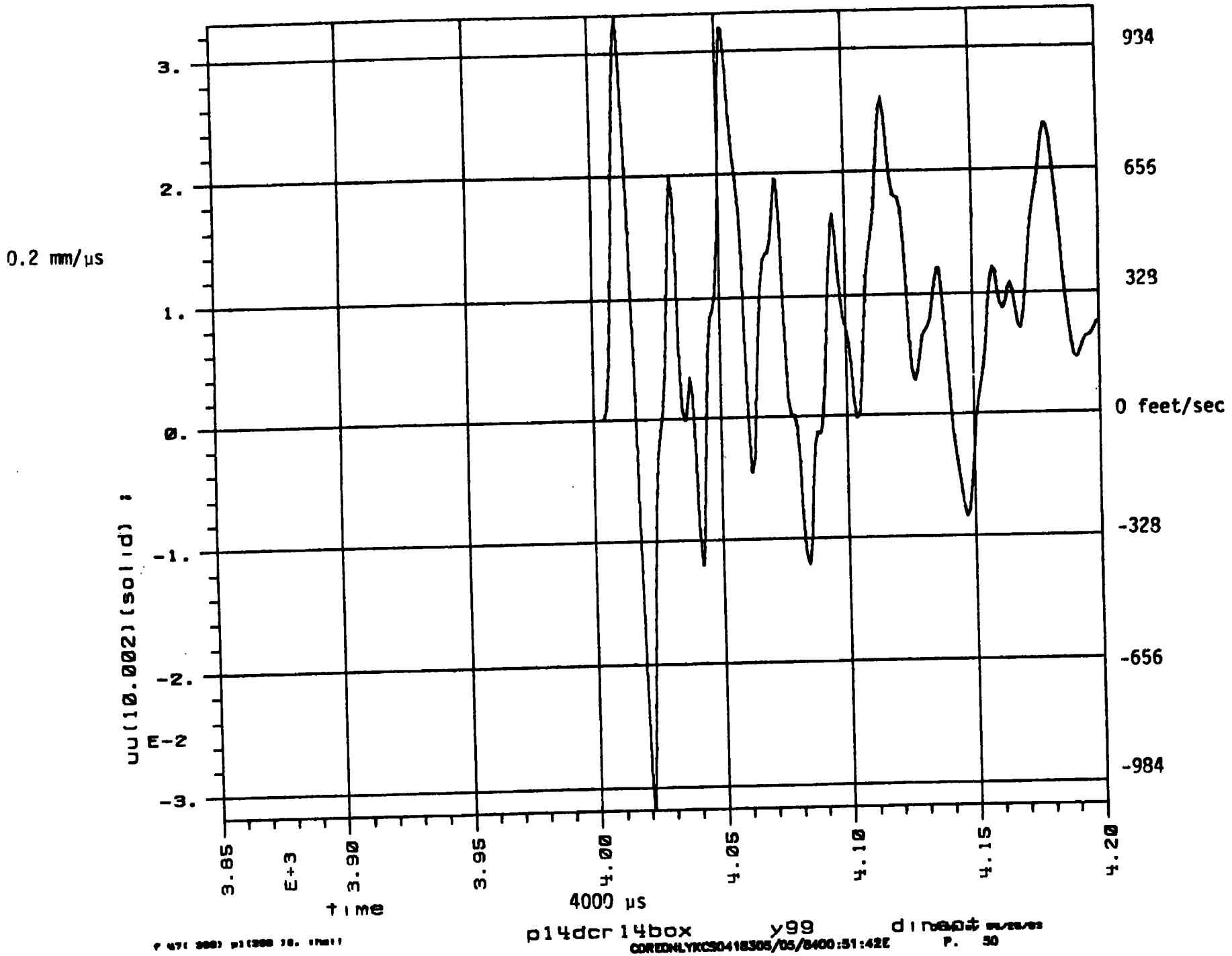

Figure B2.2-4 Uranium Dioxide velocity versus time, fine resolution

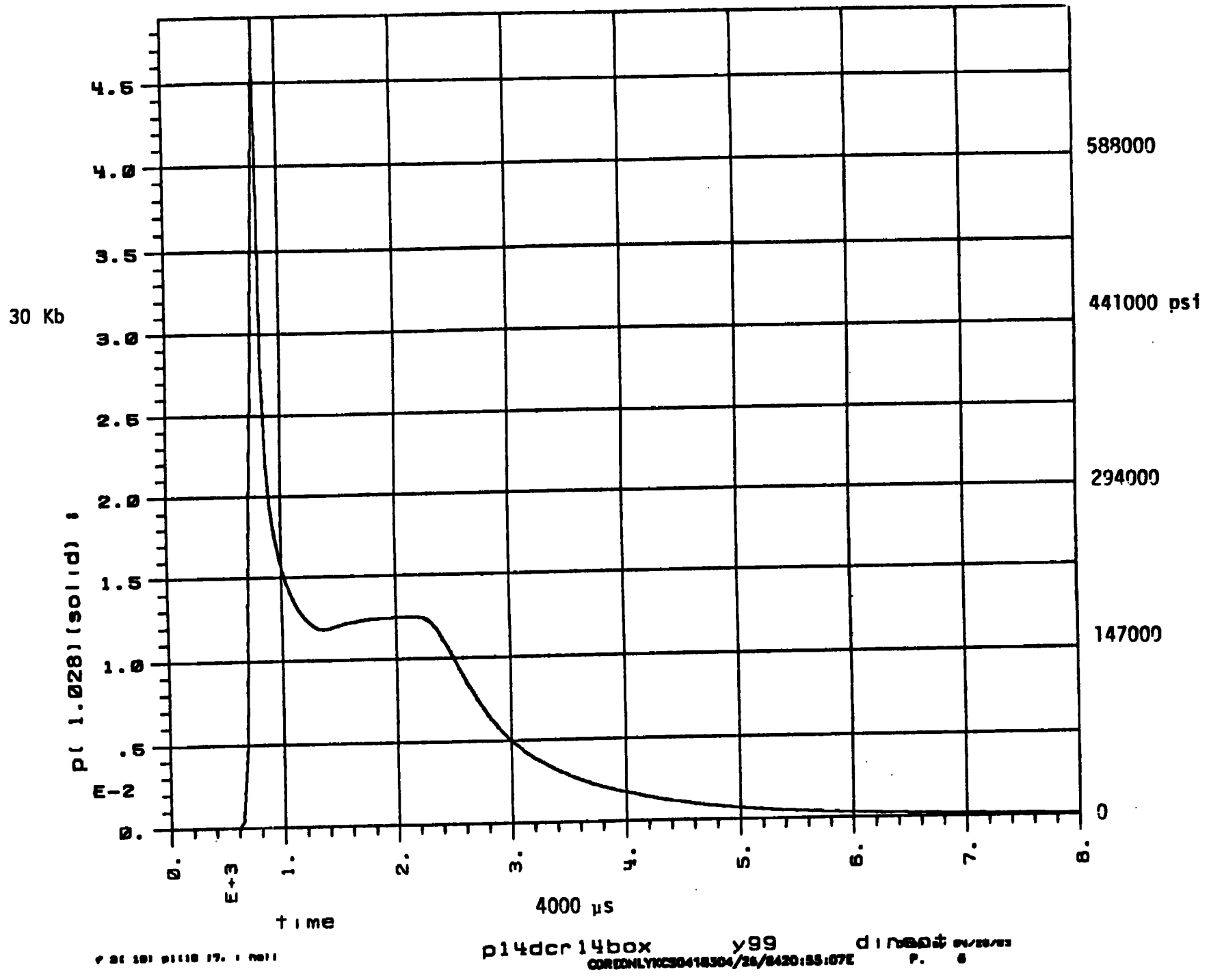

Figure B2.2-5 Middle zone ANFO pressur versus time, coarse resolution.

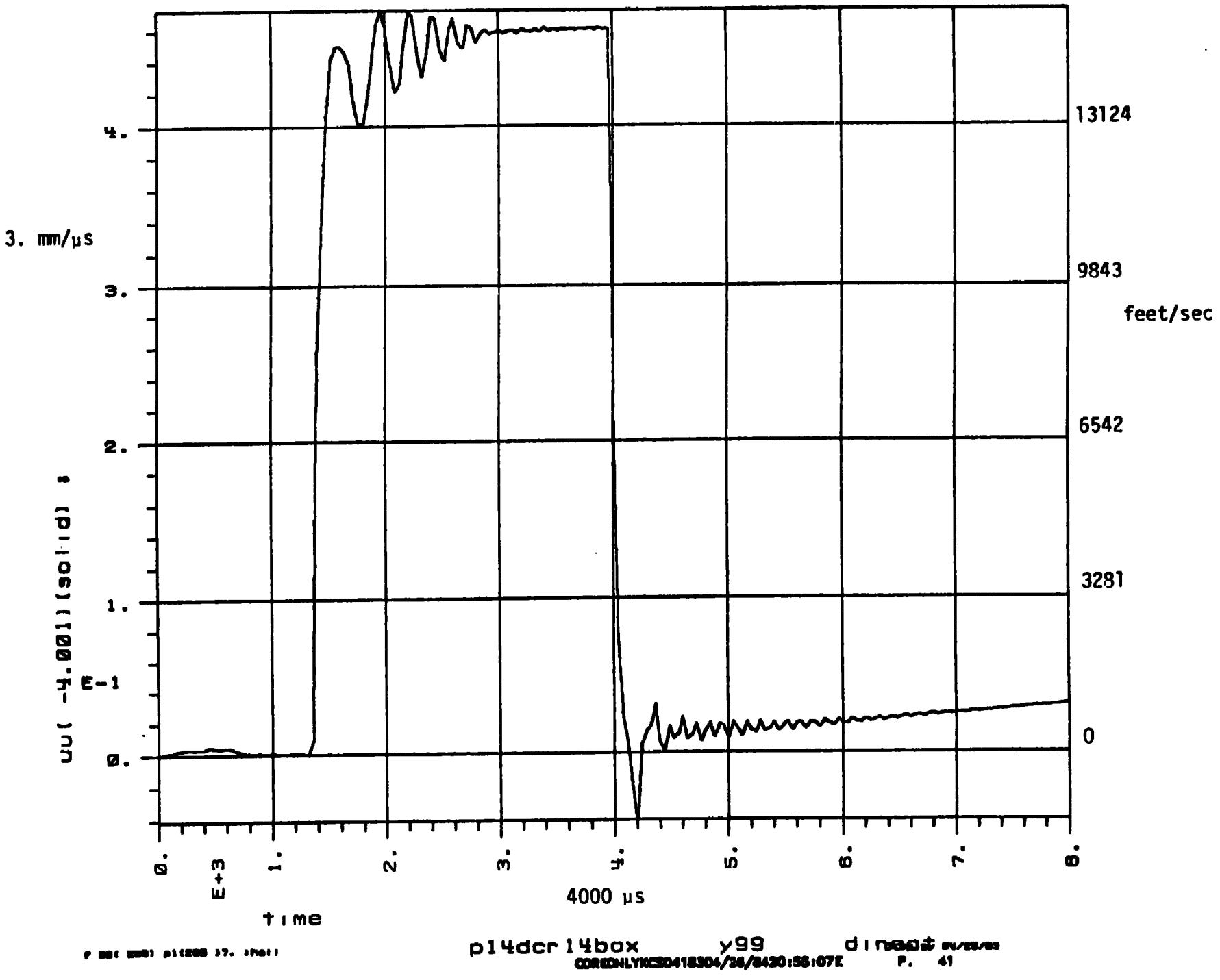

Figure B2.2-6 Outer ANFO case velocity versus time, coarse resolution.

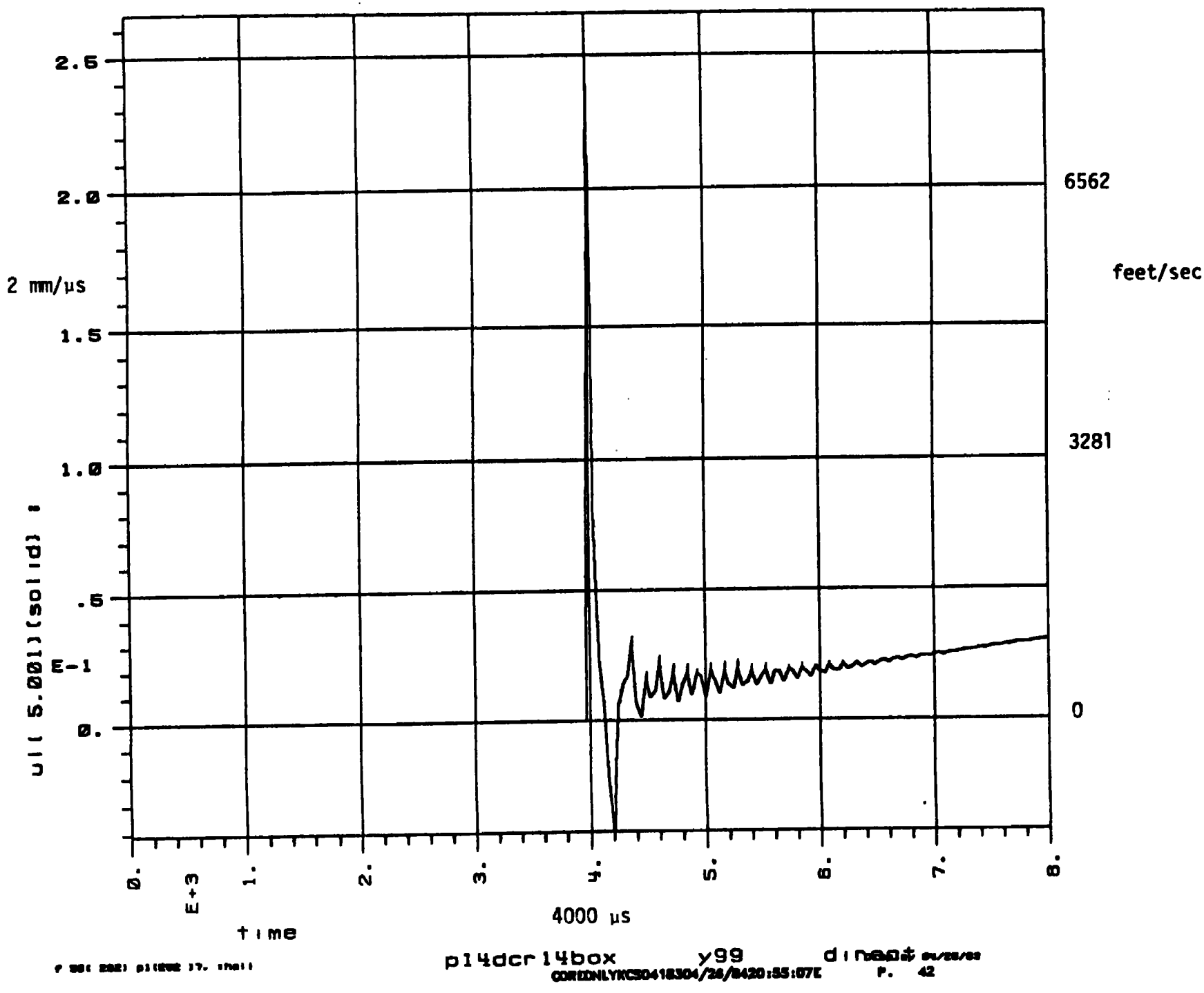

Figure B2.2-7 RTG Aluminum case velocity versus time, coarse resolution.

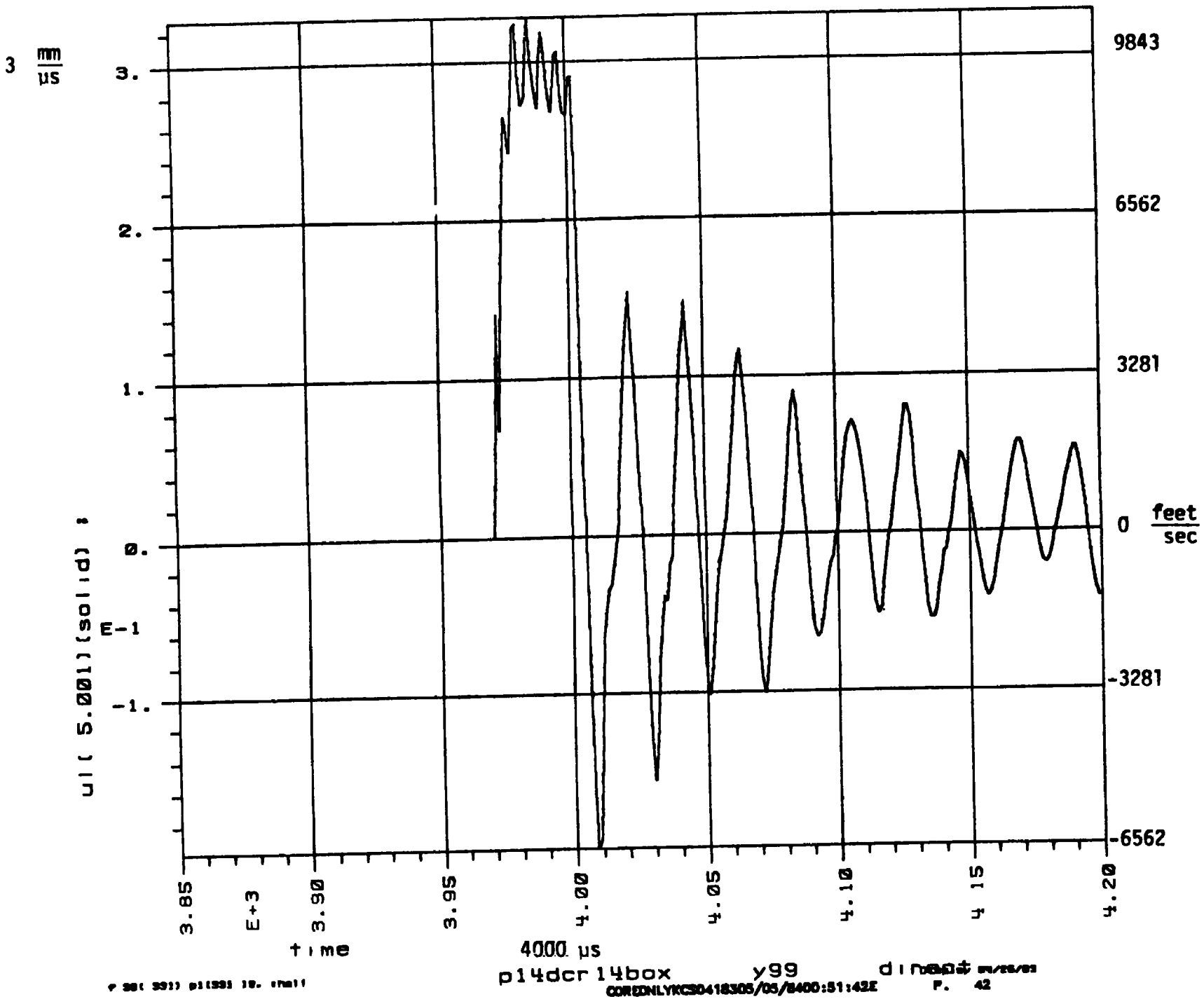

FIGURE B2.2-8 RTG ALUMINUM CASE VELOCITY VERSUS TIME, FINE RESOLUTION

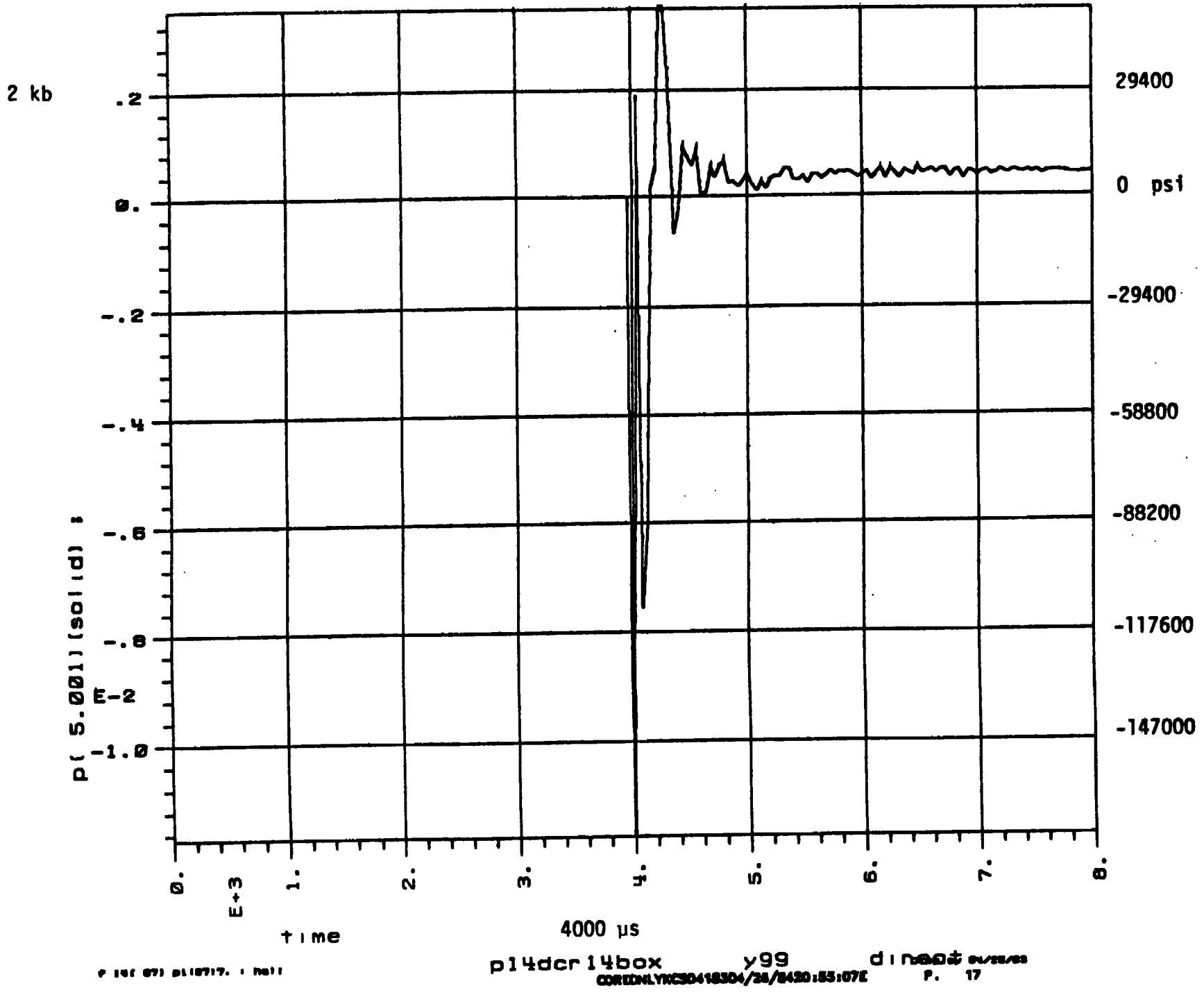

FIGURE B2.2-9 RTG ALUMINUM CASE PRESSURE VERSUS TIME, COARSE RESOLUTION

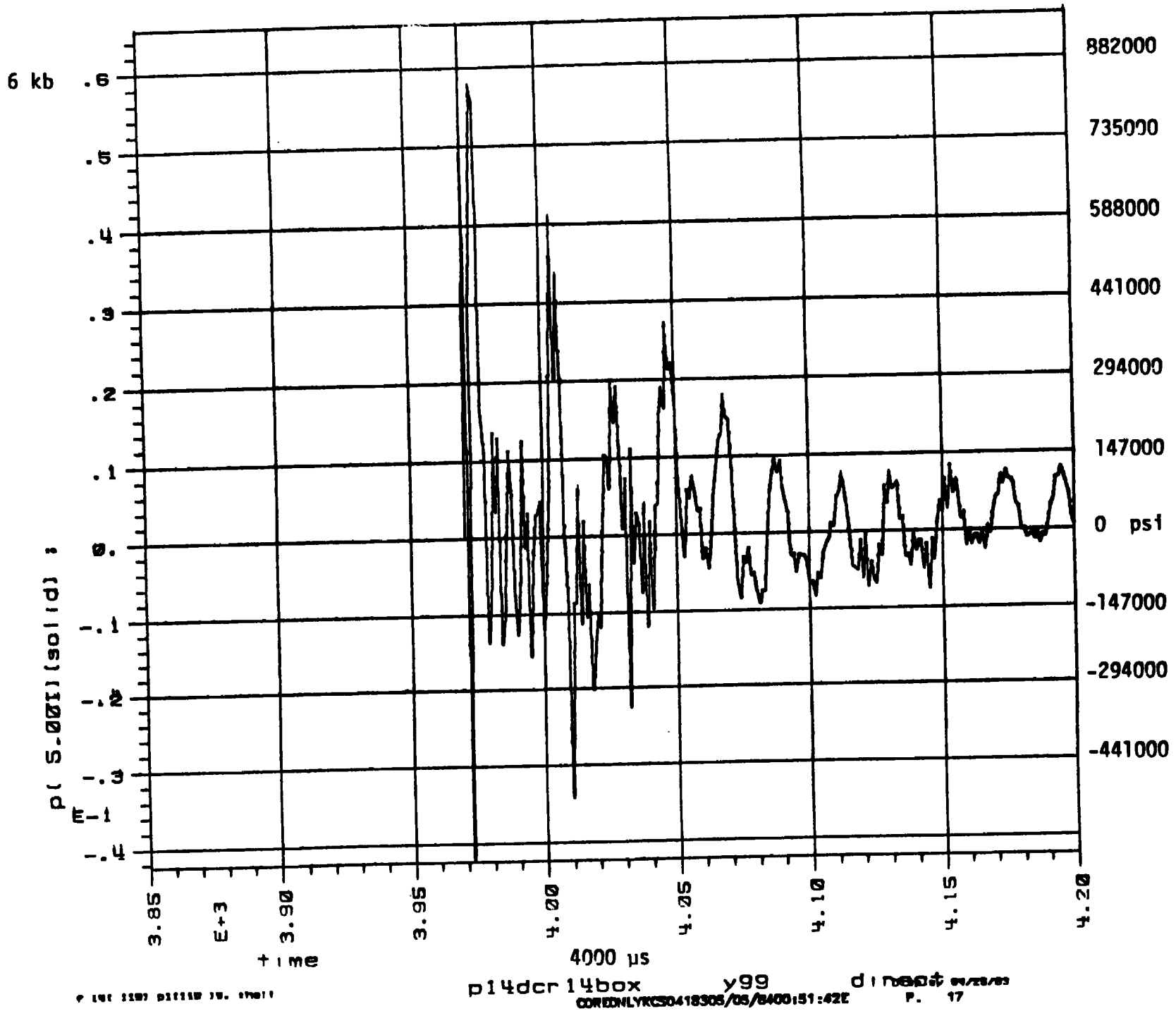

FIGURE B2.2-10 RTG ALUMINUM CASE PRESSURE VERSUS TIME, FINE RESOLUTION

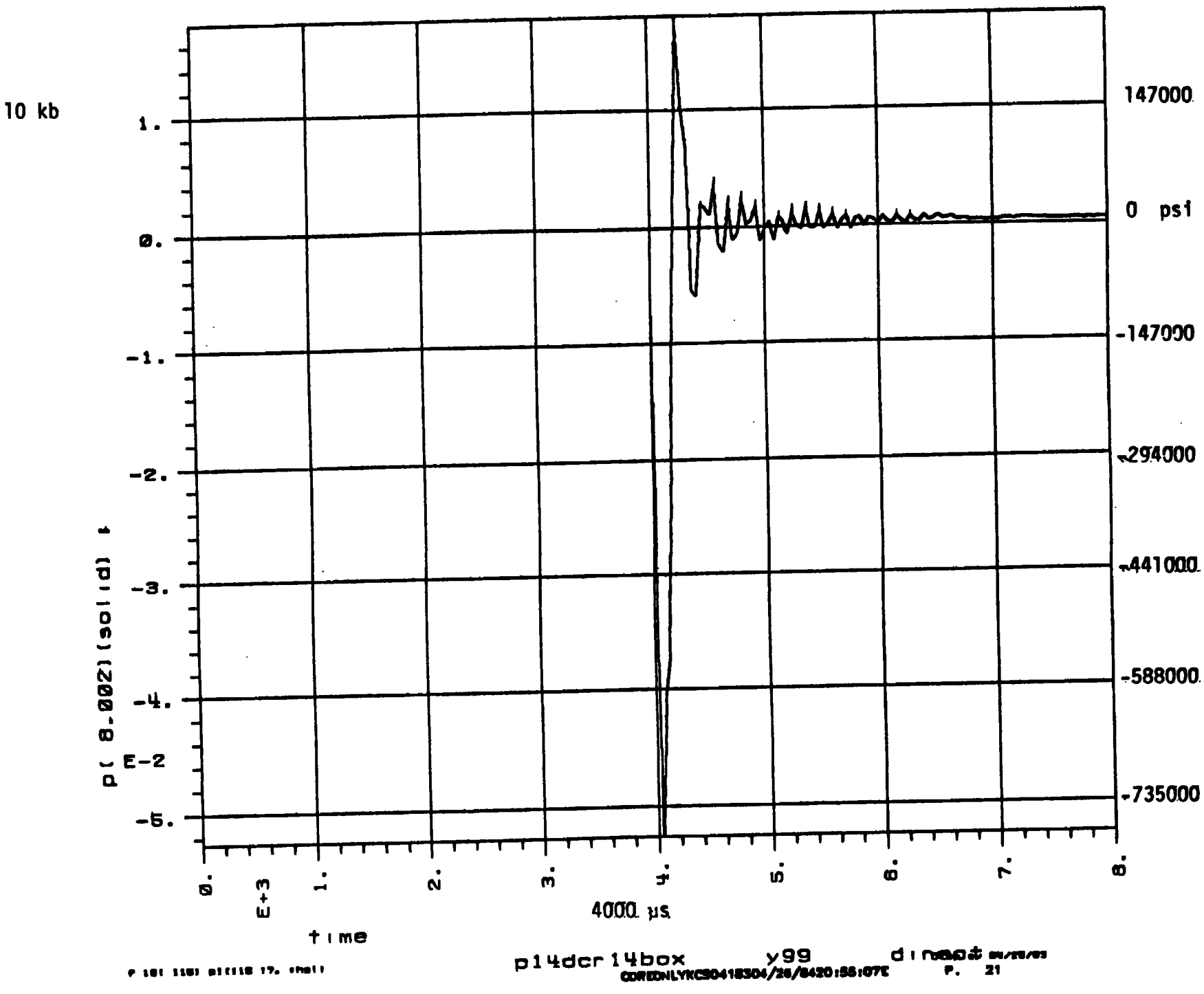

FIGURE B2.2-11 RTG GRAPHITE PRESSURE VERSUS TIME, COARSE RESOLUTION

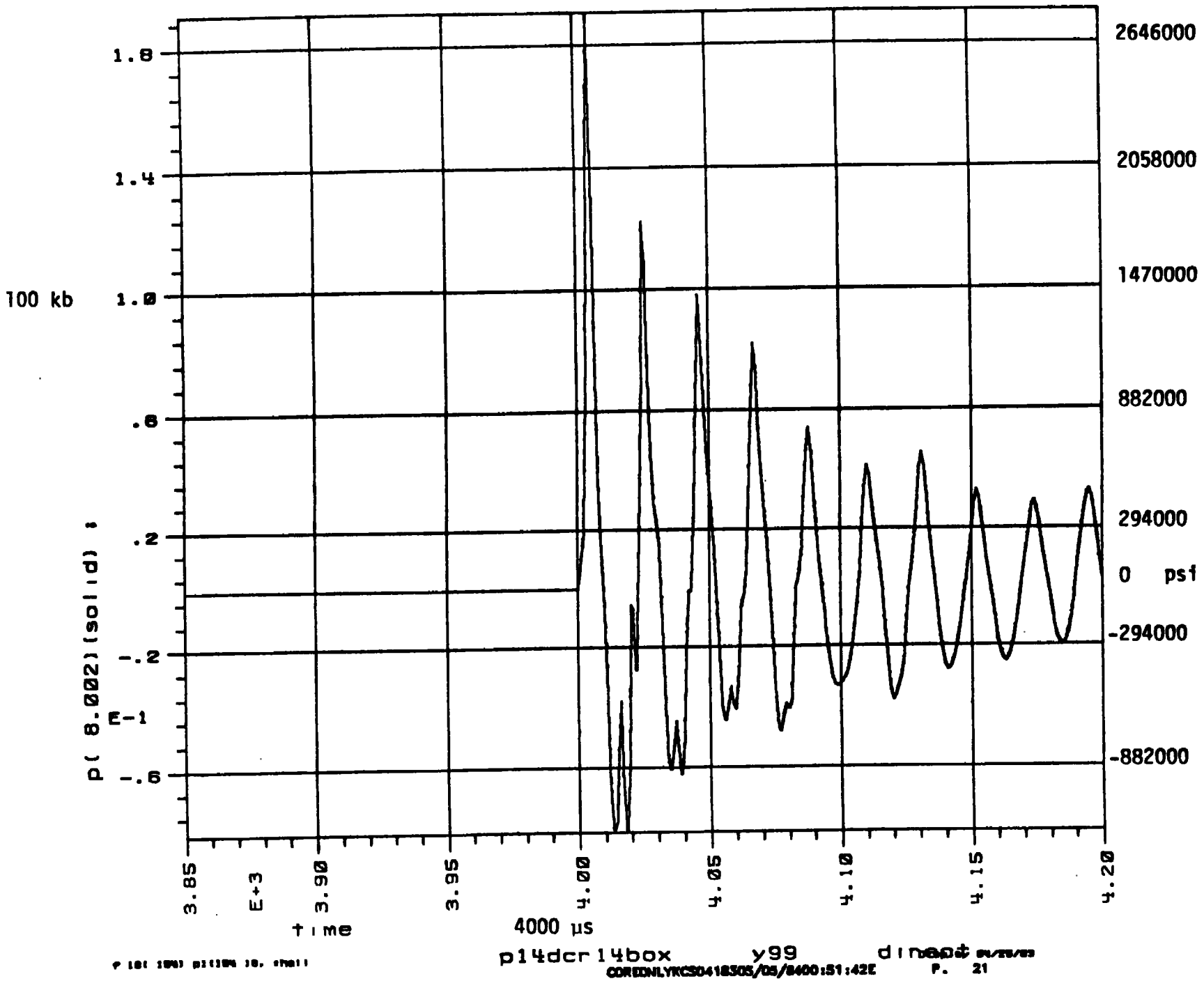

FIGURE B2.2-12 RTG GRAPHITE PRESSURE VERSUS TIME, FINE RESOLUTION

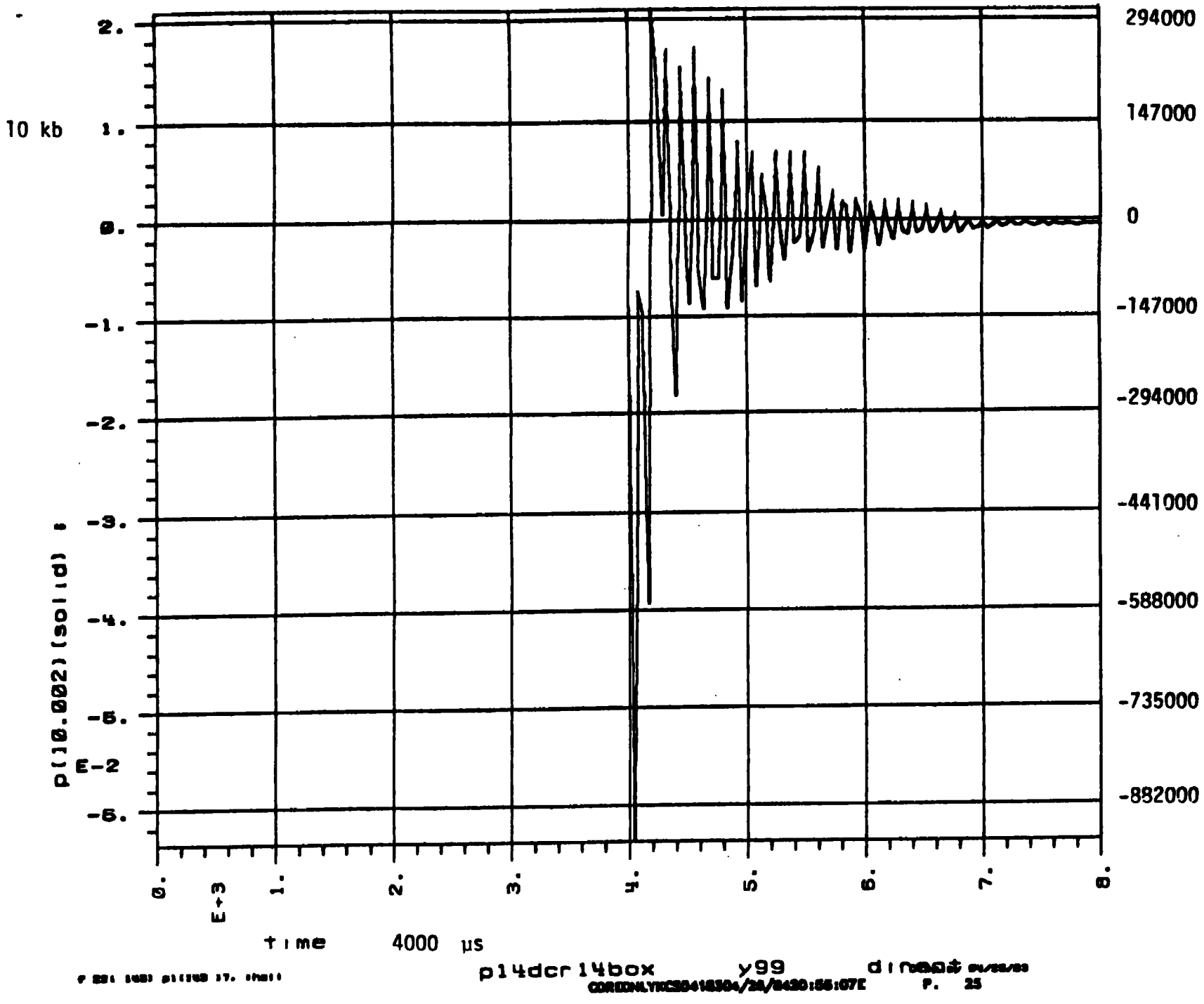

FIGURE B2.2-13 RTG URANIUM DIOXIDE PRESSURE VERSUS TIME, COARSE RESOLUTION

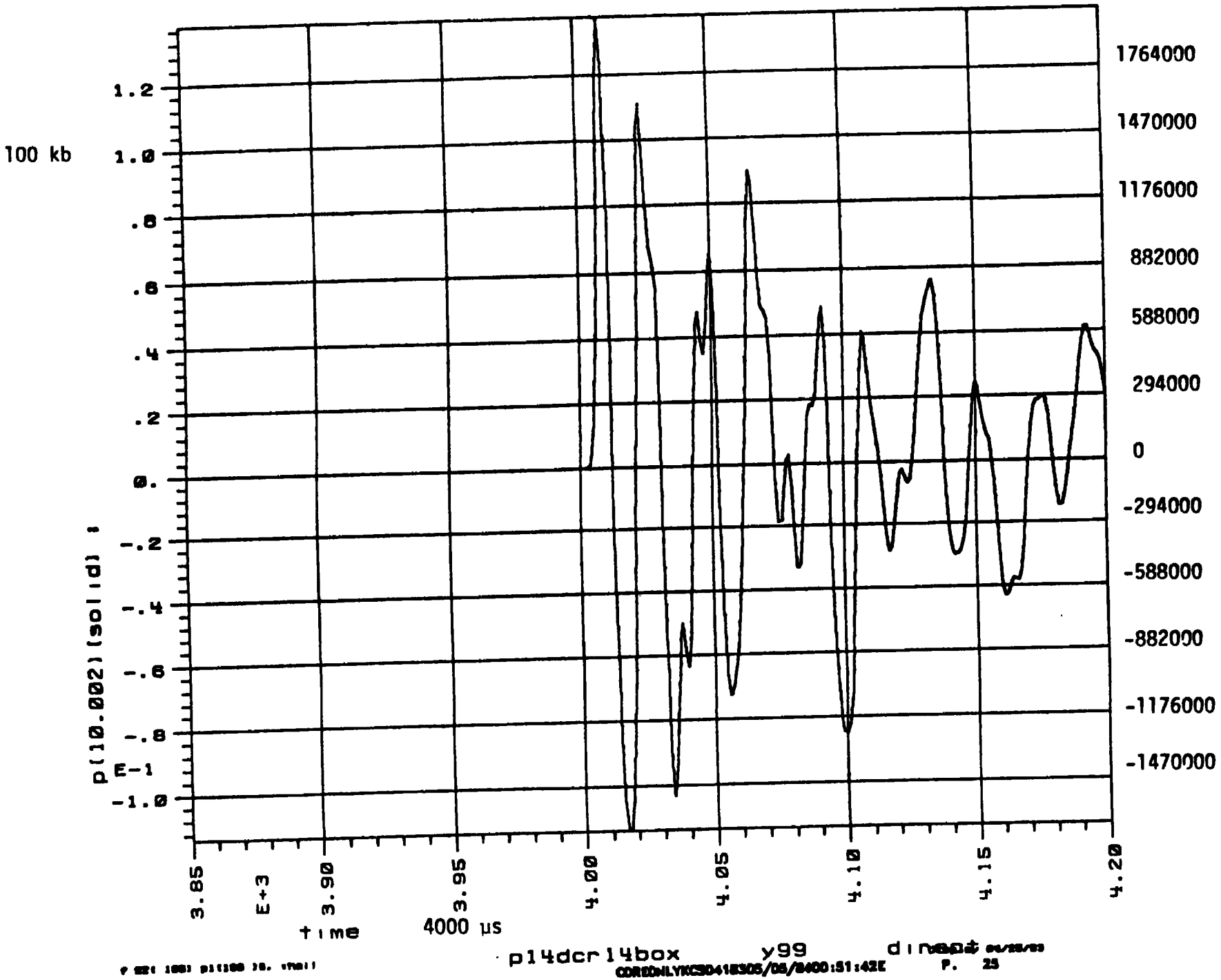

FIGURE B2.2-14 RTG URANIUM DIOXIDE PRESSURE VERSUS TIME, FINE RESOLUTION

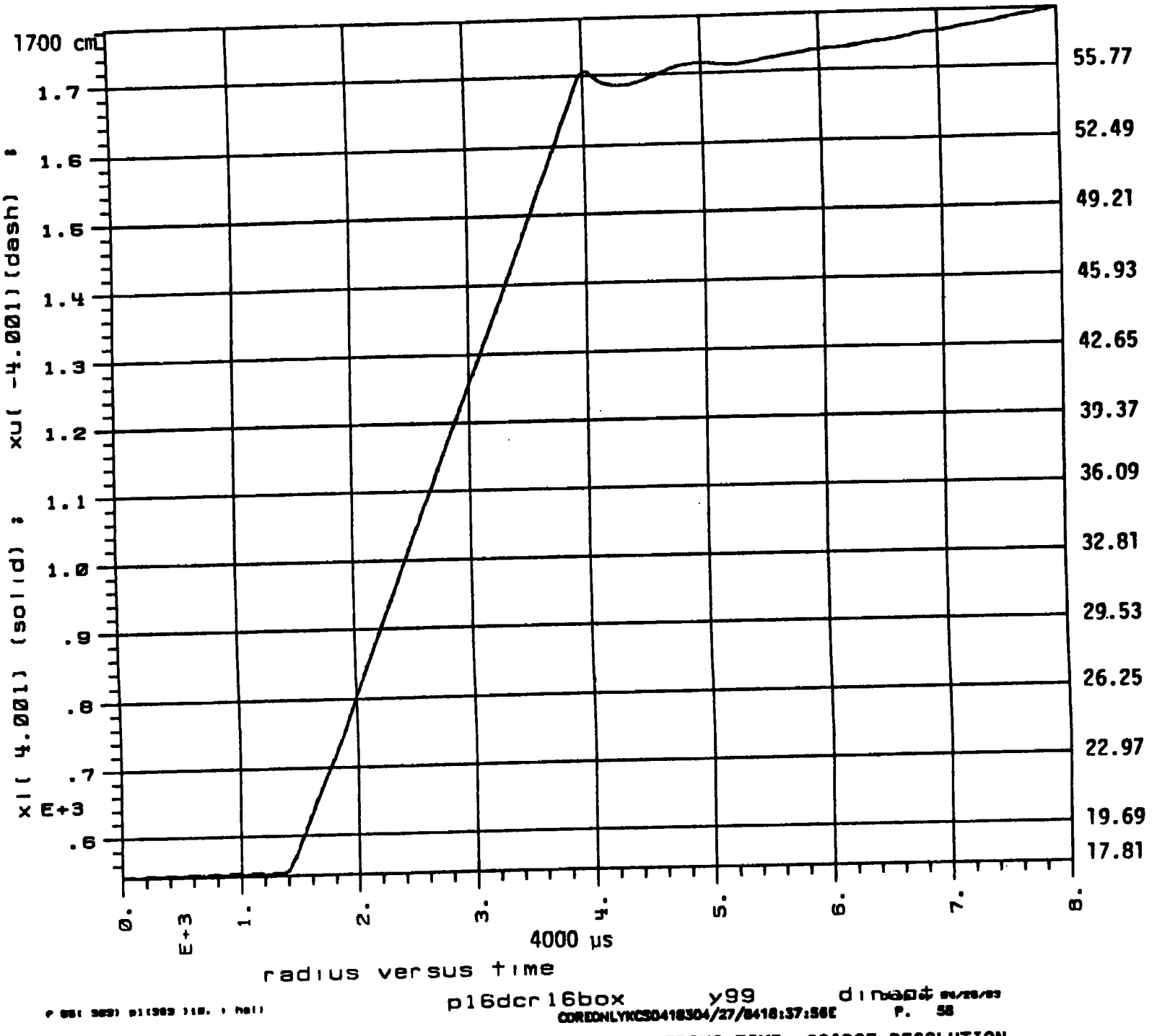

FIGURE B2.2-15 OUTER ANFO CASE POSITION VERSUS TIME, COARSE RESOLUTION

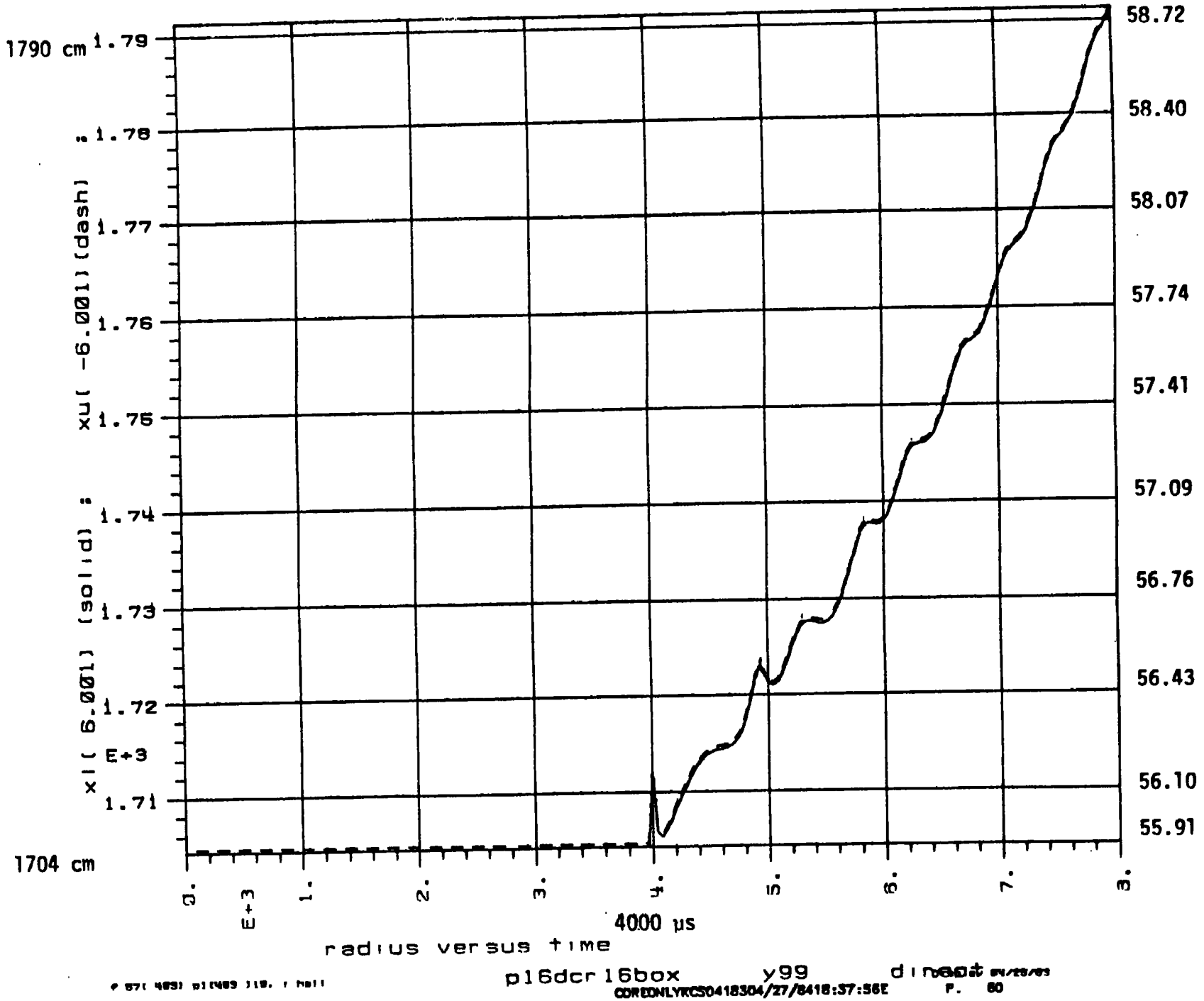

FIGURE B2.2-16 RTG ALUMINUM CASE POSITION VERSUS TIME, COARSE RESOLUTION

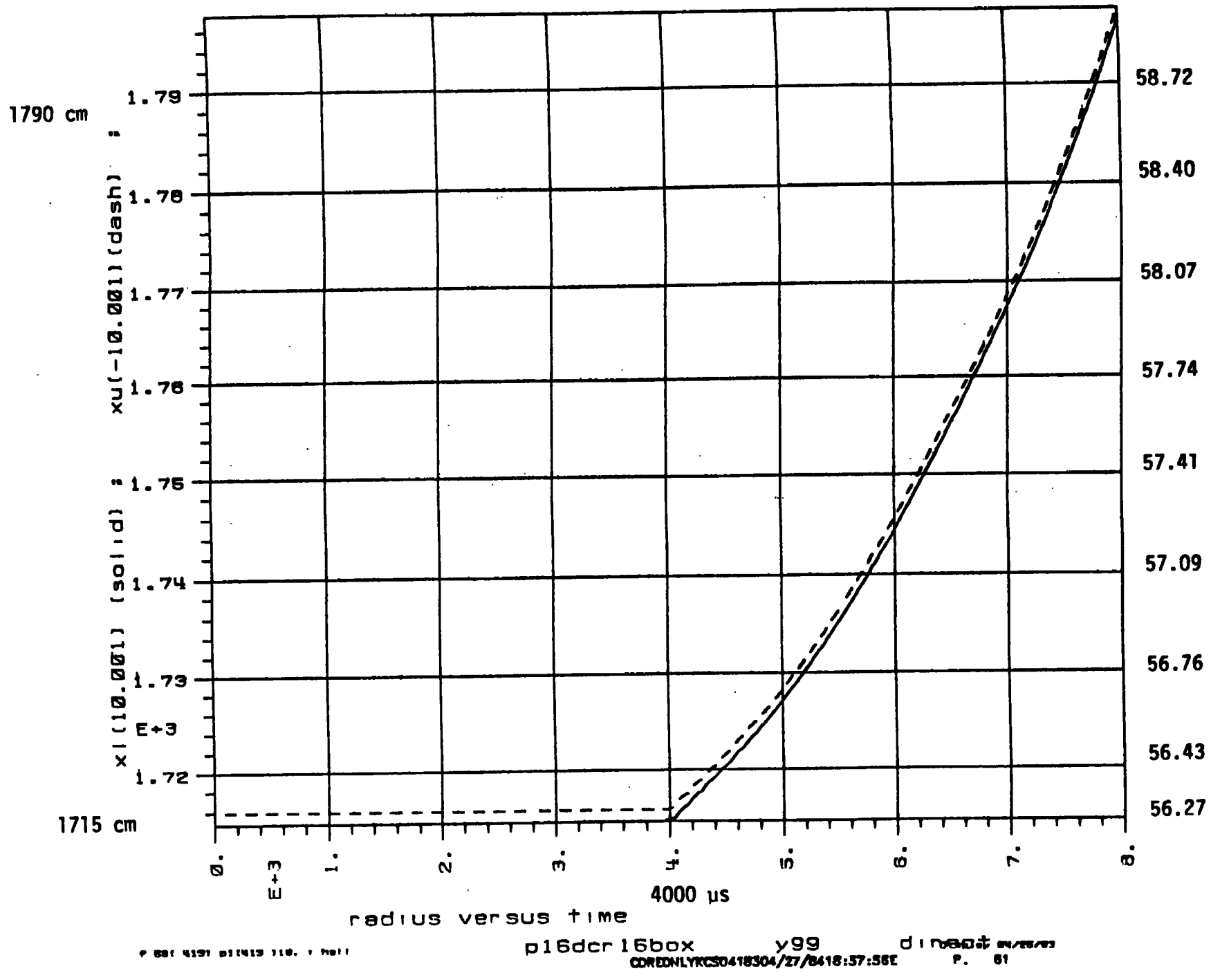

FIGURE B2.2-17 RTG RAPHITE POSITION VERSUS TIME, COARSE RESOLUTION

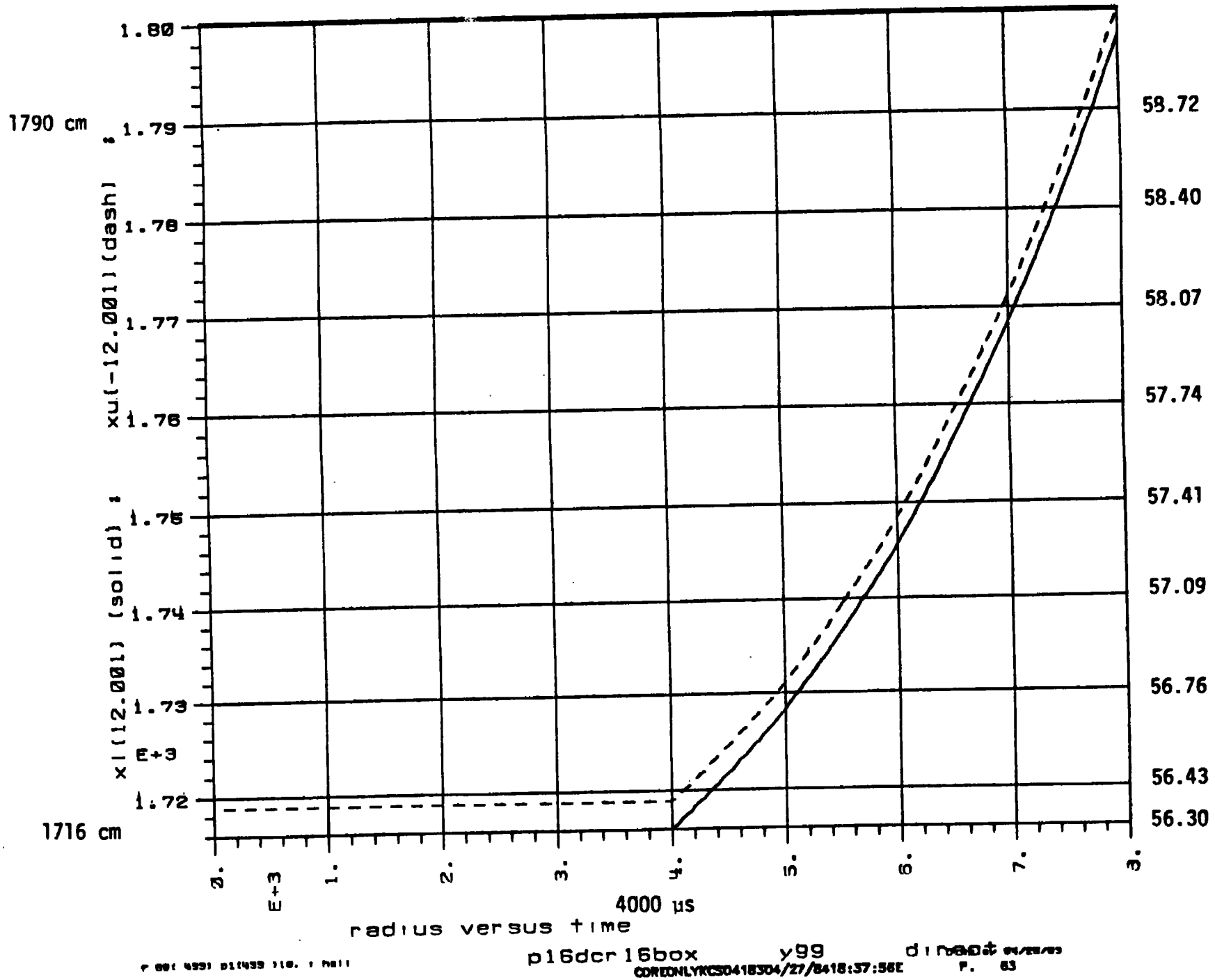

FIGURE B2.2-18 RTG URANIUM DIOXIDE POSITION VERSUS TIME: COARSE RESOLUTION

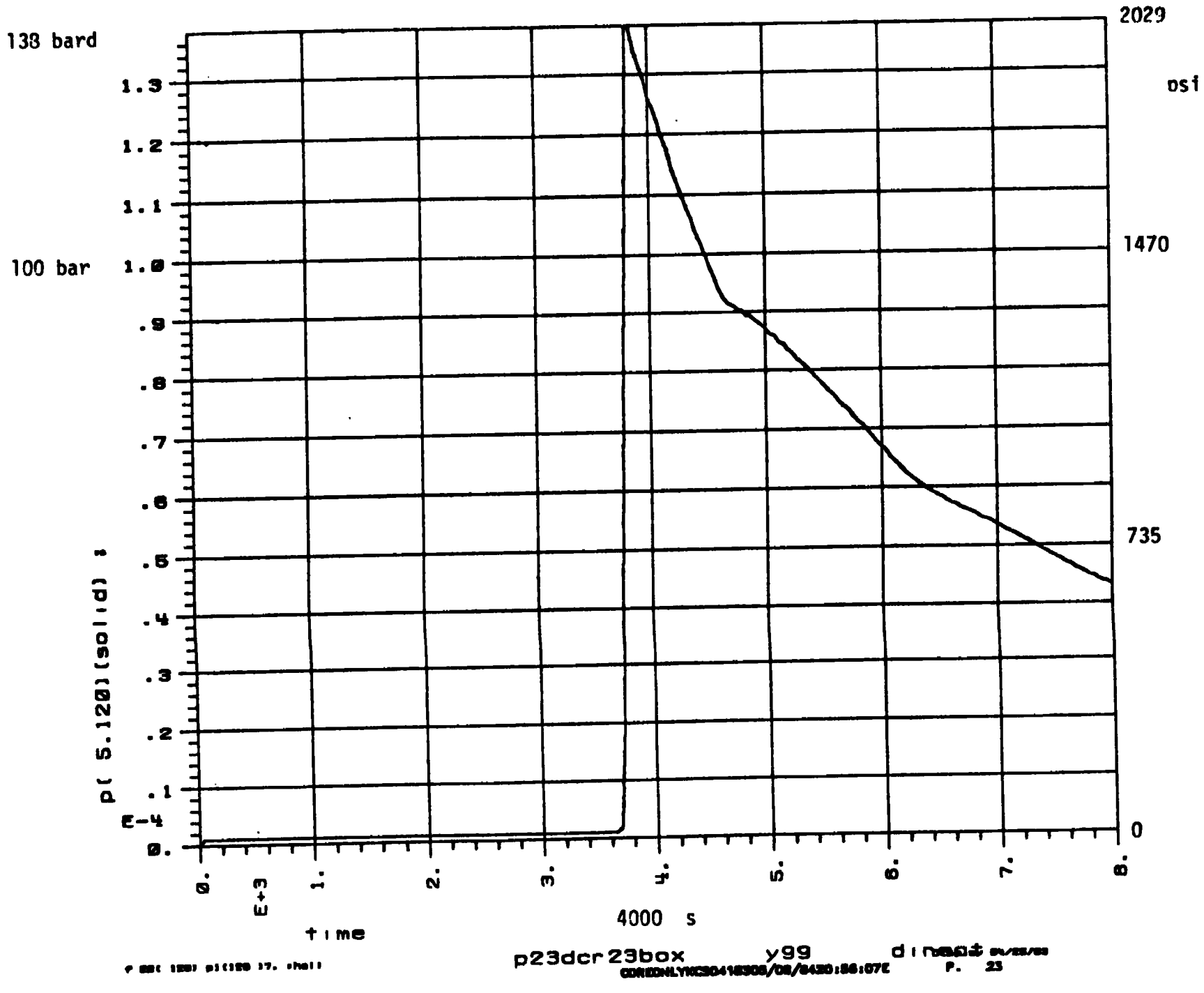

Figure B2.2-19 Free field overpressure peak forward of RTG radius.

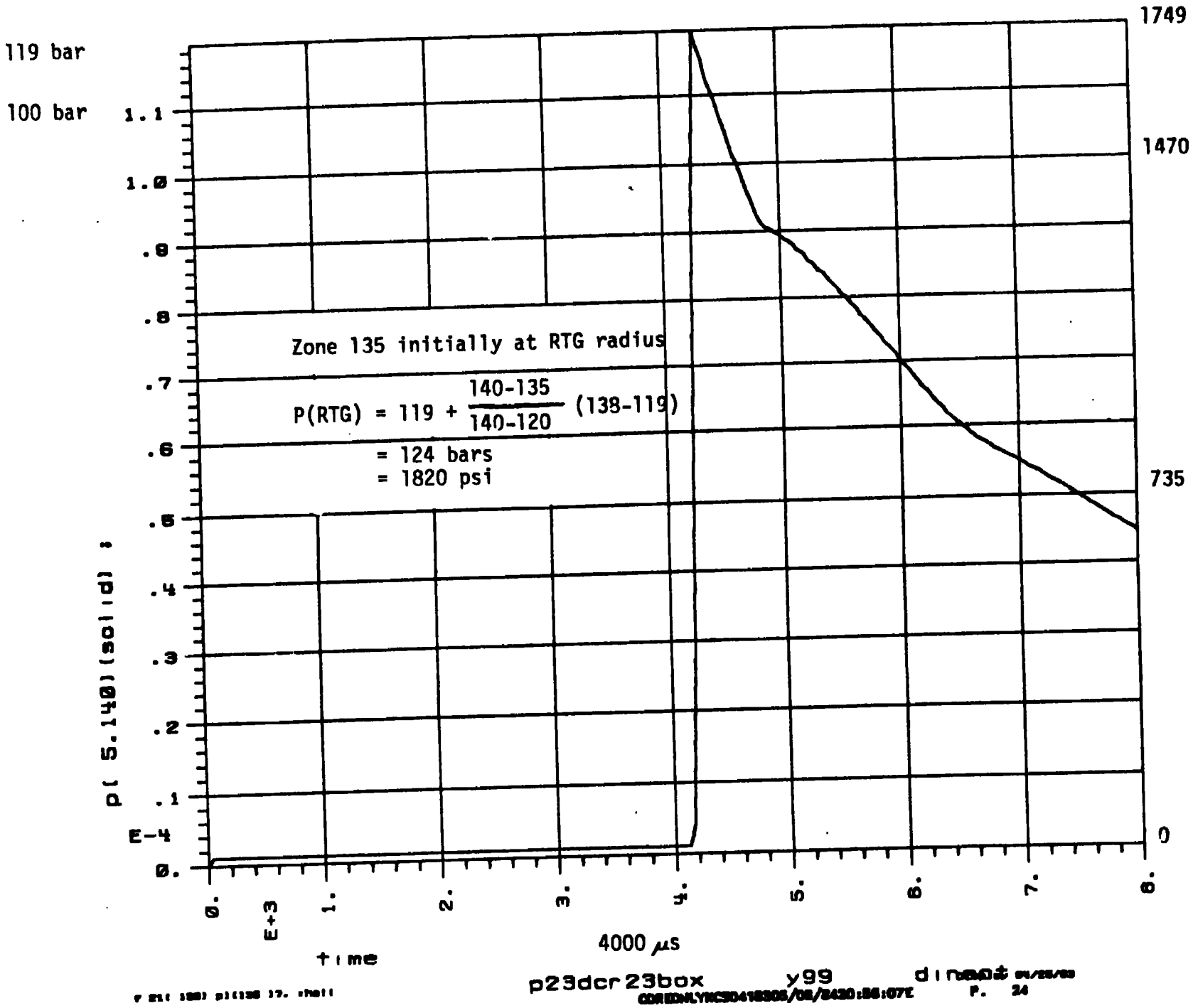

Figure B2.2-20 Free field overpressure peak behind RTG radius.

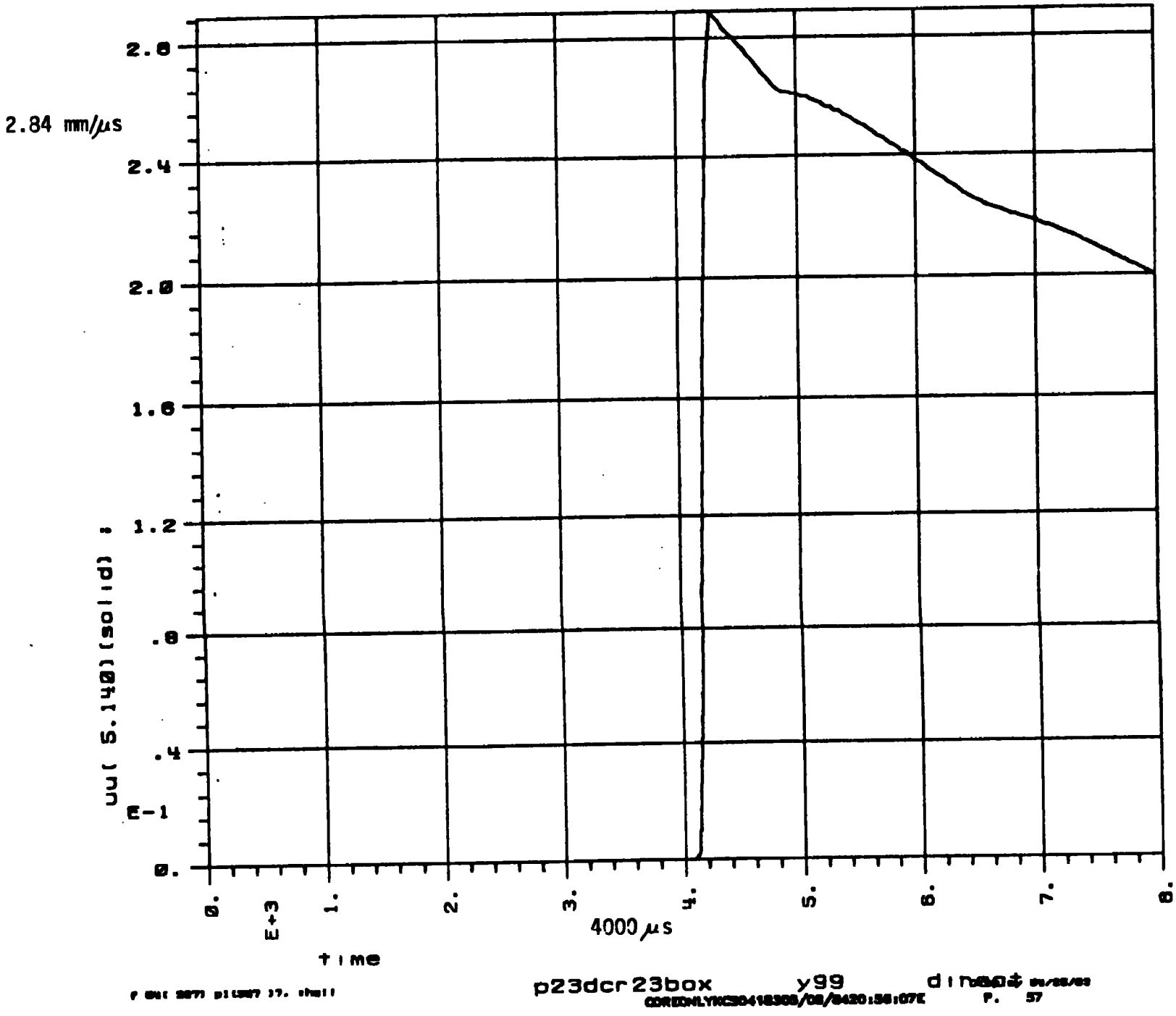

Figure B2.2-21 Free field particle velocity near RTG

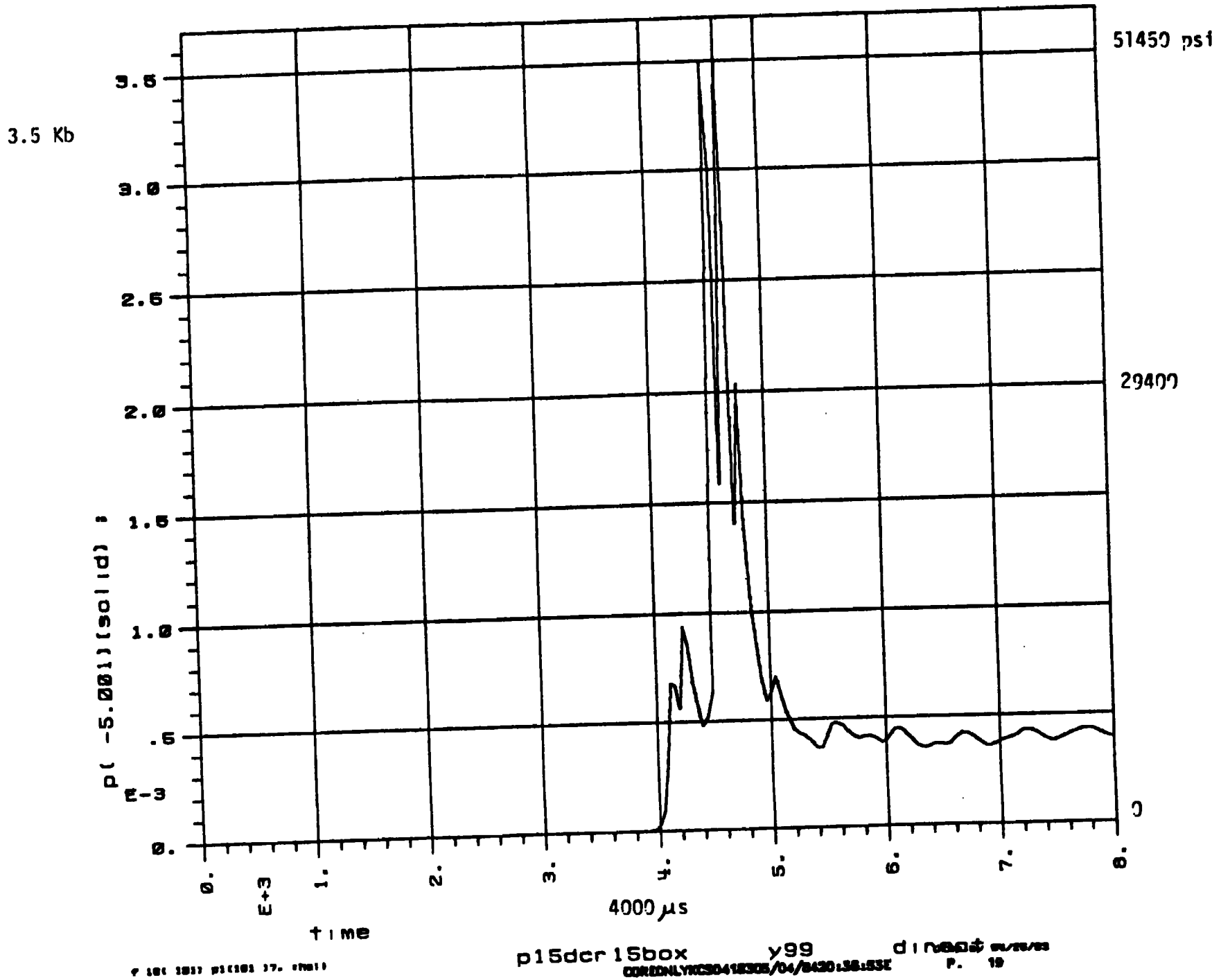

Figure B2.2-22 Air pressure vs. time on RTG surface, ANFO + case with air

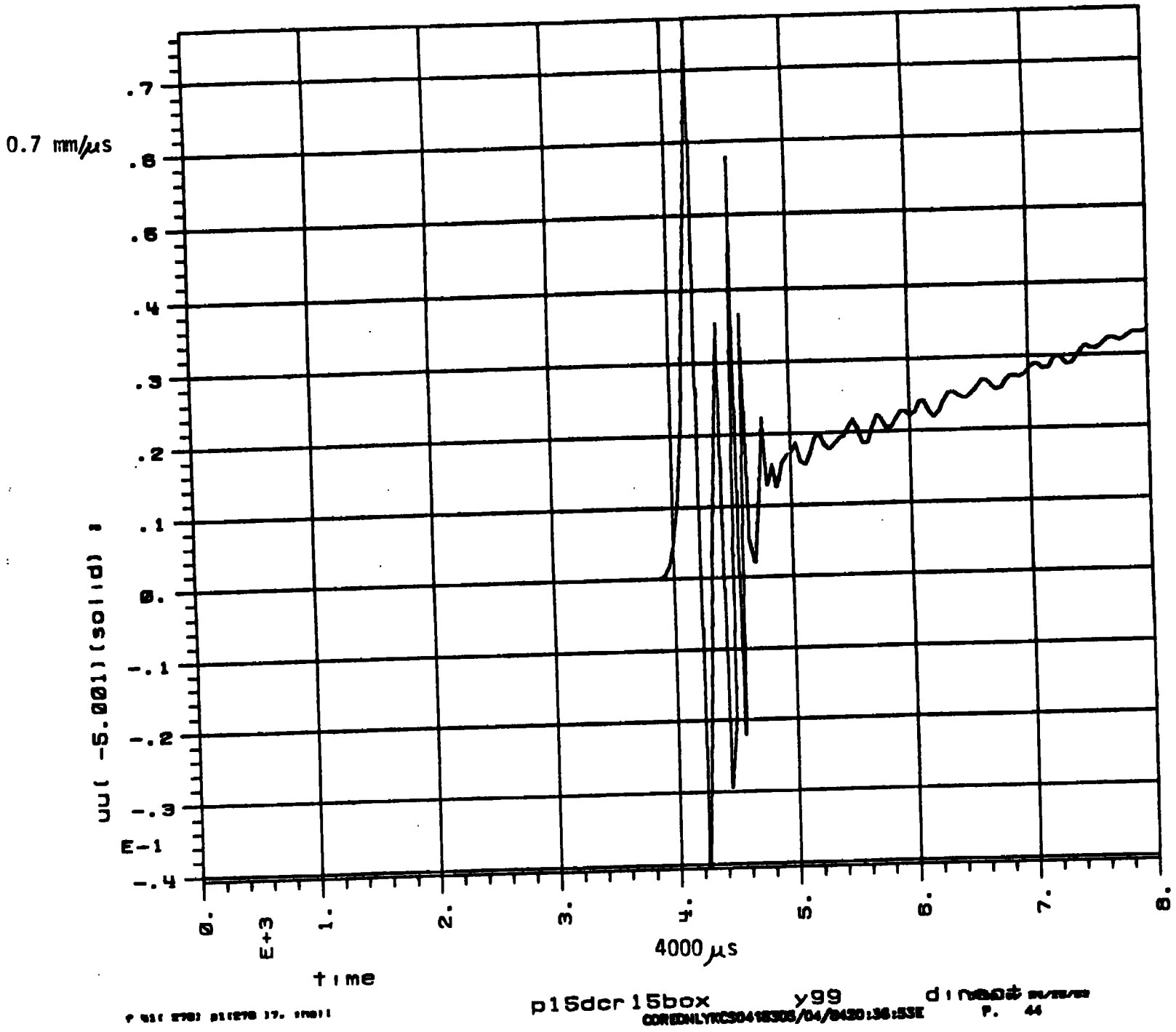

Figure B2.2-23 Air velocity vs. time at RTG surface, ANFO + case with air

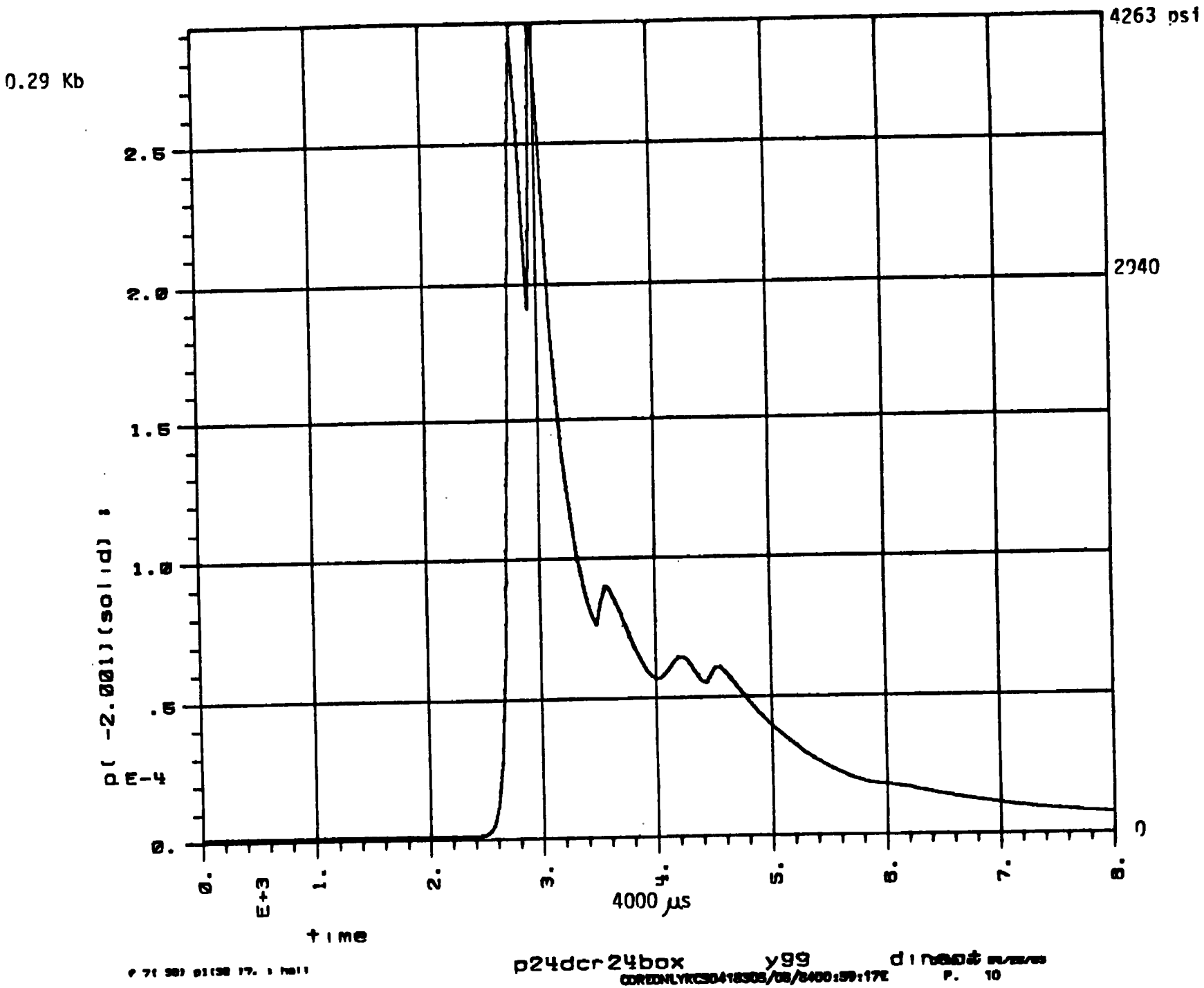

Figure B2.2-24 Air pressure vs. time on RTG surface, gas explosion, no case

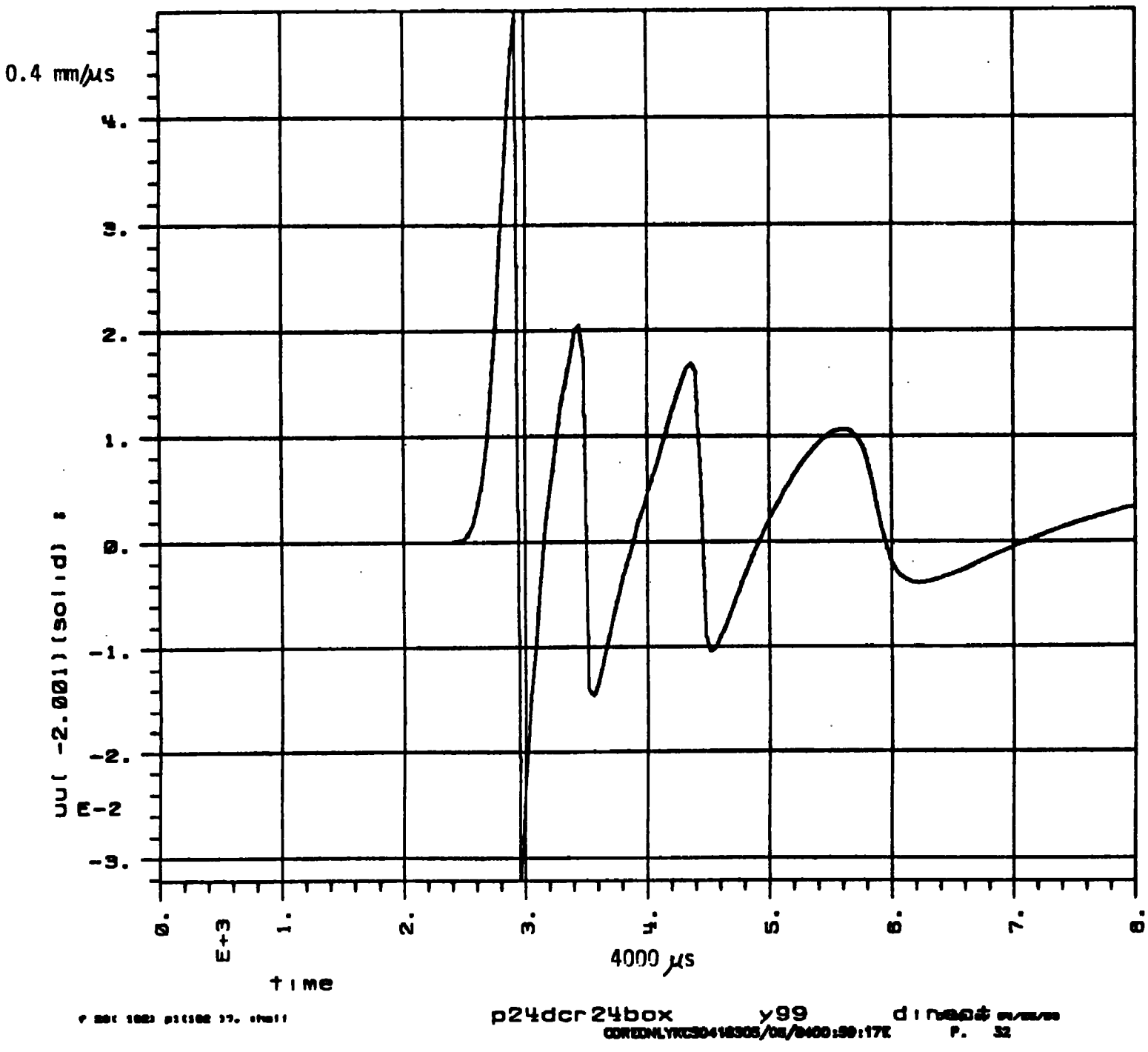

Figure B2.2-25 Air velocity vs. time at RTG surface, gas explosion, no case

DESCRIPTION	KOVEC EOS EOS NO.	THICKNESS CM	NO OF ZONES	CUMULATED DIMENSIONS CM
				0.0
GRAPHITE	73	1.1881	3	11.5691
IRIDIUM	79	0.070	1	11.6341
URANIUM DIOXIDE	95	2.833	3	14.4721
IRIDIUM	79	0.070	1	14.5421
GRAPHITE	73	1.2958	3	15.9379
IRIDIUM	79	0.070	1	16.0079
URANIUM DIOXIDE	95	2.833	3	18.8409
IRIDIUM	79	0.070	1	18.9109
GRAPHITE	73	1.1881	3	20.0990

TABLE B2.3-1 GPHS MODEL DIMENSIONS, ZONES, AND MATERIAL IDENTITY FOR SHOCK TUBE CALCULATIONS.

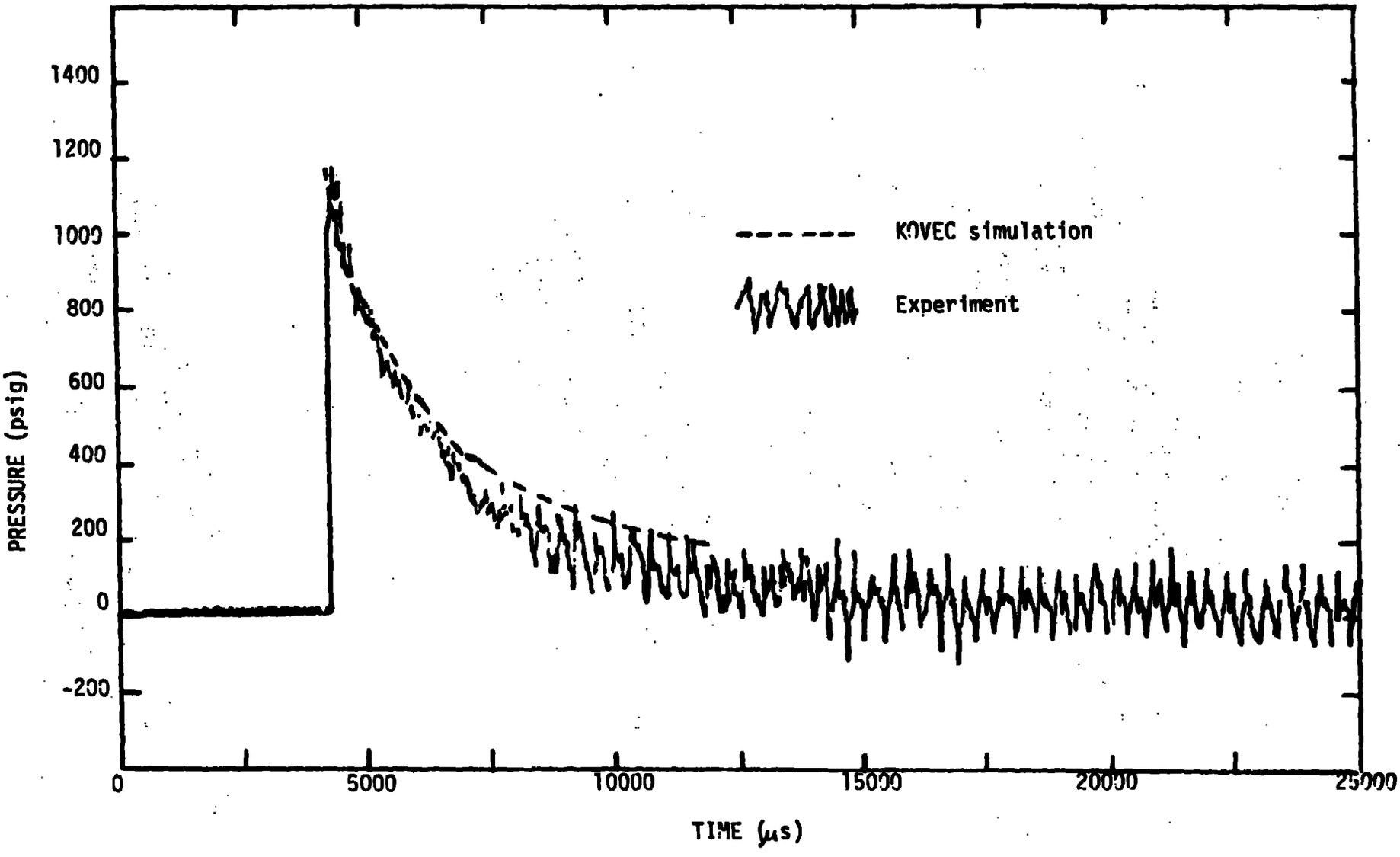

Pressure time history measured in the tube sidewall 10.3 ft. upstream from the GPHS location.

Figure B2.3-1 GPHS Shock Tube Test, Free Field Pressure versus Time.

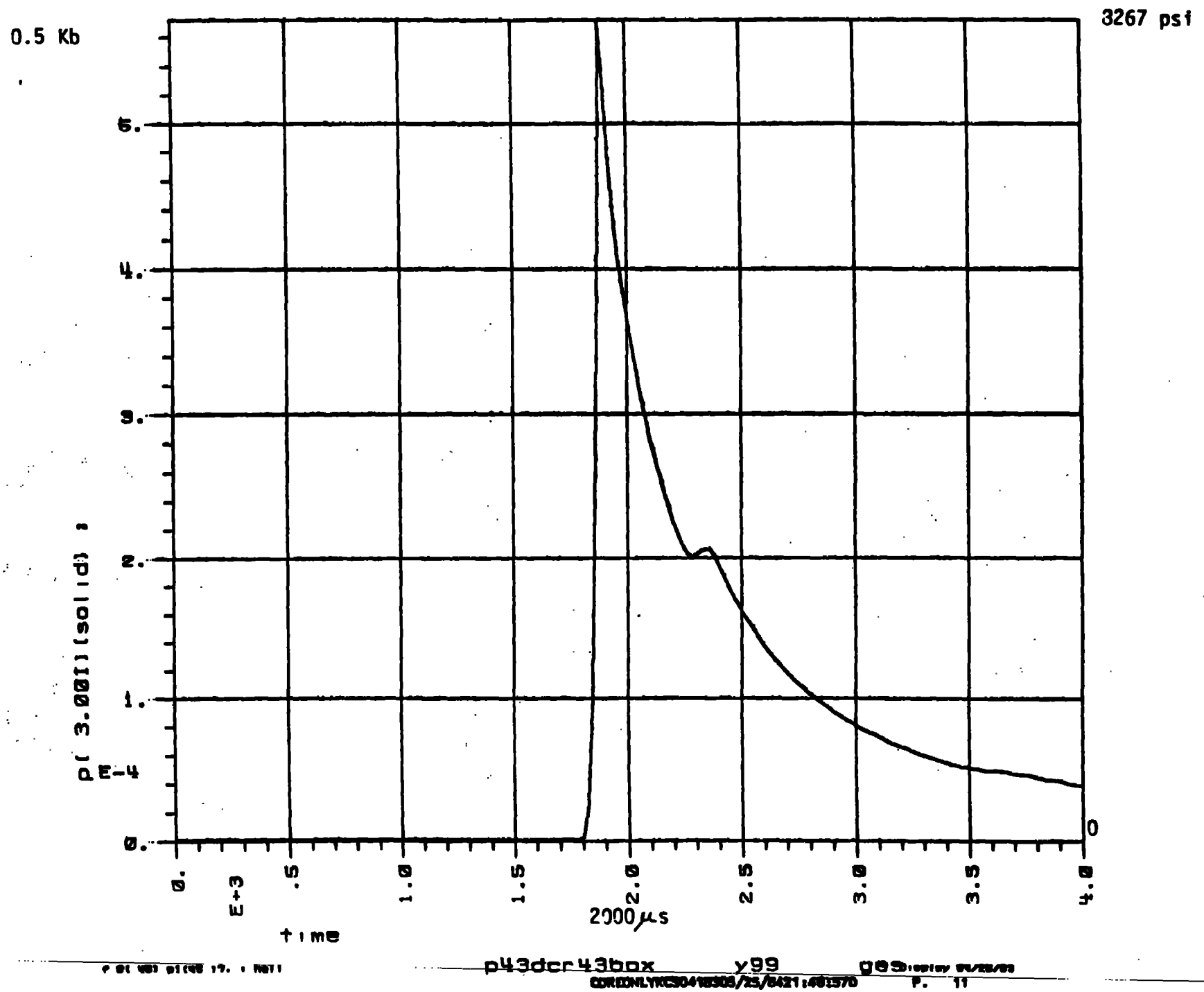

Figure B2.3-2 Shock Tube Test, pressure versus time, first graphite cell.

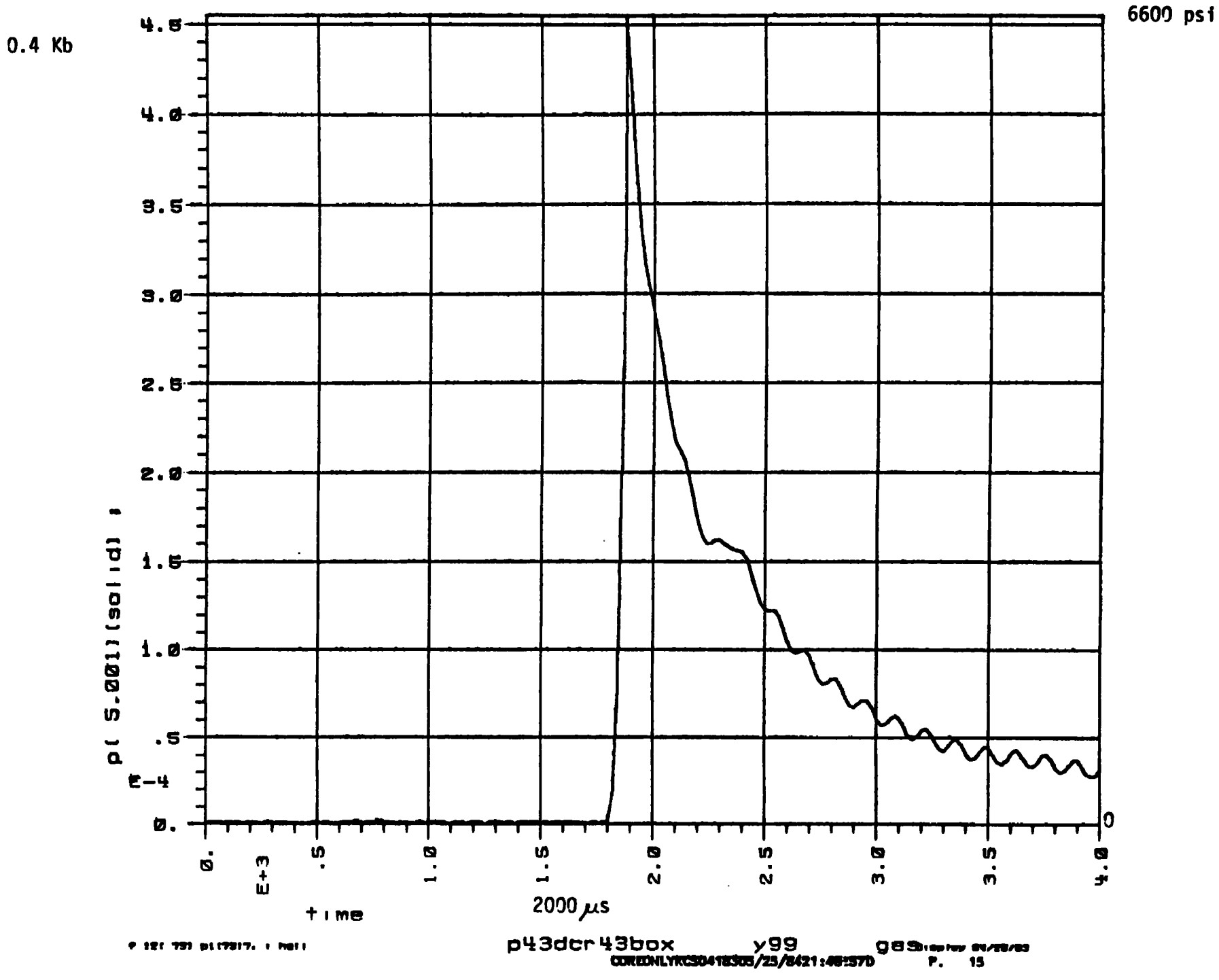

Figure B2.3-3 Shock Tube Test, pressure versus time, First UO_2 cell.

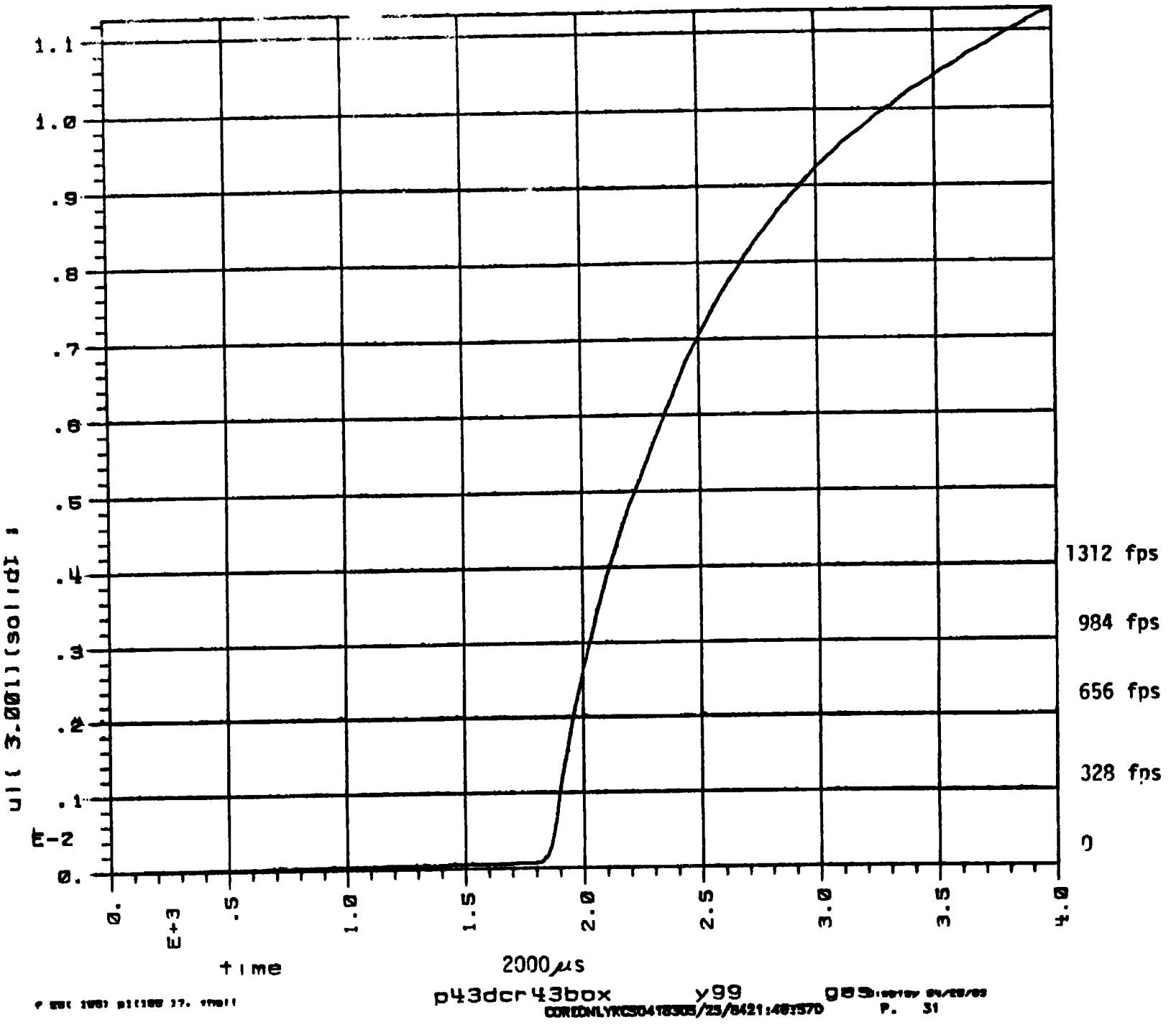

Figure B2.3-4 Shock Tube Test, Velcoity versus time, first graphite cell

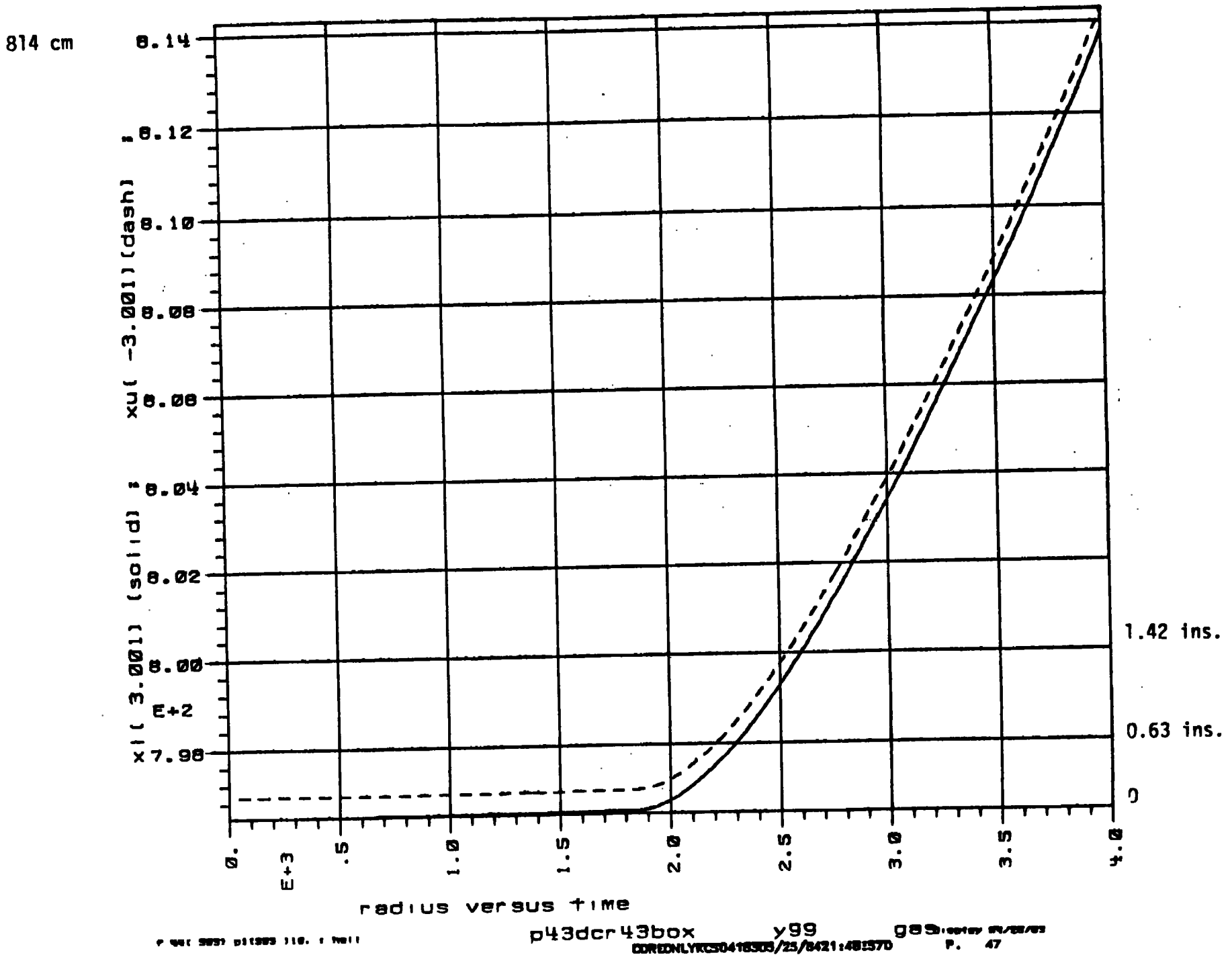

Figure B2.3-5 Shock tube test, location versus time for graphite layer

DESCRIPTION	KOVEC EOS NO.	THICKNESS CM	NO. OF ZONES	CUMULATED DIMENSION CM
				0
ALUMINUM CASE	25	0.3175	3	0.3175
CELLULAR SILICONE	90	1.9304	1	2.2479
AIR	51	8.1331	3	10.3810
GRAPHITE	73	1.2580	3	11.6390
URANIUM DIOXIDE	95	2.8330	3	14.4720
GRAPHITE	73	1.5358	3	16.0078
URANIUM DIOXIDE	95	2.8380	3	18.8408
GRAPHITE	73	1.2580	3	20.0988
AIR	51	8.1331	3	28.2319
CELLULAR SILICONE	90	1.9304	1	30.1623
ALUMINUM CASE	25	0.3175	3	30.480

TABLE I-1 RTG MODEL DIMENSIONS, ZONES, AND MATERIAL IDENTITY FOR STS FLYER PLATE CALCULATIONS.

ACTUAL MATERIAL	DENSITY	ROVEC MATERIAL	DENSITY	EOS TYPE	CONSTANTS FOR EQUATION OF STATE	SHEAR MODULUS	YIELD STRESS
Unknown mixture $LOX + LH_2$		Stoichiometric solid $O_2 + LH_2$	0.4025	JWL	A = 0.328236 R1 = 4.6 W = 0.25 B = 0.0127811 R2 = 1.4 E_0 = 0.050	0	0
Liquid Oxygen (LOX)		Liquid Oxygen (LOX)	1.149	Polynomial	A0 = 0. A2 = 0.062122 B0 = 0.8 A1 = 0.062555 A3 = 0.012703 B1 = 4.8 B3 = 0.	0	0
Liquid Hydrogen (LH_2)		Liquid Hydrogen (LH_2)	0.07	Polynomial	A0 = 0 A2 = 0.0051871 B0 = 0.8 A1 = 0.0066533 A3 = -0.0001656 B1 = 0.2 B3 = 0.	0	0
Aluminum		Aluminum 6061-T6	2.703	Gruneisen	C = 0.524 S2 = 0 γ_0 = 1.97 S1 = 1.4 S3 = 0 a = 0.48	0.276	0.0029
Air and Argon		Air	0.001195	JWL (Gamma Law)	A = 0 W = 0.4 B = 0 E_0 = 2.533E-06	0	0
301SS, Centaur Alloy STL, SRB		304SS	7.90	Gruneisen	C = 0.457 S2 = 0 γ_0 = 1.93 S1 = 1.49 S3 = 0 a = 0.35	0.77	0.0045
Magnesium		Magnesium	1.78	Gruneisen	C = 0.452 S2 = 0 γ_0 1.54 S1 = 1.242 S3 = 0 a = 0.33	0.165	0.0017
Various fiber-glass type insulations Ceramic tile	2 PCF 2.4 PCF 5.21 PCF 8 PCF 9 PCF	Cellular Silicone	0.128	Gruneisen	C = 0.178 S2 = 0 γ_0 = 1.1 S1 = 1.62 S3 = 0 a = 0	0.001	0.0001
Acrylic Nitride Butadiene rubber Asbestos & S_iO_2 filled - SRB	1.274	Boron Rubber (orig. density = 1.786)	1.274	Gruneisen	C = 0.127 S2 = -14.93 γ_0 = 0.4 S1 = 6.125 S3 = 12.7 a = 0	0.05	1.E-06
SRB Propellant		Non reactive "SOPHY" prop. AAB 3225	1.735	Polynomial	A0 = 0 A2 = 0.24307 B0 = 0.93 A1 = 0.060866 A3 = 0.40373 B1 = 11.0 B2 = 0.	0.04	0.001
Graphite		Graphite	1.98	Gruneisen	C = 0.39 S2 = 1.54 γ_0 = 0.24 S1 = 2.16 S3 = -0.43 a = 0	0.02	0.0001
Uranium Dioxide		Uranium Dioxide	10.5	32 bit	A11 = 1.638 A21 = 1.545 A31 = 0.1662 A12 = 0.00371 A22 = 3.243 A32 = 0.02028 A13 = 0.03645 A23 = 0.0002098 A50 = 0.77255 A20 = 0.2445 A30 = 1.261 A60 = 1. A70 = -70.37	0.365	0.0013

No material was allowed to carry negative pressure (volumetric tension)

TABLE I-2 MATERIALS DATA FOR STS EXPLOSION MODELS

RUN NO.	DESCRIPTION BURNABLE WT.	GEOMETRY	BURN PRESSURE Kb	GRAPHITE PRESSURE Kb	UO_2 PRESSURE Kb	UO_2 FINAL VELOCITY mm/μs	FLYER PLATE VELOCITIES					
							ANFO CASE mm/μs	ET WALL mm/μs	ORBITER FLOOR mm/μs	CENTAUR STL mm/μs	CENTRAL MAG. mm/μs	SRB STL. mm/μs
	Direct Course											
14A	Vac. fine res.	Spherical	47	186/-72	132/114							
14	Vac. coarse res.			53	64	0.3 ↑	4.6					
15	Air			11	37.5	0.33 ↑	3.					
16	Vac + Air Blkt.			104	36	0.32 ↑	4.6					
21	Vac + Air Blkt.			46	31	0.32 ↑	4.6					
24	Gas, no case		12	2.8	5.6							
	ET to RTG											
26	1664 lbs/ft	Planar	18.2	14.9	26.2	0.8 →		2.6	2.8			
28	555 lbs/ft			14.8	14.2	0.47 →		2.15	1.36			
40	185 lbs/ft			2.36	2.53	0.23 →		1.34	.84			
27	1664 lbs/ft	Cylindrical		18.4	12.9	0.44 →		2.3	2.2			
29	555 lbs/ft			8.8	8.3	0.29 →		1.52	1.16			
41	185 lbs/ft			3.2	2.8	0.17 →		1.18	.75			
	Centaur to RTG											
30	14773 lbs/ft	Spherical	18.2	10.6	43	0.31 →				1.6	1.8	
31	4925 lbs/ft			12.5	14.6	0.19 →				1.2	1.44	
32	702 lbs/ft			3	4.5	0.08 →				0.63	0.8	
	Flyer Plates											
37	ET/Orbiter Pl.	Planar	-0-	12.2	7.6	0.58 →		1.6	0.78			
38	Into RTG with			1.92	2.2	0.234 →		.9144	0.42			
39	ET initial Vel.			.043	.035	.0082 →		.3048	0.112			
	ET → SRB*											
33	1664 lbs/ft	Cylindrical	18.2					2.3				0.2

* Run 33, ET → SRB resulted in 7 Kb, 700 μs pulse into propellant with energy fluence = 60 MJ/M^2

TABLE I-3 Flyer Plate Summary Results

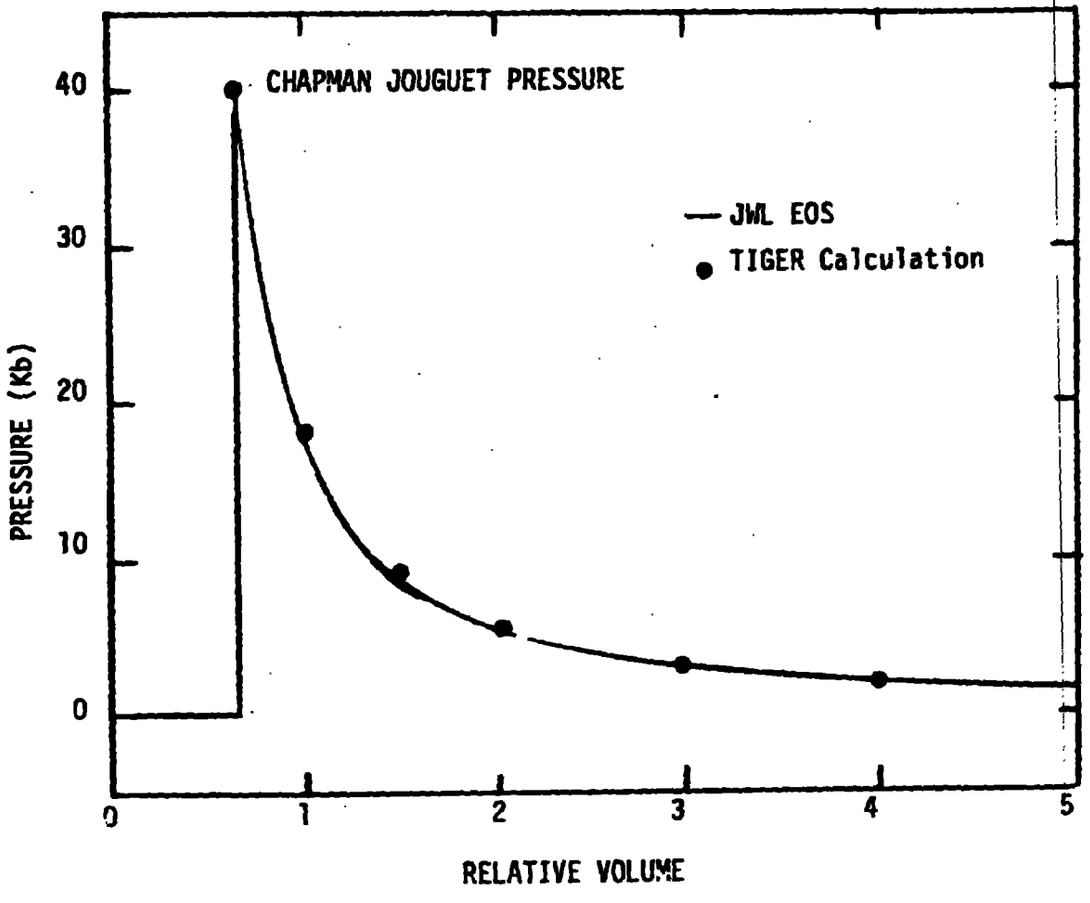

Figure I-1 Reacted Hugoniot pressure vs. relative volume JWL Equation of State fitted to equilibrium thermochemical calculation (TIGER) stoichiometric $LH_2 + SO_2$, ρ_0 = 0.4025

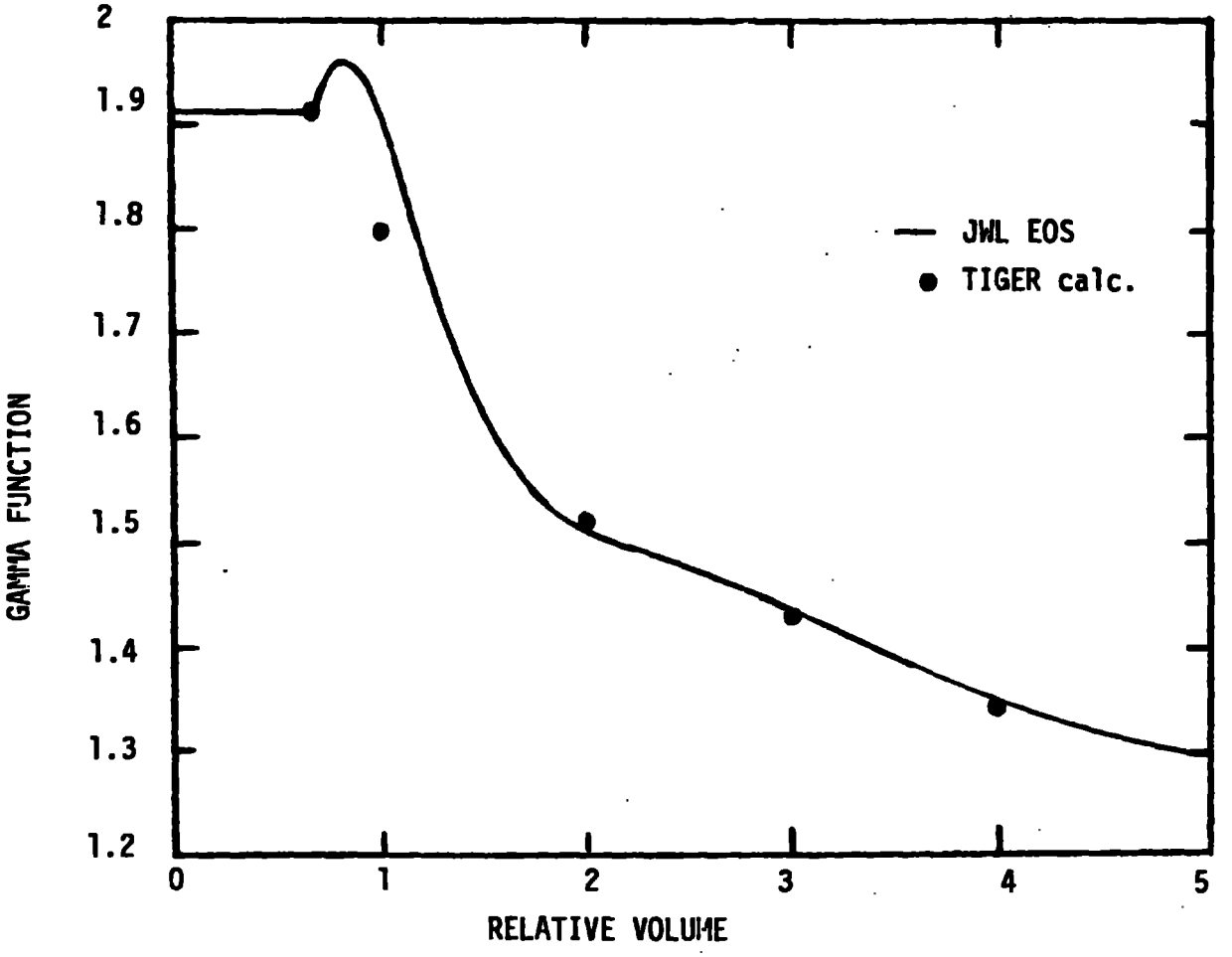

Figure I-2 Gamma function vs. relative volume JWL Equation of State fitted to equilibrium thermochemical calculation (TIGER) stoichiometric $LH_2 + SO_2$, $\rho_0 = 0.4025$

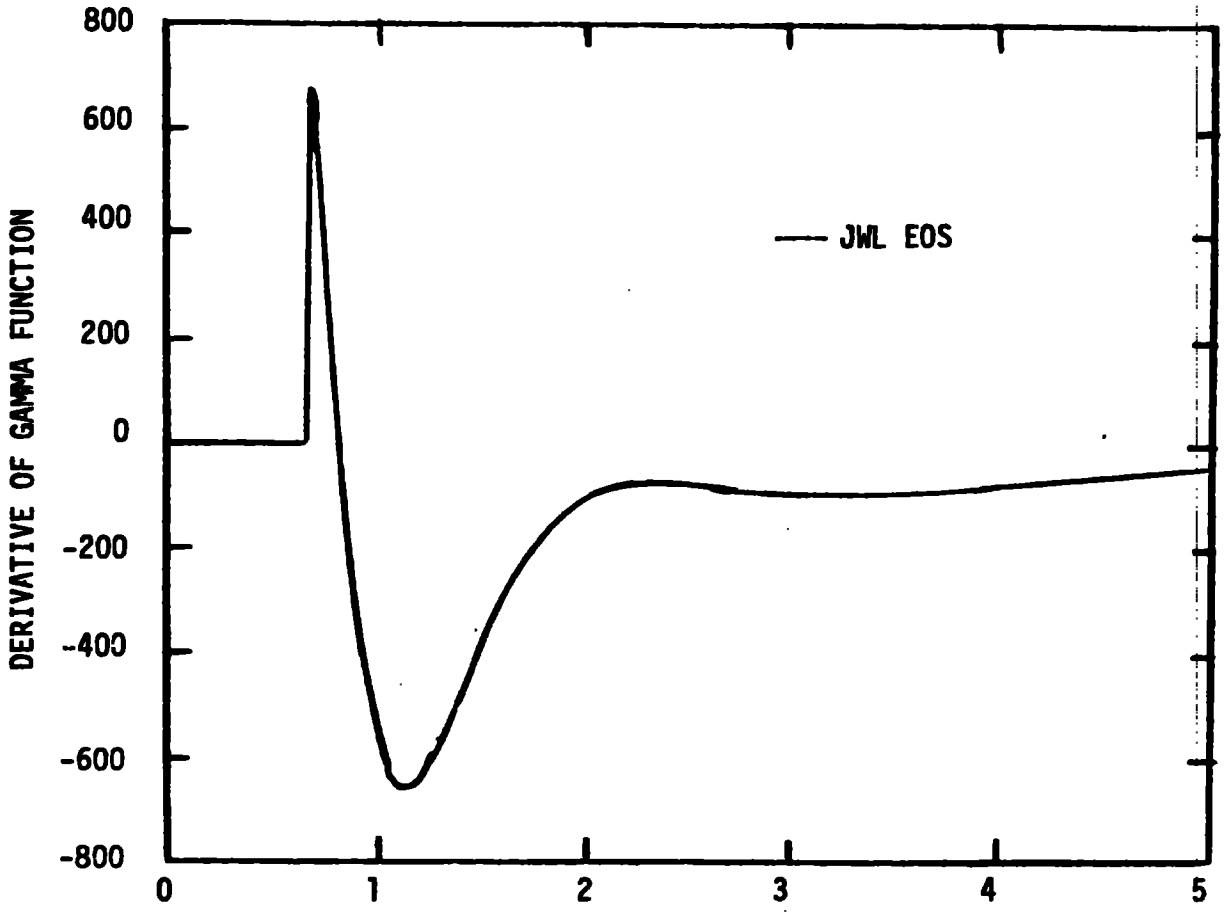

Figure I-3 Derivative of Gamma Function vs. relative volume JWL Equation of State fitted to equilibrium thermochemical calculation (TIGER) stoichiometric $LH_2 + SO_2$, $\rho_o = 0.4025$

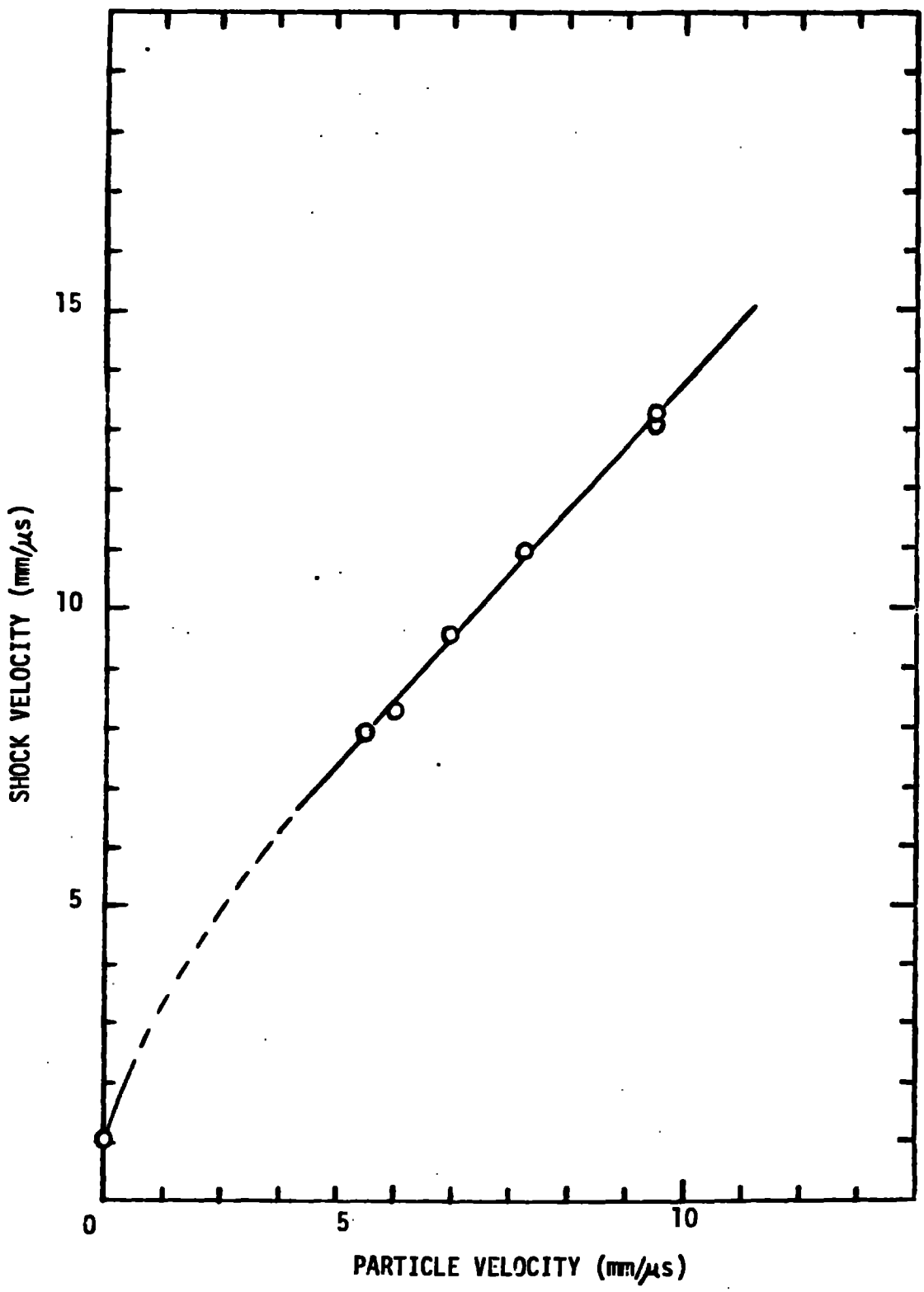

Figure I-4 U_s-U_p shock Hugoniot for LH_2 initial density is 0.07 g/cc

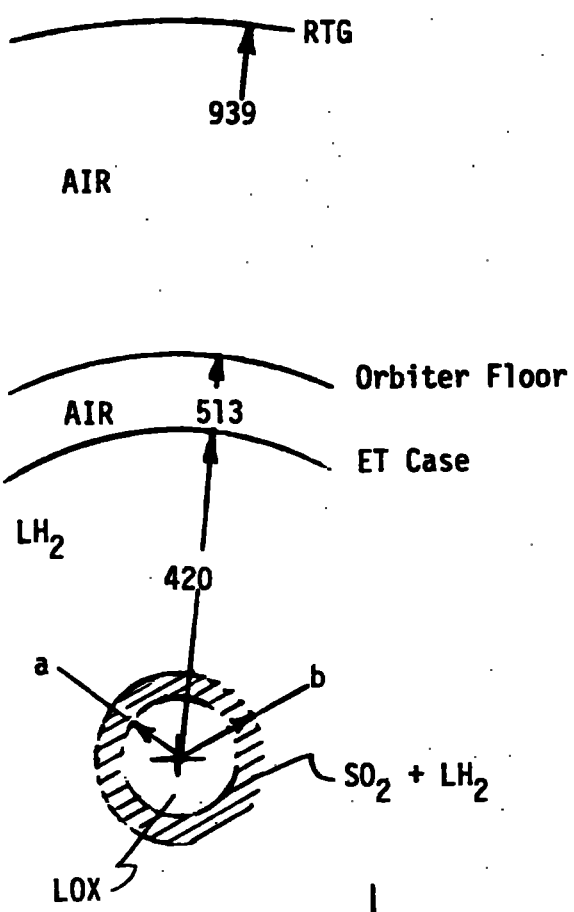

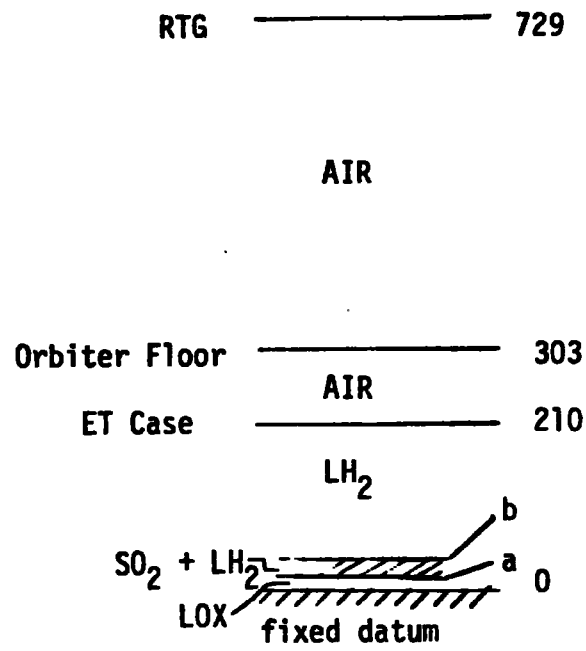

	Detonable Wt. lbs/ft	Planar A cm	Planar B cm	Cylindrical A cm	Cylindrical B cm
26,27	1664	23	47	140	198
28,29	555	8	16	81	114
40,41	185	2.6	5.2	46	65

Figure I-5 Cylindrical and Planar Explosion Models ET Case to RTG

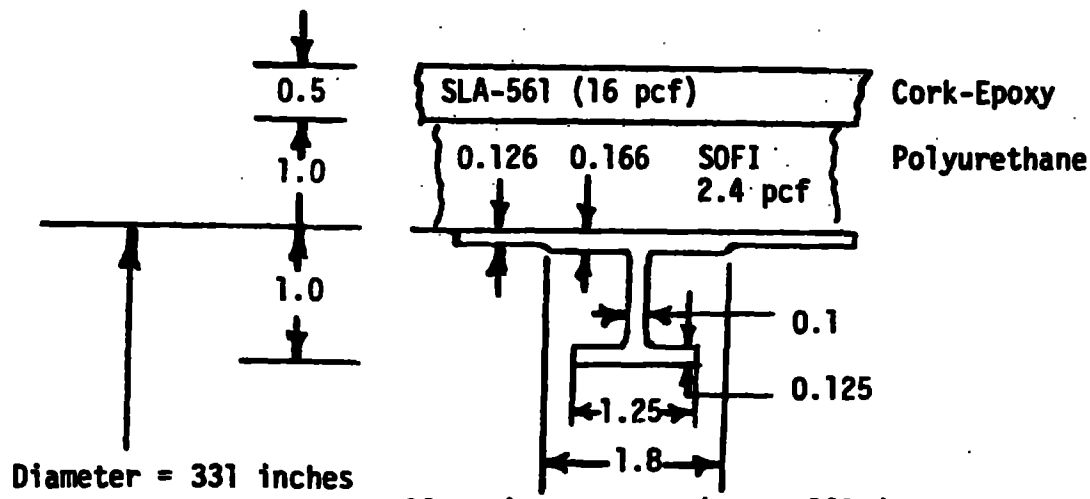

PHYSICAL STRUCTURE

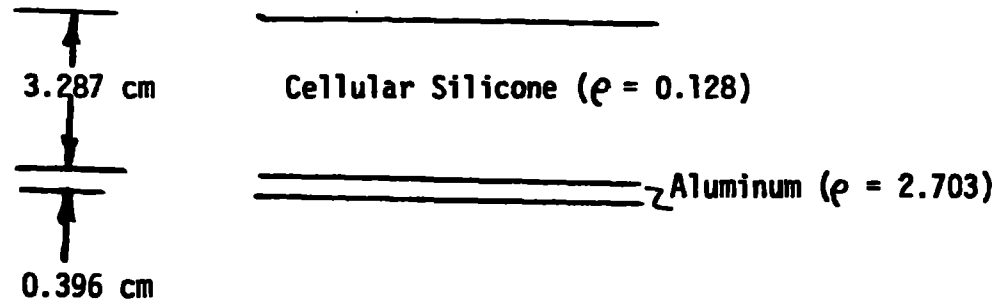

KOVEC MODEL

Figure I-6 Representation of External Tank Wall (ET)

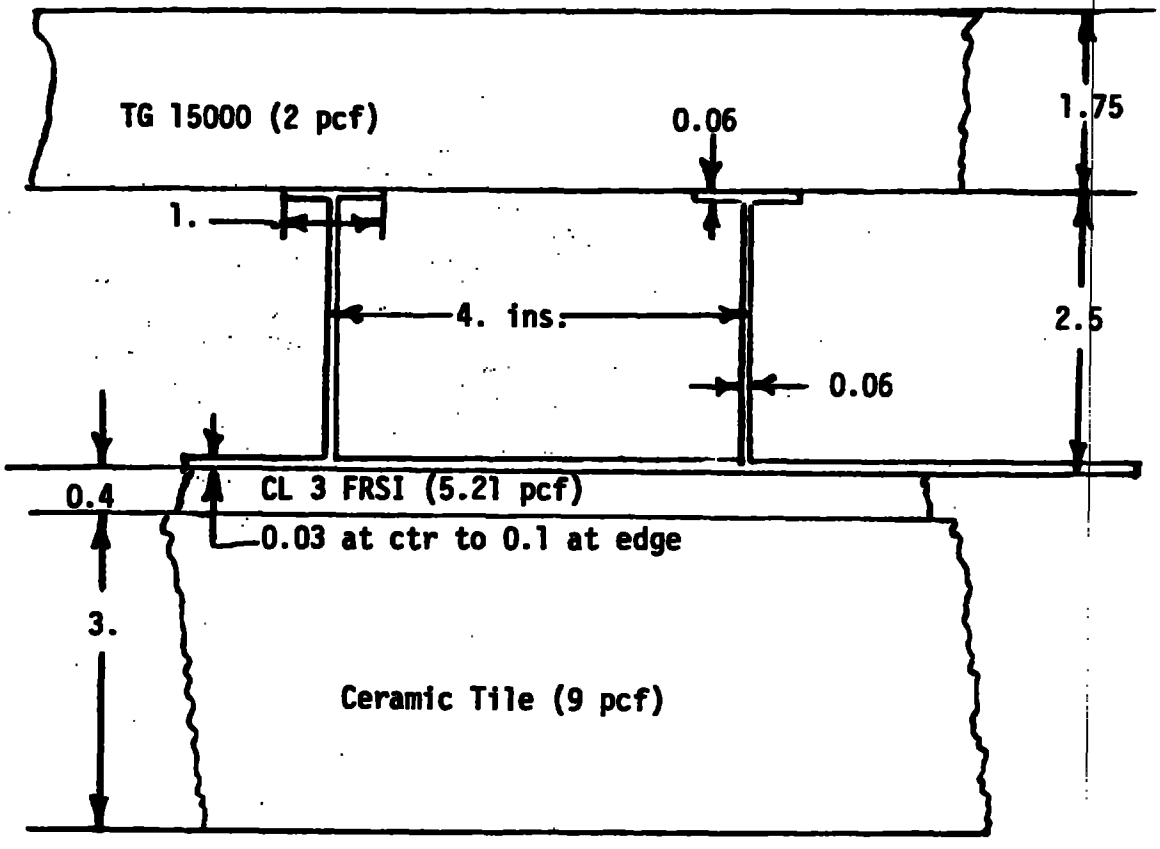

PHYSICAL STRUCTURE

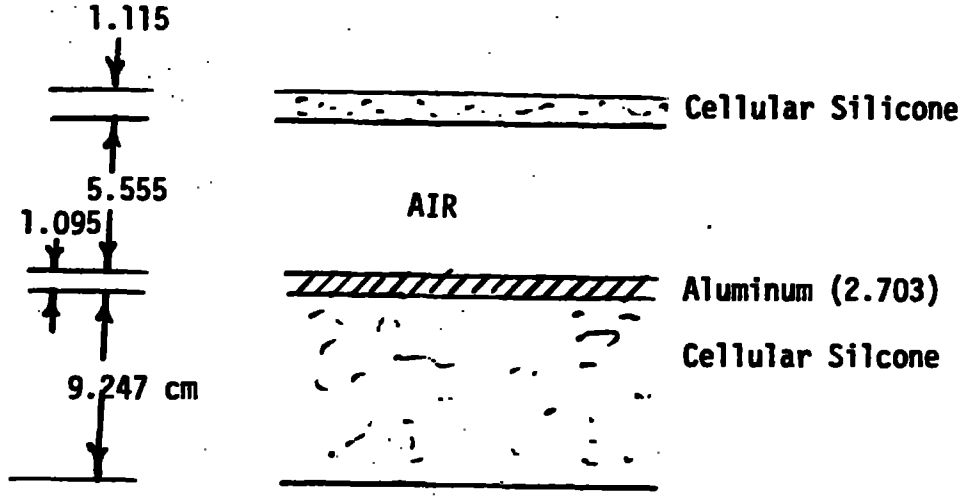

KOVEC MODEL

Figure I-7 Representation of Orbiter Floor

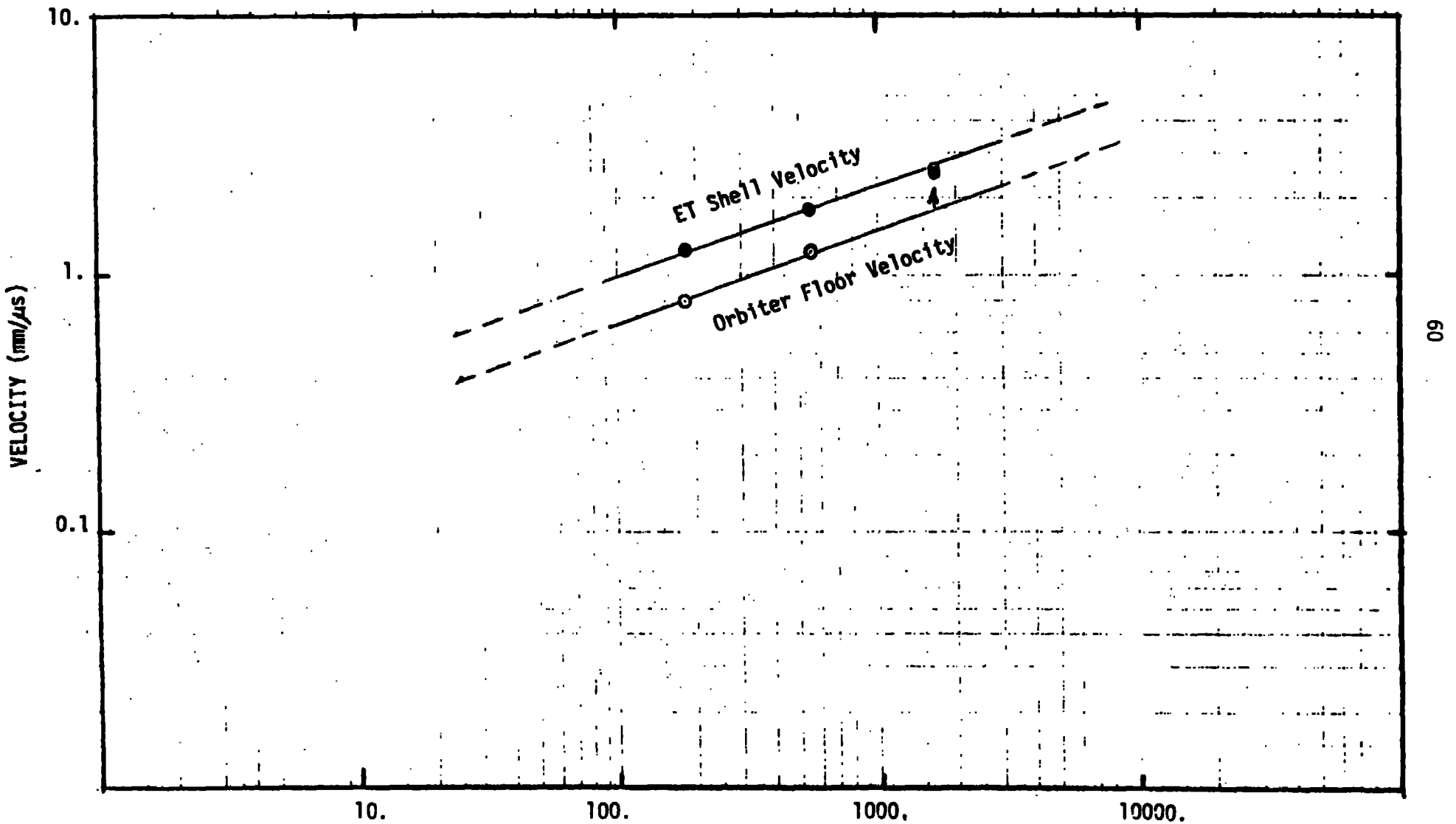

Figure I-8a ET Stoichiometric Mixture Weight (lbs/ft).

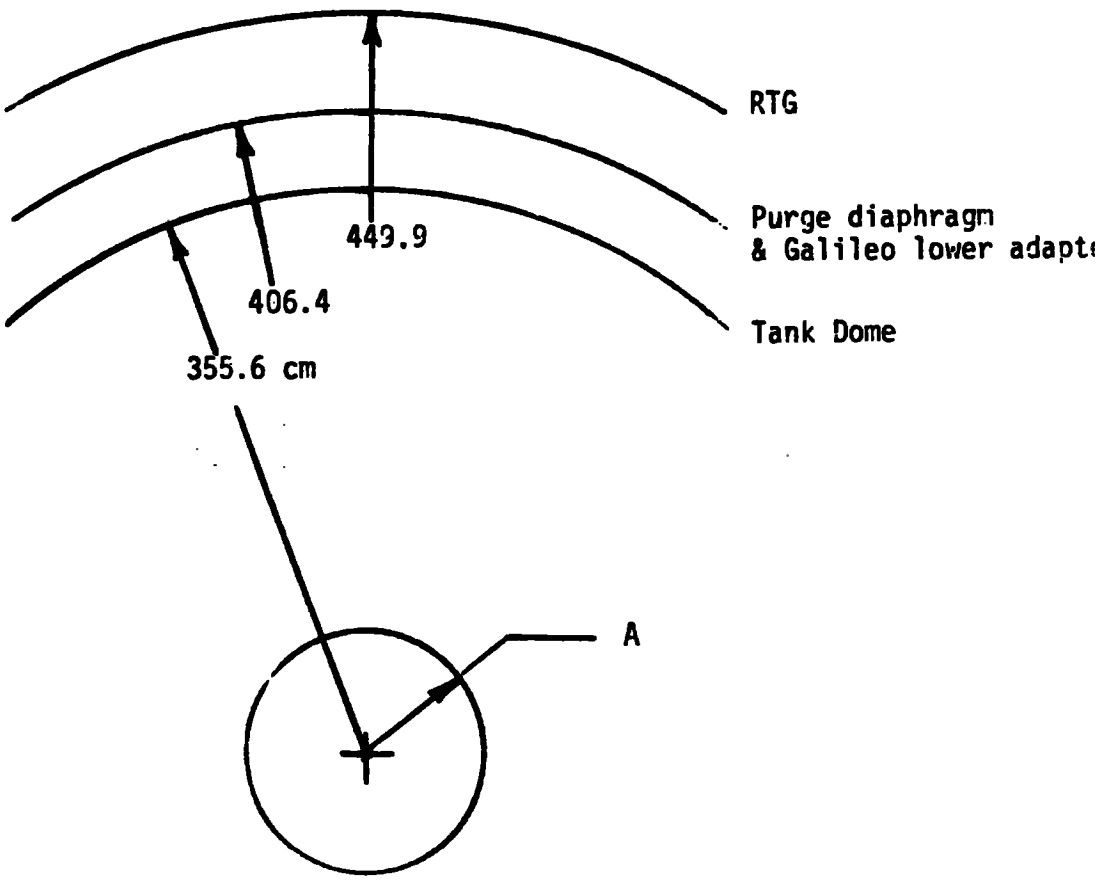

Run No.	Det. wt. lbs.	A cm.
30	14773	110.99
31	4925	75.40
32	702	52.28

Figure I-8b Centaur Tank Explosion to RTG

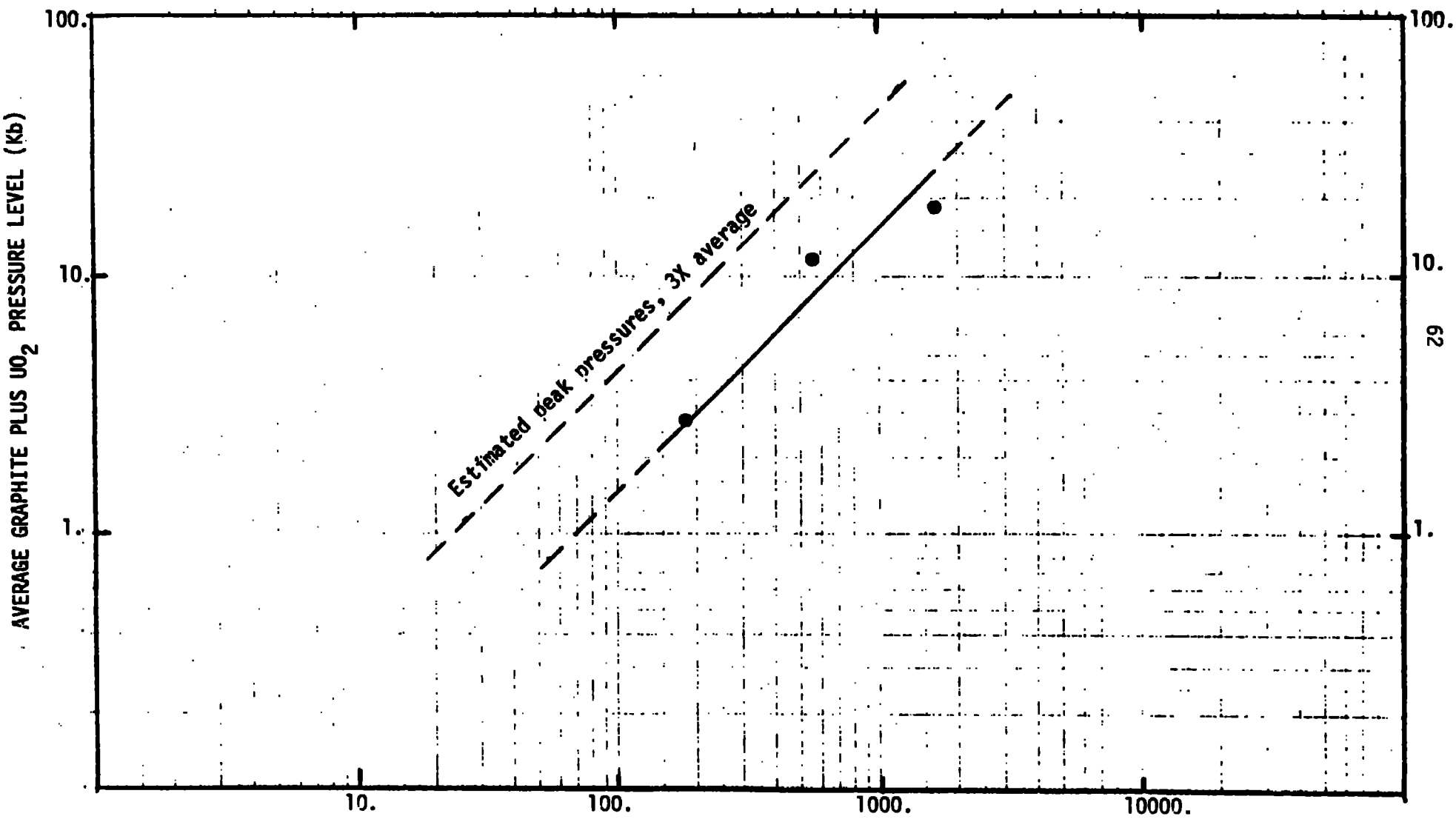

Figure I-9a ET Stoichiometric Mixture Weight (lbs/ft).

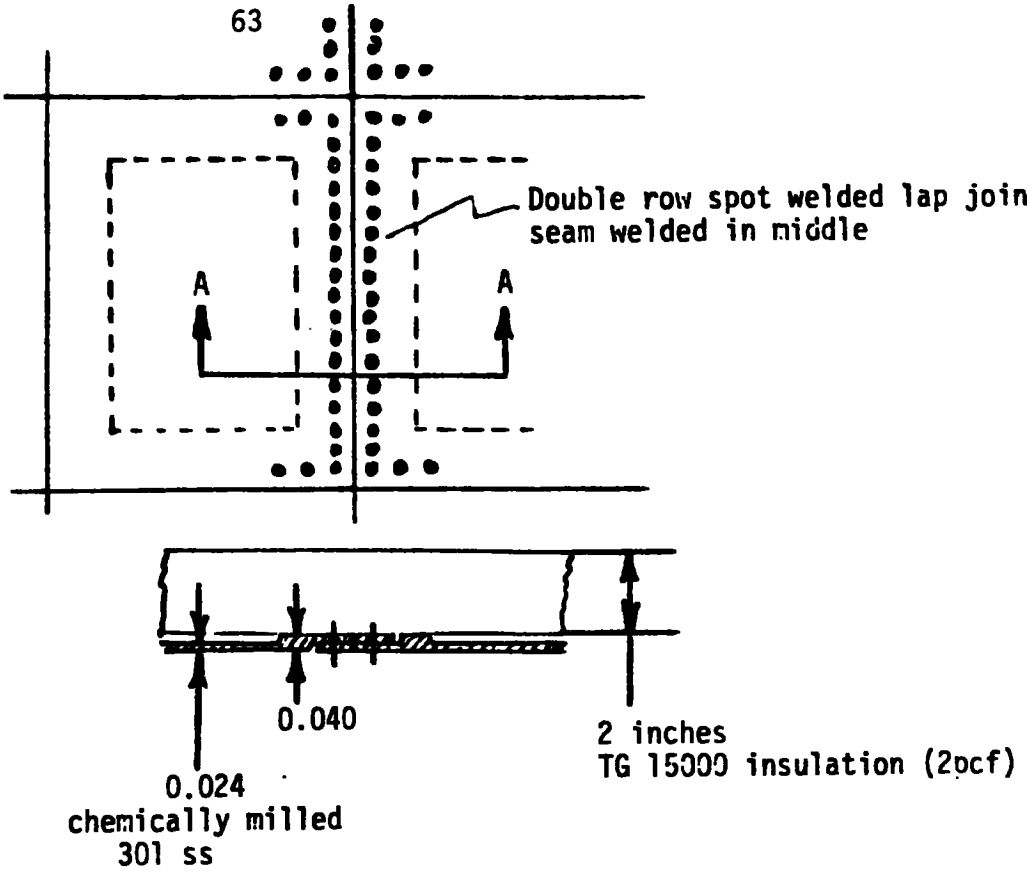

Section AA
Physical Structure of Tank Dome

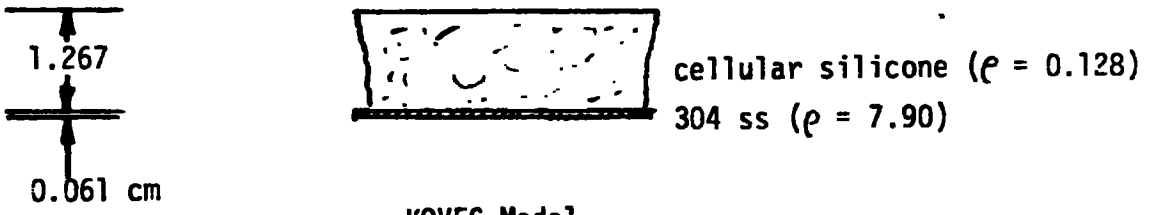

KOVEC Model

Figure I-9b Flyer plate model for Centaur Tank Dome

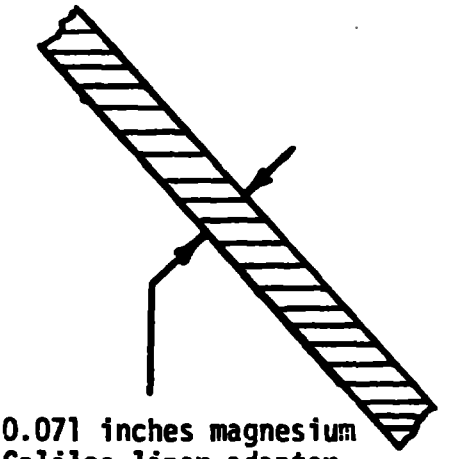

0.071 inches magnesium
Calileo liner adapter

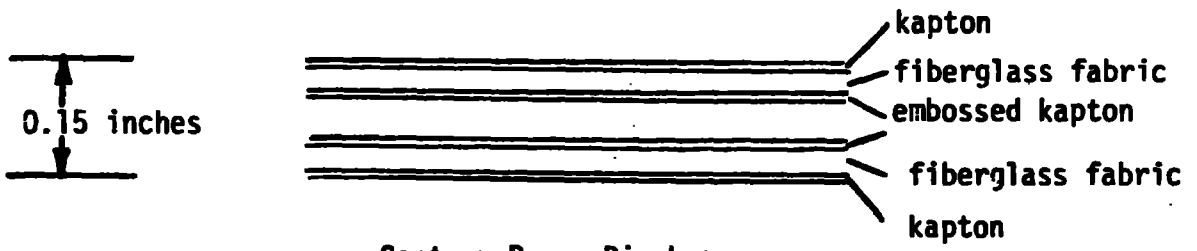

Centaur Purge Diaphragm

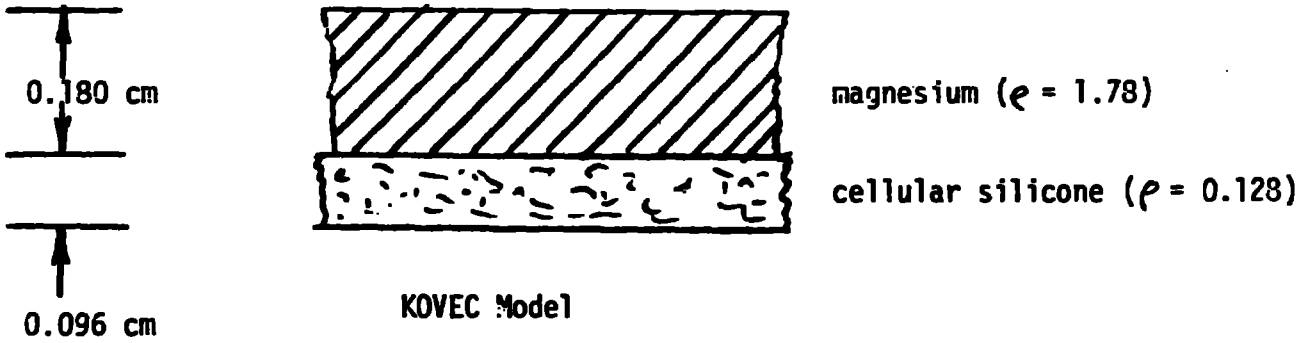

KOVEC Model

Figure I-10 Flyer plate model for Centaur purge diaphragm and Galileo lower adapter.

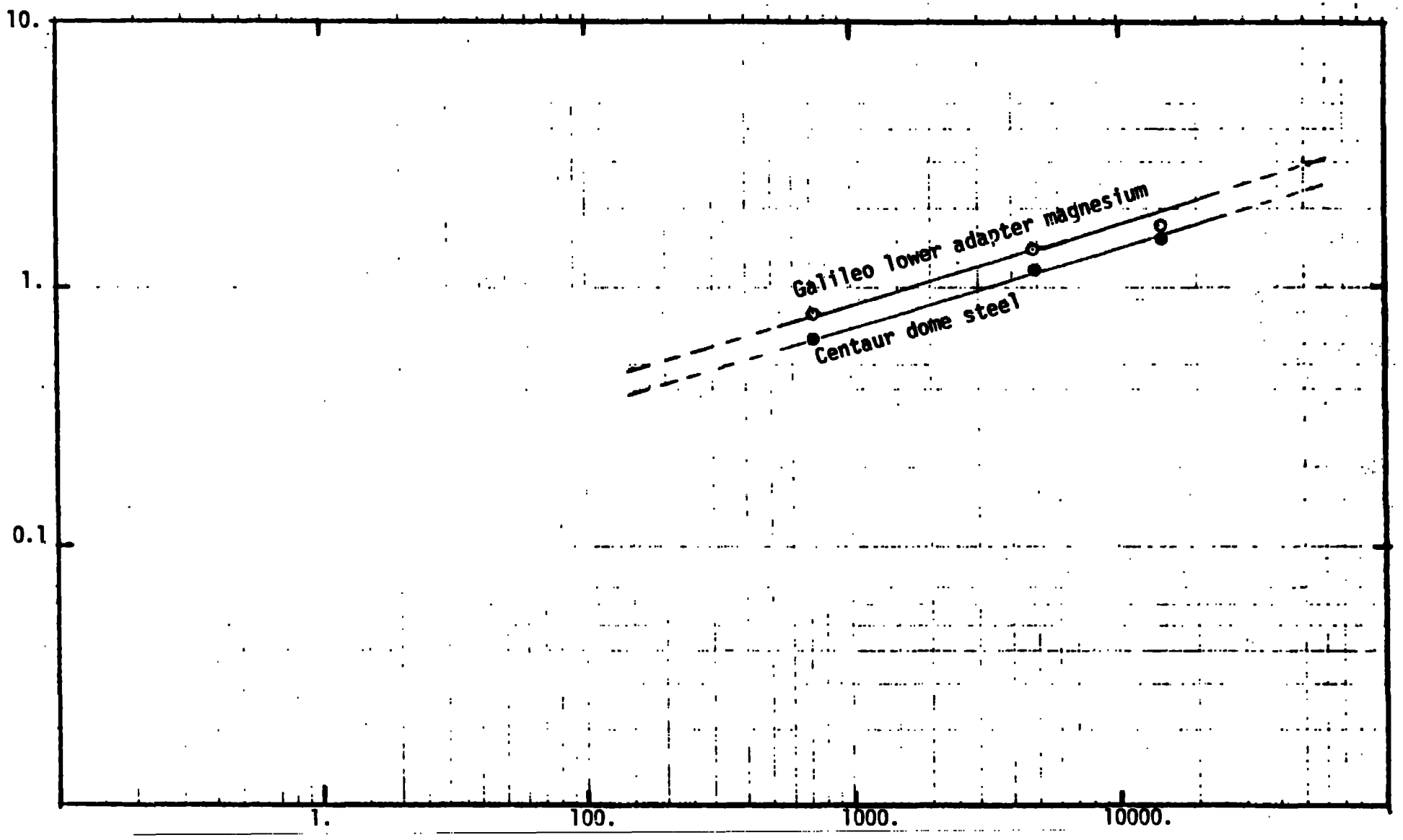

Figure I-11 Centaur Explosion Stoichiometric Mixture Weight (lbs.)

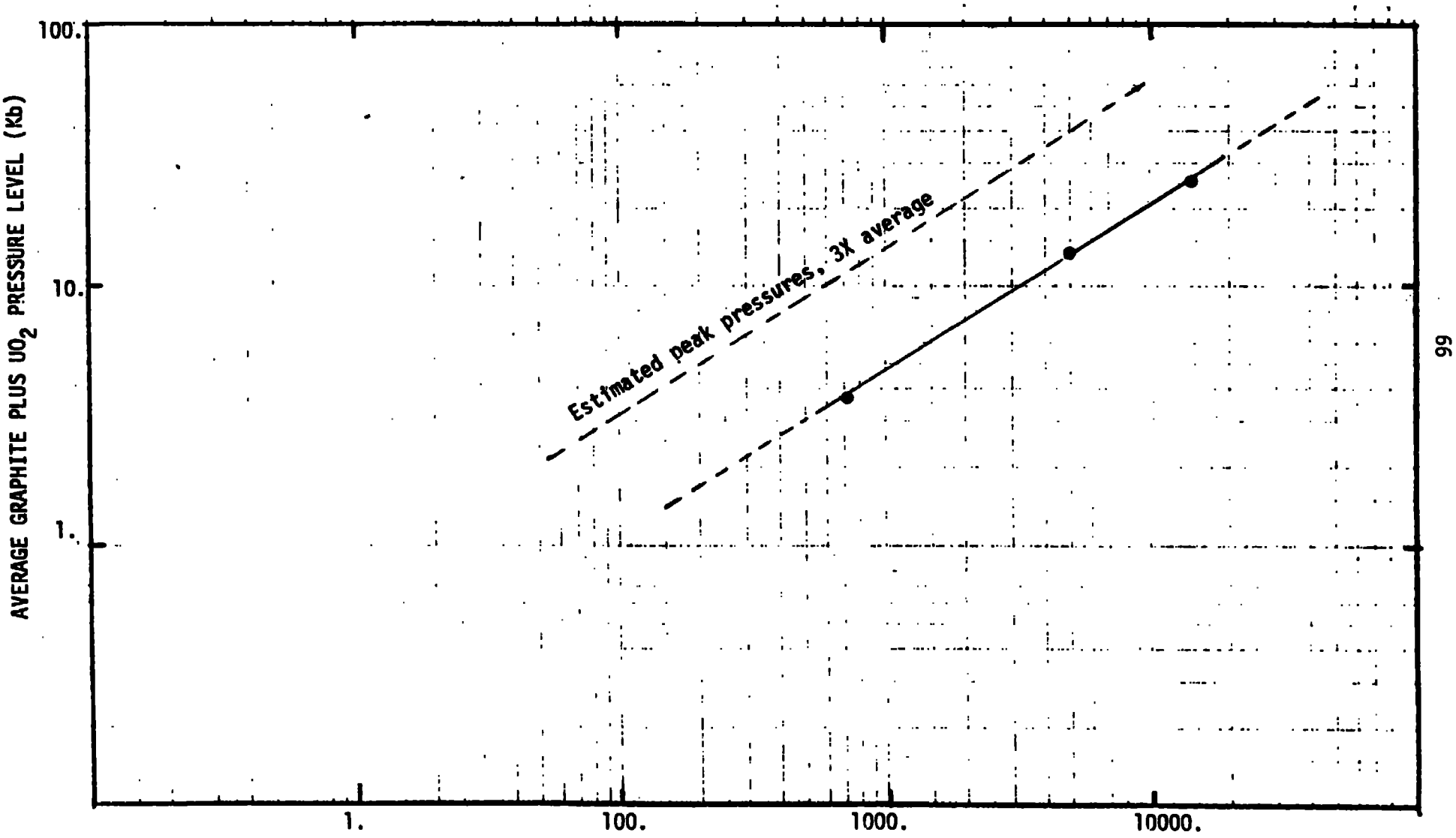

Figure I-12 Centaur Explosion Stoichiometric Mixture Weight (lbs.)

Centaur Tank Explosion to RTG, I5

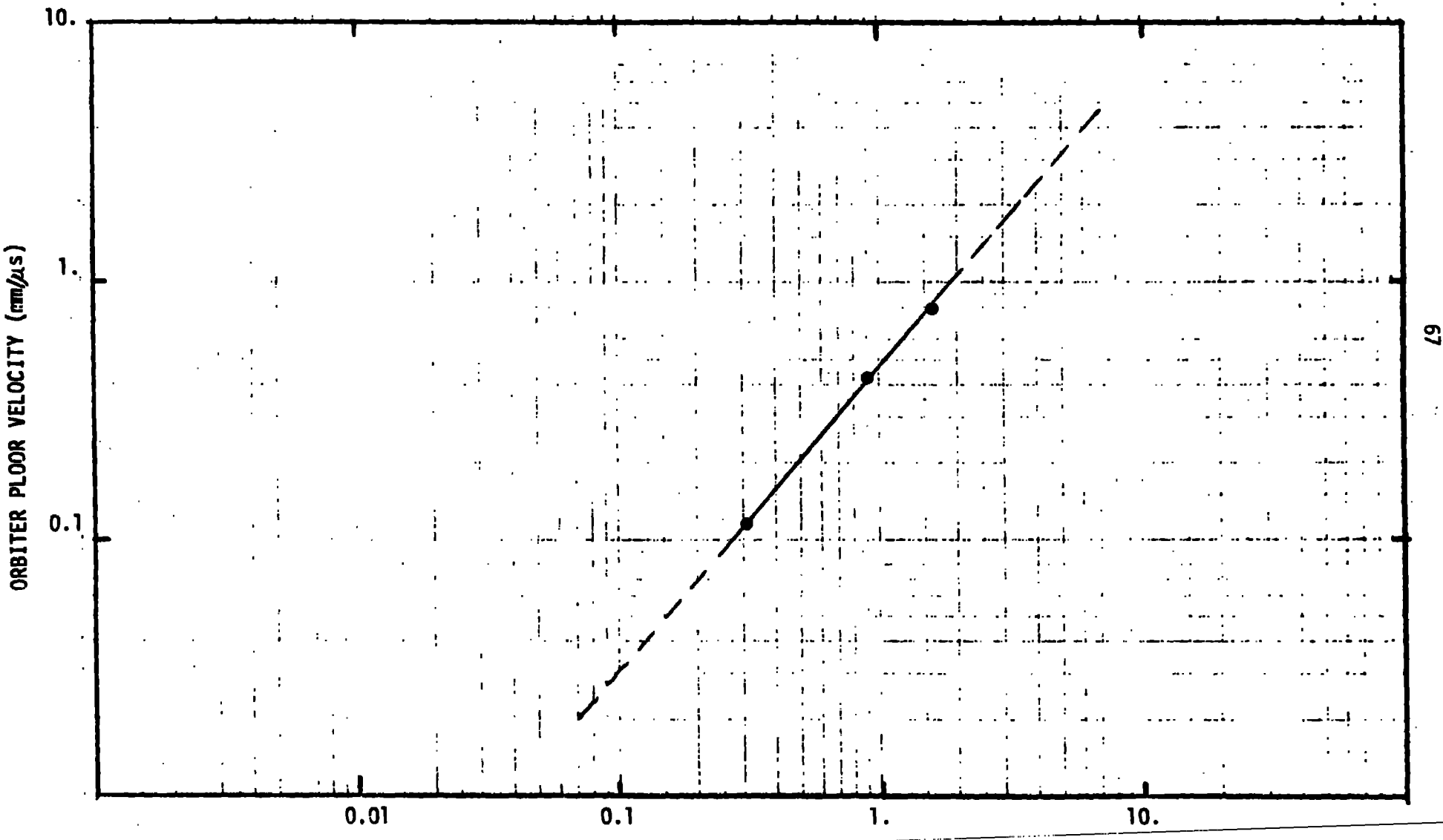

~~Figure I-13 ET~~ Shell Initial Velocity (mm/μs)

Flyer Plate Initial Velcoity Impacts, I6

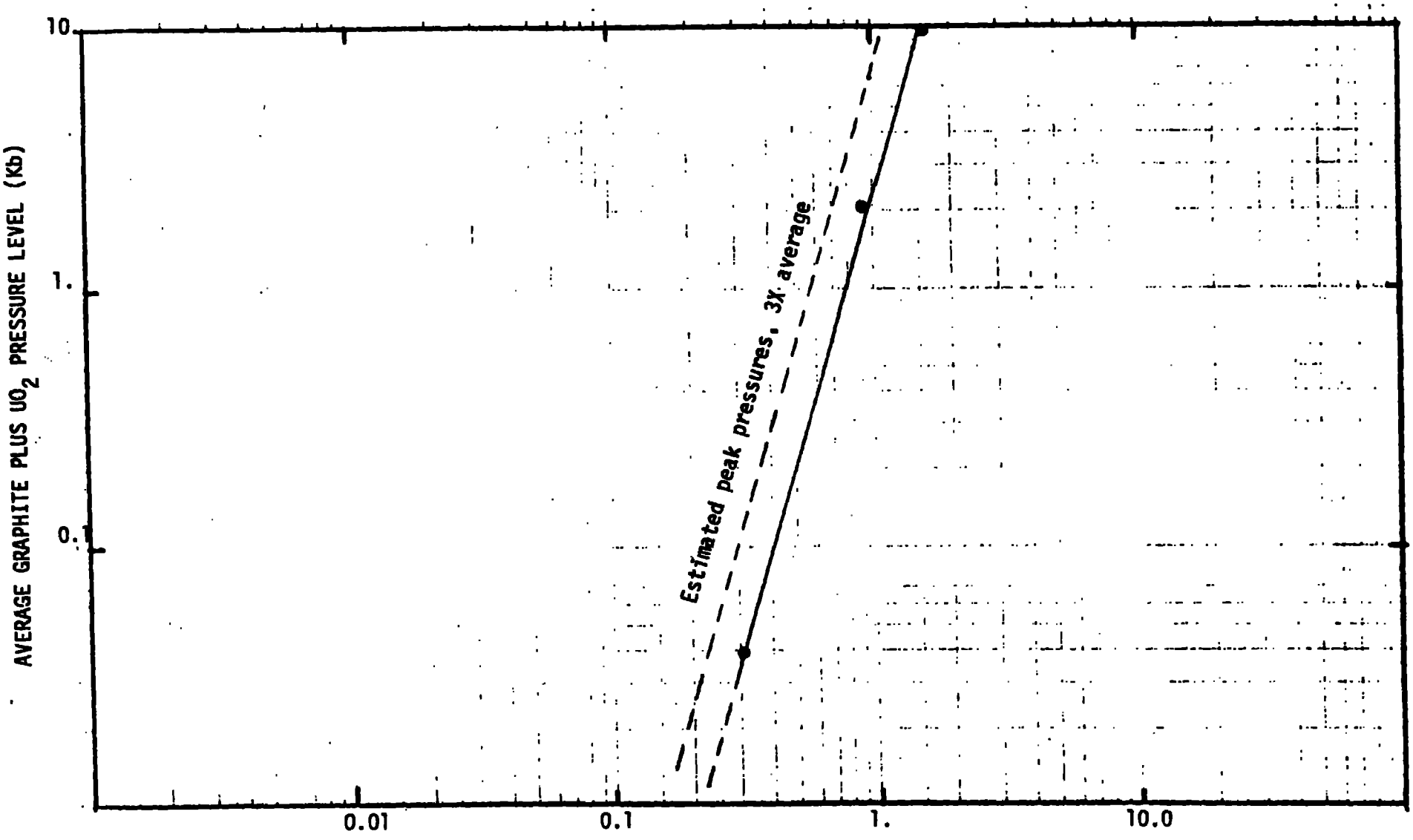

Figure I-14 ET Shell Initial Velocity (mm/μs)

Flyer Plate Initial Velocity Impact, I6

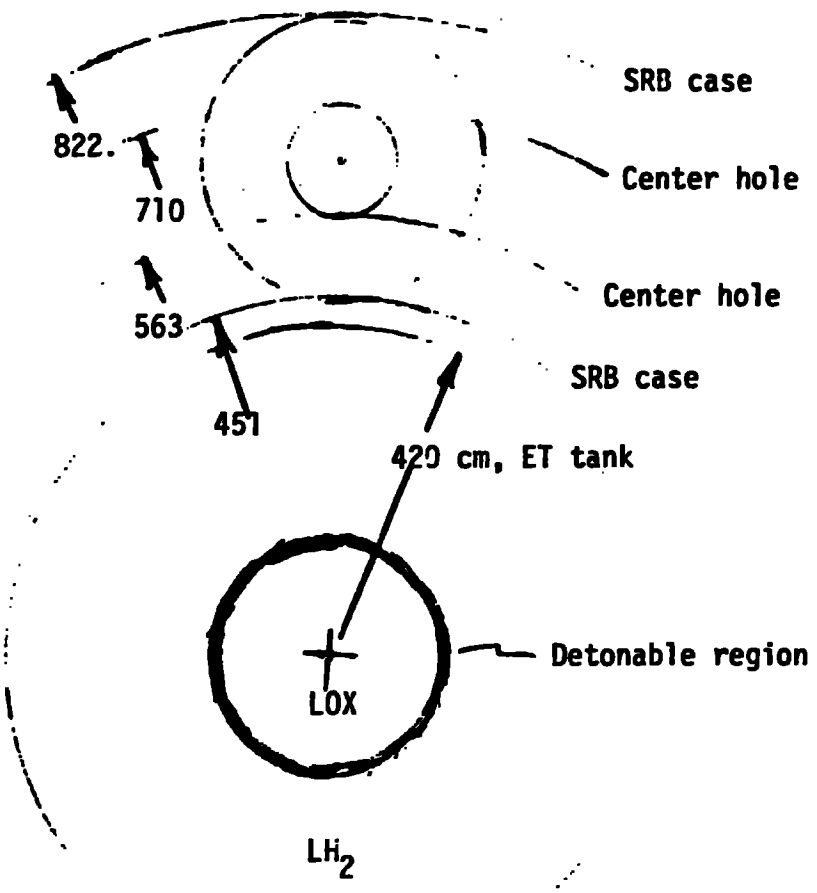

Figure I-15 Explosion Model, ET to SRB

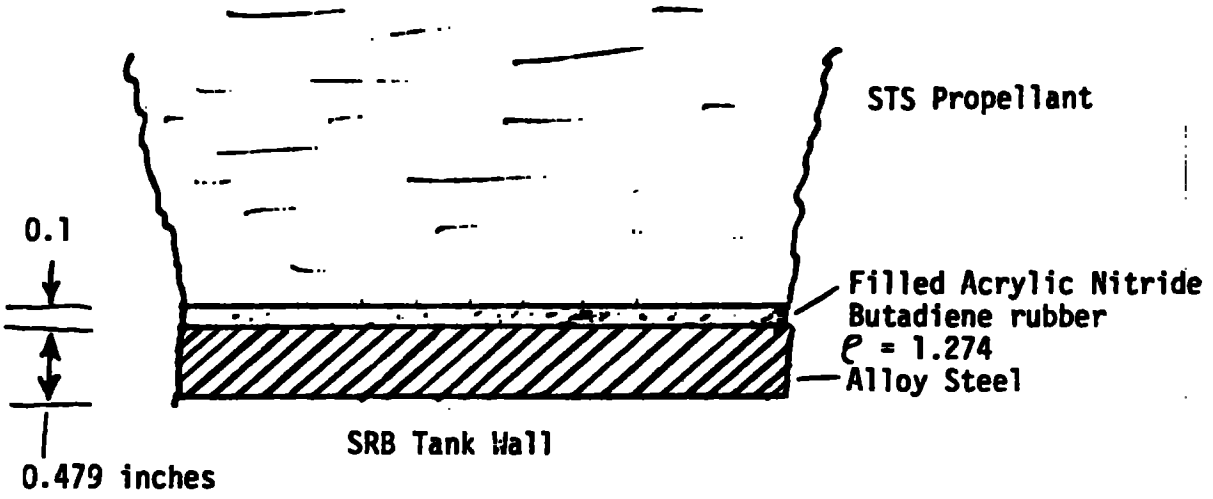

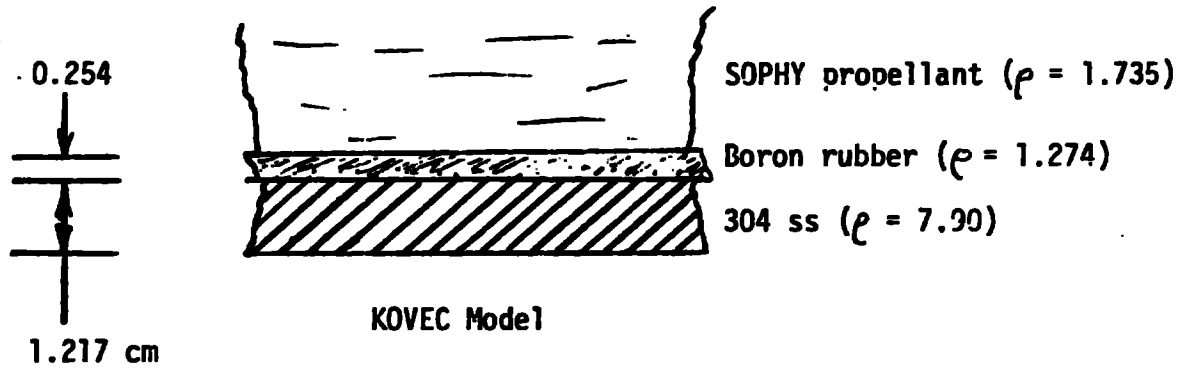

Figure I-16 Flyer plate model for SRB tank wall.

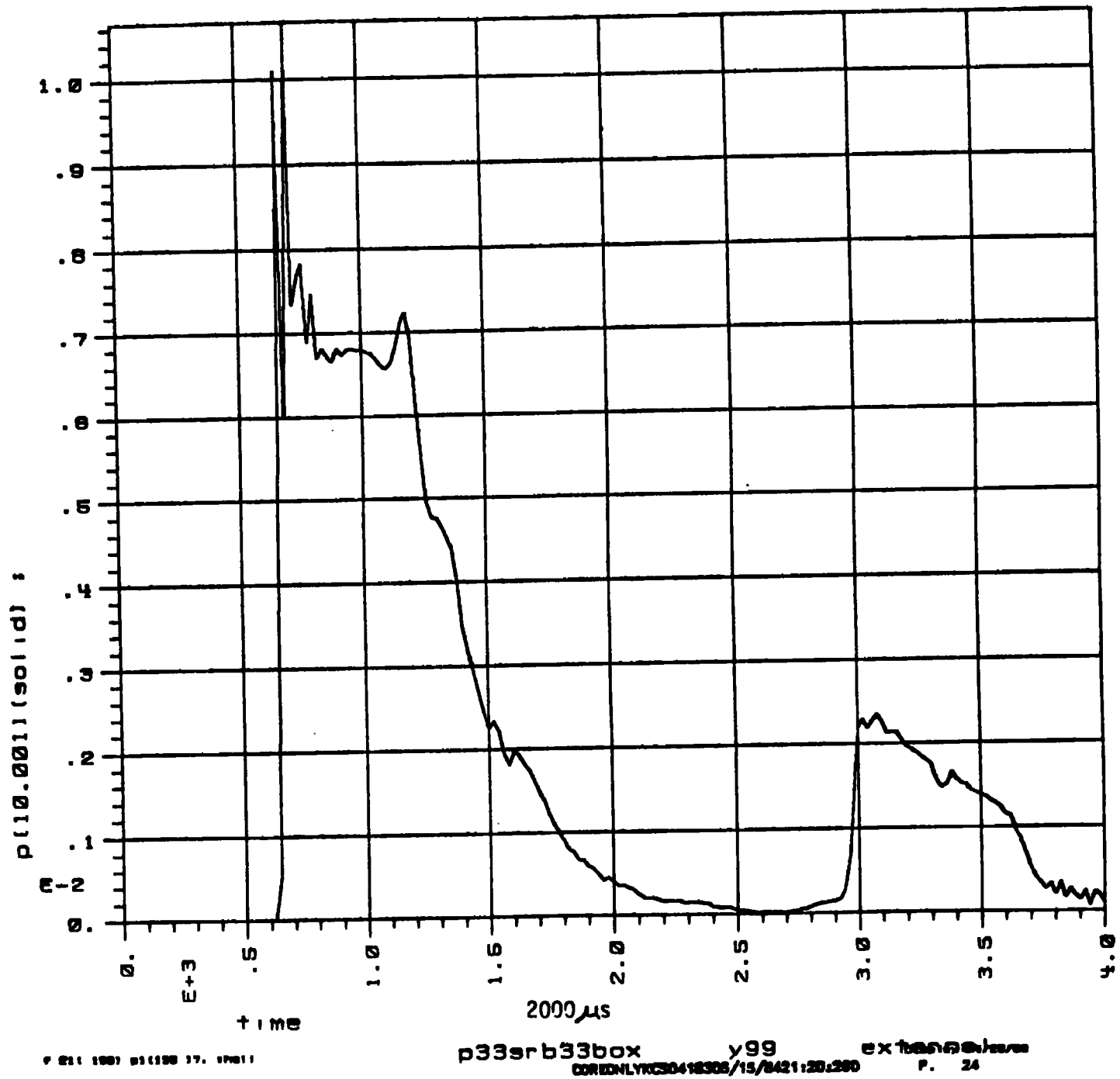

Figure I-17 Pressure versus time into SRB propellant for 1664 lbs/ft of ET detonable mixture weight

0.3 mm/μs

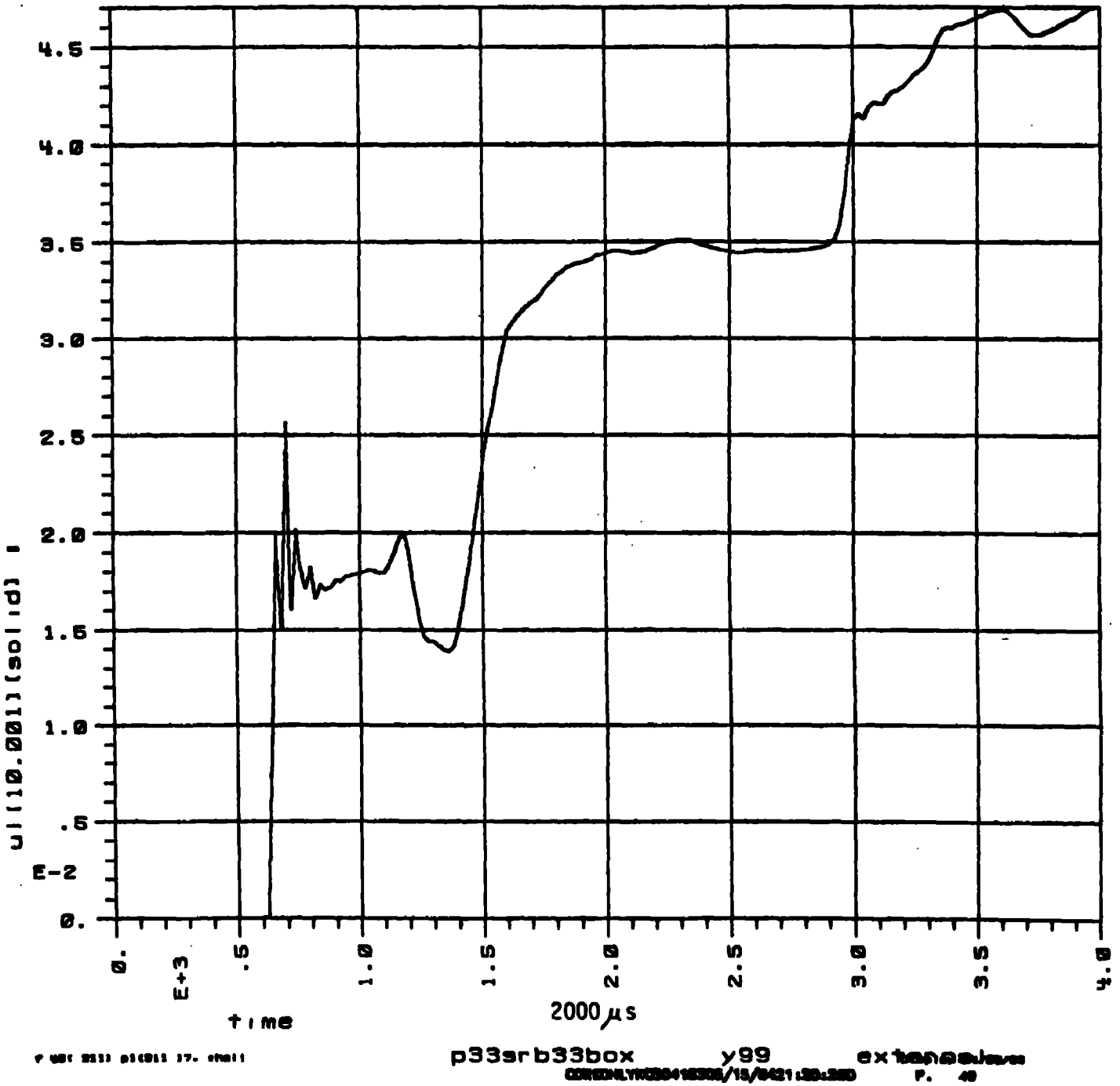

Figure I-18 Velocity versus Tume into SRB propellant for 1664 lbs/ft of ET detonable mixture weight

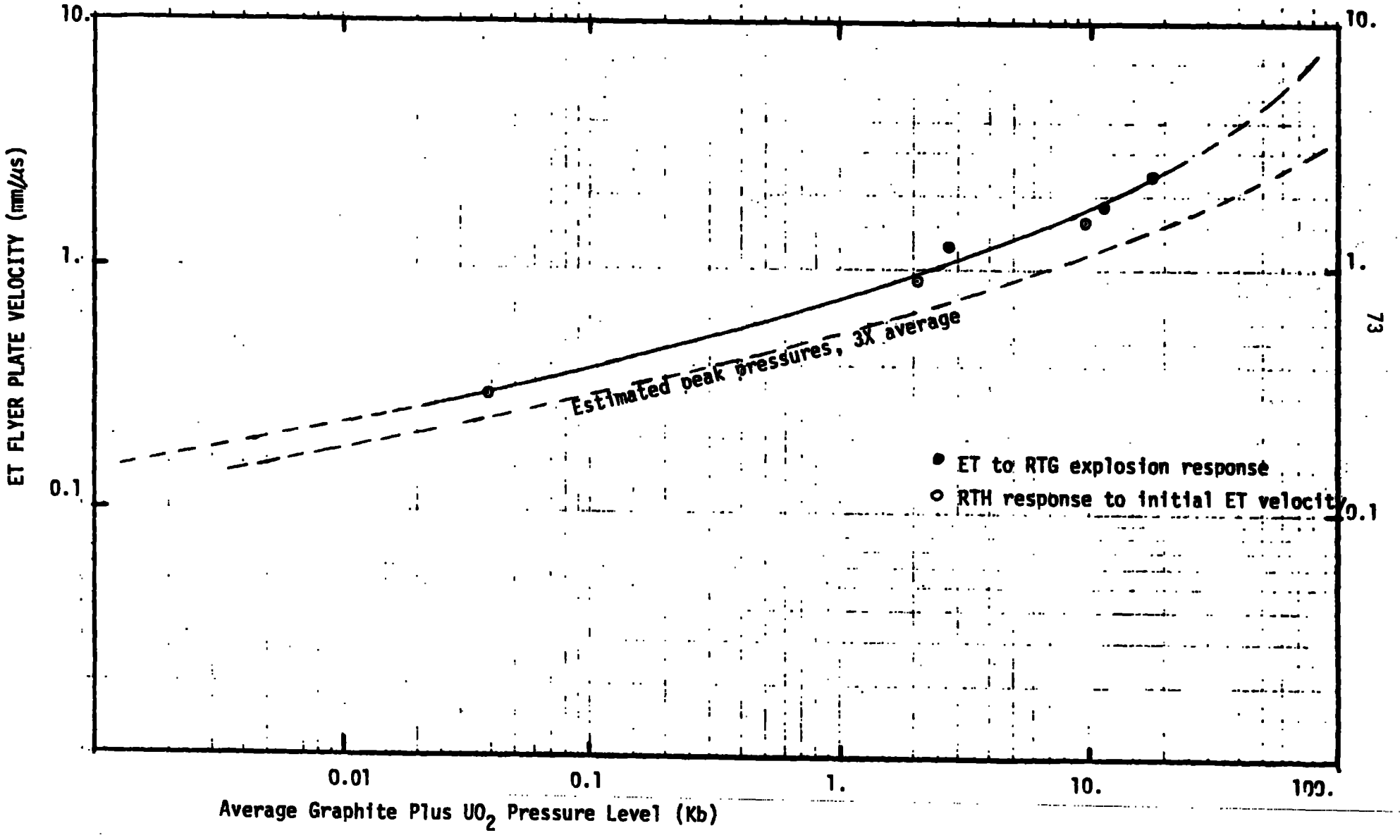

Figure I-19 ET Flyer Velocity Versus RTG Response Pressure. Summary Section, I8